

a NASA facsimile reproduction  
PROPERTY OF: ACCS / JET PROP

**REPRODUCED FROM MICROFORM**

by the  
Reproduced From  
Best Available Copy  
Scientific and Technical Information Facility

**DISTRIBUTION STATEMENT A**  
Approved for Public Release  
Distribution Unlimited



**20011221 111**

**B057148**

N64  
17765  
UNCLASS  
CODE 1

2

1

N64-17765

SUMMARY STATEMENT

RESEARCH AND DEVELOPMENT OF S-1C  
HEAT SHIELD/HONEYCOMB PANELS

ER-764

G.F.R.E.C. MARSHALL SPACE FLIGHT CENTER  
HUNTSVILLE, ALABAMA

Contract No. NASA-S221  
Request No. TP-385174

Period of Performance: January 29, 1963  
to January 29, 1964, inclusive.

Submitted by:

ATRONCA MANUFACTURING CORPORATION  
MIDDLETON, OHIO

Prepared by:

DONALD Y. POTTER  
GEORGE W. SOMERS

MSFC Technical Supervisor  
James O. Lysaght

DISTRIBUTION STATEMENT  
Approved for Public Release  
Distribution Unlimited

January 28, 1964

ABSTRACT

This report describes the work accomplished on Research and Development of S-1C Heat Shield Panels utilizing brazed stainless steel honeycomb sandwich construction, for the period January 29, 1963, to January 29, 1964, inclusive.

The principal effort in this program was the stress, thermal and design analysis of two S-1C heat shield panel designs which differed by virtue of the panel mounting system. As a consequence of this analytical study and the NASA S-1C Heat Shield Panel Test conducted at Wyle Laboratories, either panel design appears to satisfy the S-1C requirements provided the M-31 insulation is retained on the panel by deformation of the honeycomb insulation reinforcement.

Additional items investigated include:

1. Application of Beryllium Sheet to S-1C Heat Shield Panels.
2. Deflection Characteristics of M-31 Insulation with Deformed Stainless Steel Honeycomb Reinforcement.
3. Analysis of Braze Defects, Braze Quality Standards and Repair Methods.
4. Analysis of Holes in Heat Shield Panels and Experimental Measurements of Stresses at Hole Boundaries.
5. Design Recommendations for Heat Shield Panels.

OTS PRICE

XEROX MICROFILM

3

4

TABLE OF CONTENTS

<u>SECTION</u>	<u>PAGE</u>	<u>NUMBER</u>	<u>PAGE</u>
ABSTRACT	1	1	1
TABLE OF CONTENTS	11	2	11
LIST OF TABLES	111	3	111
LIST OF ILLUSTRATIONS	v	4	v
I. TRANSIENT THERMAL ANALYSIS FOR S-1C HEAT SHIELD PANELS	1-32	5	1-32
II. STRESS ANALYSIS FOR S-1C HEAT SHIELD PANELS 30M12571 AND 60B20210	33-46	6	33-46
III. DESIGN PARAMETERS FOR BRAZED HONEYCOMB HEAT SHIELD PANELS WITH SIMPLY SUPPORTED EDGES	47-52	7	47-52
IV. APPLICATION OF BERYLLIUM SHEET TO S-1C HEAT SHIELD PANELS	53-70	8	53-70
V. DEFLECTION CHARACTERISTICS OF M-31 INSULATION WITH DEFORMED STAINLESS STEEL HONEYCOMB REINFORCEMENT	71-74	9	71-74
VI. ANALYSIS OF BRAZE DEFECTS, BRAZE QUALITY STANDARDS AND REPAIR METHODS FOR 30M12571 HEAT SHIELD PANEL	75-97	10	75-97
VII. ANALYSIS OF HOLES IN HEAT SHIELD PANELS AND EXPERIMENTAL MEASUREMENTS OF STRESSES AT HOLE BOUNDARIES	98-120	11	98-120
VIII. DESIGN RECOMMENDATIONS FOR S-1C HEAT SHIELD PANELS Nomenclature	121-123 36-37	12	121-123 36-37
		13	
		14	
		15	
		16	
		17	
		18	
		19	
		20	
		21	
		22	
		23	
		24	
		25	
		26	
		27	
		28	
		29	
		30	
		31	
		32	
		33	
		34	
		35	
		36	
		37	
		38	
		39	
		40	
		41	
		42	
		43	
		44	
		45	
		46	
		47	
		48	
		49	
		50	
		51	
		52	
		53	
		54	
		55	
		56	
		57	
		58	
		59	
		60	
		61	
		62	
		63	
		64	
		65	
		66	
		67	
		68	
		69	
		70	

LIST OF TABLES

<u>NUMBER</u>	<u>PAGE</u>
1	1
2	2
3	3
4	4
5	5
6	6
7	7
8	8
9	9
10	10
11	11
12	12
13	13
14	14
15	15
16	16
17	17
18	18
19	19
20	20
21	21
22	22
23	23
24	24
25	25
26	26
27	27
28	28
29	29
30	30
31	31
32	32
33	33
34	34
35	35
36	36
37	37
38	38
39	39
40	40
41	41
42	42
43	43
44	44
45	45
46	46
47	47
48	48
49	49
50	50
51	51
52	52
53	53
54	54
55	55
56	56
57	57
58	58
59	59
60	60
61	61
62	62
63	63
64	64
65	65
66	66
67	67
68	68
69	69
70	70

5

6

LIST OF TABLES (Cont'd)

NUMBER	PAGE
17	FLEXURE TEST OF HEAT SHIELD TEST SAMPLE
18	SIZE AND SHAPE OF CORE TO FACING - ROSS VOID EFFECTS WITH MINIMUM SPACING REQUIREMENTS
19	SIZE AND SHAPE OF CORE TO FACING, INTERMITTENT CELL WALL VOIDS
20	METAL TO METAL AND CORE TO METAL BRAZE REQUIREMENTS
21	VALUES OF THE STRESS CONCENTRATION FACTOR K FOR VARIOUS SHAPED HOLES WITHOUT FINGER TIPPER
22	A UNIAXIAL STRESS TEST PANEL DEFLECTION DATA
23	SUMMARY OF EXPERIMENTAL AND THEORETICAL VALUES OF STRESS CONCENTRATION FACTOR K FOR BIAXIAL LOADING

LIST OF ILLUSTRATIONS

NUMBER	PAGE
1	TYPICAL S-IC HEAT SHIELD HEATING RATES & SURFACE TEMPERATURE AS A FUNCTION OF FLIGHT TIME (NASA SUPPLIED DATA 2-11-63)
2	TEMPERATURE PROFILE FOR HEAT SHIELD PANEL 3OM12571; 100% NODE FLOW (.010 INCH WIDTH)
3	TEMPERATURE PROFILE - "W" TYPE PANEL ATTACHMENT PANEL 3OM12571
4	TEMPERATURE PROFILE FOR HEAT SHIELD PANEL SK60B20091 WITH 100% NODE FLOW (.010 INCH WIDTH)
5	TEMPERATURE PROFILE - CUP-TYPE PANEL EDGE ATTACHMENT THERMAL CONDUCTIVITY OF HEAT SHIELD PANEL VS. CELL WIDTH AND NODE FLOW WIDTH
6	EFFECT OF NODE FLOW SIZE ON PANEL UNIT WEIGHT AND THERMAL CONDUCTIVITY
7	EFFECT OF NODE FLOW WIDTH & CELL SIZE ON TEMPERATURE DIFFERENTIALS ACROSS THE 3OM12571 PANEL DESIGN FOR THREE DIFFERENT LOAD BEARING CORE SIZES
8	TEMPERATURE DIFFERENTIALS ACROSS THE HONEYCOMB AS FUNCTION OF CELL DEPTH AND NODE FLOW WIDTH. CORE SIZE 4-15
9	TEMPERATURE PROFILES IN HEAT SHIELD PANEL NO. 3OM12571 ZERO NODE FLOW--CELL SIZE 4-15, VARIABLE M-31 REIN- FORCEMENT
10	TEMPERATURE PROFILES, PANEL NO. 3OM12571, ZERO NODE FLOW - CELL SIZE 3-15, OPEN CORE SIZE 8-15
11	TEMPERATURE PROFILES, PANEL NO. 3OM12571, *005 INCH NODE FLOW WIDTH - CELL SIZE 3-15, OPEN CORE SIZE 8-15
12	TEMPERATURE PROFILES, PANEL NO. 3OM12571, *005 INCH NODE FLOW WIDTH - CELL SIZE 3-15, OPEN CORE SIZE 8-15
13	TEMPERATURE PROFILES, PANEL NO. 3OM12571, *010 INCH NODE FLOW WIDTH - CELL SIZE 3-15, OPEN CORE SIZE 8-15
14	TEMPERATURE PROFILES, PANEL NO. 3OM12571, *015 INCH NODE FLOW WIDTH -- CELL SIZE 3-15, OPEN CORE SIZE 8-15
15	TEMPERATURE PROFILES - PANEL NO. 3OM12571, ZERO NODE FLOW - CELL SIZE 4-15, OPEN CORE SIZE 8-15

7

8

LIST OF ILLUSTRATIONS (Cont'd)

NUMBER	PAGE	
16	TEMPERATURE PROFILES - PANEL NO. SK601001 ZERO NODE FLOW - CELL SIZE 4-15, OPEN CORE SIZE 8-15	24
17	TEMPERATURE PROFILES - PANEL NO. SK6010001, .005 INCH NODE FLOW WIDTH - CELL SIZE 4-15, OPEN CORE SIZE 8-15	25
18	TEMPERATURE PROFILES - PANEL NO. SK6012001, .015 INCH NODE FLOW WIDTH - CELL SIZE 4-15 OPEN CORE SIZE 8-15	26
19	TEMPERATURE PROFILES IN HEAT SHIELD EASEL NO. 30M12571 .015 INCH NODE FLOW WIDTH - CELL SIZE 8-15, VARIABLE M-31 REINFORCEMENT	27
20	TEMPERATURE PROFILES - PANEL NO. 30M12571, ZERO NODE FLOW - CELL SIZE 6-20, OPEN CORE SIZE 8-15	28
21	TEMPERATURE PROFILES - PANEL NO. 30M12571, .005 INCH NODE FLOW WIDTH - CELL SIZE 6-20, OPEN CORE SIZE 8-15	29
22	TEMPERATURE PROFILES - PANEL NO. 30M12571, .010 INCH NODE FLOW WIDTH - CELL SIZE 6-20, OPEN CORE SIZE 8-15	30
23	TEMPERATURE PROFILES - PANEL NO. 30M12571, .015 INCH NODE FLOW WIDTH - CELL SIZE 6-20, OPEN CORE SIZE 6-20	31
24	MOUNTING SYSTEM FOR 60B2020 PANEL SHOWING CALCULATION DIMENSIONS ONLY	38
25	VARIATION OF MODULUS OF ELASTICITY WITH TEMPERATURE (ELASTIC PROPERTIES OF PH15-7Mo (TH 1050) BASED ON 1958 ARMC DATA IN ARDC TR 59-66)	39
26	DEFLECTION AT CENTER OF PANEL VS. CORE THICKNESS	48
27	THERMAL DEFLECTION AT CENTER OF PANEL VS. HEIGHT OF PANEL FOR CONSTANT TEMPERATURE DIFFERENCES	49
28	THERMAL + AIR LOAD DEFLECTION AT CENTER OF PANEL VS. HEIGHT OF PANEL FOR CONSTANT TEMPERATURE DIFFERENCES AND 1 psf	50
29	THERMAL + AIR LOAD DEFLECTION AT CENTER OF PANEL VS. HEIGHT OF PANEL FOR CONSTANT TEMPERATURE DIFFERENCES AND 1 psi	51
30	THERMAL + AIR LOAD DEFLECTION AT CENTER OF PANEL VS. TEMPERATURE DIFFERENCE FOR CONSTANT CORE THICKNESS ( $\bar{t}$ )	52
NUMBER	PAGE	
31	FLEXURE TEST OF SANDWICH SECTION WITH M-31 INSULATION	73
32	FLEXURE TEST OF SANDWICH SECTION WITH M-31 INSULATION AT FAILURE	74
33	QUALITY MODIFYING CONDITIONS REVEALED BY RADIOPHASIC EXAMINATION	76
34	QUALITY MODIFYING CONDITIONS REVEALED BY RADIOPHASIC EXAMINATION	77
35	QUALITY MODIFYING CONDITIONS REVEALED BY RADIOPHASIC EXAMINATION	78
36	QUALITY MODIFYING CONDITIONS REVEALED BY RADIOPHASIC EXAMINATION	79
37	QUALITY MODIFYING CONDITIONS REVEALED BY RADIOPHASIC EXAMINATION	80
38	QUALITY MODIFYING CONDITIONS REVEALED BY RADIOPHASIC EXAMINATION	81
39	BASIC VOID AND BUCKLING CONFIGURATIONS	83
40	EFFECT OF CROSS VOIDS - LOCAL UNIAXIAL COMPRESSION ALLOWABLE PH15-7Mo (RH1050)	85
41	EFFECT OF CELL WALL VOIDS - LOCAL UNIAXIAL COMPRESSION ALLOWABLE PH15-7Mo (RH1050)	87
42	EFFECT OF UNDERSIZE FILLET ON FACE SHEET STABILITY	88
43	TYPICAL METAL TO METAL BRAZE VOID REPAIR WITH MECHANICAL FASTENERS (RIVETS)	95
44	HOLE DIAGRAMS, TYPICAL	100
45	STRESS CONCENTRATION FACTOR, K AT $\theta = \pi/4$ FOR SQUARE AND DIAMOND HOLES	101
46	VACUUM BOX TEST FIXTURE	109
47	SIDE VIEW, TEST ASSEMBLY, PANEL NO. 1	110
48	END VIEW, TEST ASSEMBLY	112
49	DIAL INDICATOR POSITIONS FOR TEST PANELS	

LIST OF ILLUSTRATIONS (Cont'd)

<u>NUMBER</u>	<u>PAGE</u>
50	113
51	114
52	115
53	116
54	117
55	120
56	123
57	124

STRESS COAT, PANEL NO. 1, INITIAL HOLE PATTERN  
CENTER HOLE STRESS COAT CLOSE-UP PANEL NO. 1,  
INITIAL HOLE PATTERN

EDGE HOLE STRESS COAT CLOSE-UP PANEL NO. 1,  
INITIAL HOLE PATTERN

CENTER HOLE STRESS COAT CLOSE-UP PANEL #1  
MODIFIED HOLE PATTERN

PANEL NO. 2, STRESS COAT PATTERN, QUARTER  
SECTION VIEW

STRAIN GAGE LOCATIONS ON TEST PANELS USED FOR  
EXPERIMENTAL DETERMINATION OF STRESS CONCENTRATION  
FACTOR, K

RECOMMENDED ZEE SECTION CORNER JOINT ASSEMBLY

ECONOMICAL ZEE SECTION CORNER JOINT ASSEMBLY

SECTION I  
TRANSIENT THERMAL ANALYSIS  
FOR S-1C HEAT SHIELD PANELS

*Stan Kline*

Introduction

Presented in this section are the transient heat transfer analyses of the Saturn base heat shield panel for design drawing Nos. 10R12571 and SK 60B-20001 and shown in Figure 1, Page 2. All analyses are three dimensional in nature and are based on heat transfer and surface temperatures derived from NASA Huntsville data. Included are the maximum temperature profiles of the edge attachment scheme for the two panel designs. The temperature profiles presented are for the condition of 100° braze joint allow node flow in the honeycomb support structure. All other assumptions and general rules which govern the analysis are presented in "Methods of Analysis".

In addition to the thermal analyses of the two panel concepts, a set of parametric curves is presented illustrating the temperature differences across the honeycomb support structure as a function of braze node flow size, cell dimensions and M-31 reinforcement honeycomb dimensions. While these parametric studies are confined to the dimensions bounded for the most part by the dimensions of the panel considered, they do present the possible trade-offs that could be considered for possible panel design optimization from thermal considerations.

Methods of Analysis

Aeronca has developed a digital computer program which has general applicability to thermal analysis of high temperature structures. For purposes of analysis the structure is represented by a set of spatially distributed points or nodes. The temperature of each node is determined by solving the generalized heat balance equation in finite difference form:

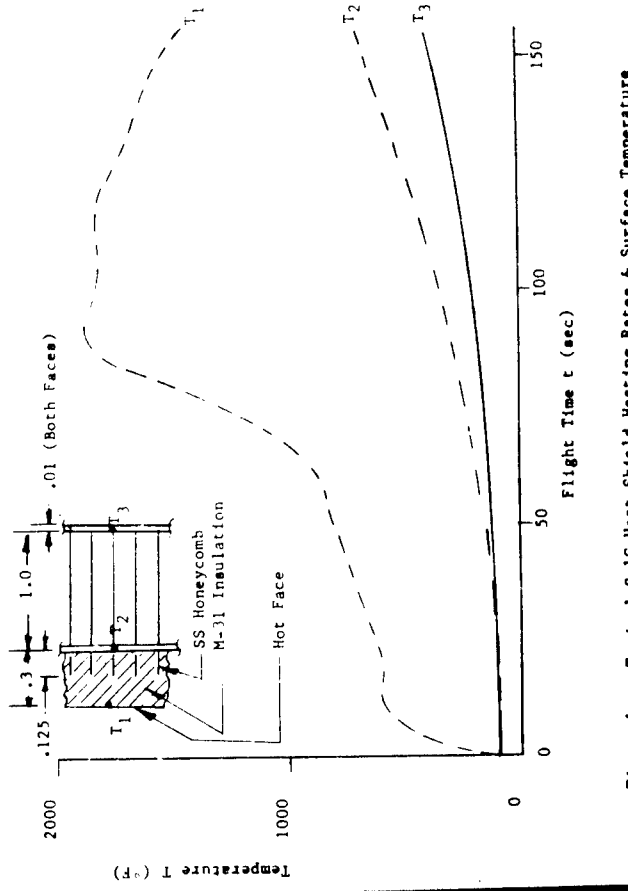
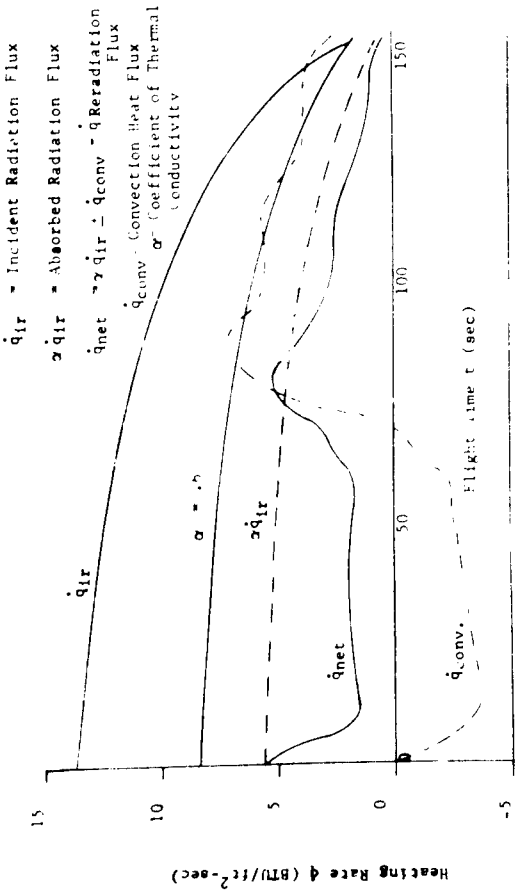
$$T_j^* - T_j = \frac{\Delta t}{\rho C_p} [Q_j + Q_{j-1} - \sum_{i=1}^n U_{ij} (T_i^* - T_j)] \quad (1)$$

$T_i^*$  and  $T_j$  represent the temperatures at the end, and beginning of the time step, respectively. The parameters  $Q_i$  and  $Q_j$  represent volumetric heating and incident surface flux, respectively.  $U_{ij}$  is the thermal conductance between the adjacent nodes i and j. The program does an iteration for  $T^*$  and re-evaluates temperature dependent functions (radiation coefficient, etc.) on the temperature at the midpoint of the time step. This is the so-called Implicit Method.

\*NSFC Memorandum, "Estimated Temperatures for S-1C Heat Shield Attachment", dated 2/11/63, M-Pave PH 26-63.  
See Figure 2.

12

11



The program can use the Explicit Method, in which  $T_j^*$  and  $T_j$  are the same as in the Implicit Method. The heat balance equation will become explicit in  $T_j^*$ .

$$T_j^* - T_j = \frac{\Delta\tau}{\rho V C_p} \left[ \dot{q}_j^{***} + \dot{q}_j^{**} - \sum_{i=1}^n U_{ij} (T_j - T_i) \right] \quad (2)$$

There is now a limit on the length of time step  $\Delta\tau$  which the program calculates and is given by  $\Delta\tau \leq \frac{\rho V C_p}{\alpha}$  and taken so that the expression  $\sum_{i=1}^n U_{ij}$  is a minimum for the entire nodal system. Here,  $n$  is the total number of thermal connections.

The expression used to evaluate zero-volume nodes (surface) and steady-state calculations is

$$\sum_{i=1}^n U_{ij} (T_j - T_i) - \dot{q}_j^{***} - \dot{q}_j^{**} = 0 \quad (3)$$

The parameters  $\dot{q}_j^{***}$  and  $\dot{q}_j^{**}$  are the same as defined previously.

The thermal conductance term,  $U_{ij}$ , is used in three basic forms: (1) solid to solid conduction, with contact coefficient; (2) solid to solid radiation, with radiation coefficient; and (3) solid to fluid, with conduction and film coefficient.

There are several important features in this computer program. The amount of data necessary to run a problem is quite large and would include such things as: (1) time, boundary temperature tables; (2) time, rate tables; (3) Nusselt number correlation tables; (4) material property tables; (5) node description data for each node; and (6) connection data for each node. Although a large amount of input data is necessary, the engineer requires little or no knowledge of computer programming or techniques to use the program. Use of stacked storage is employed rather than the bulkier reserved storage, so that problems with greater than 1000 nodes can be run.

The program is divided into five chains: Chain 1 accepts data in a form which is easy for the user to prepare and stores it for further processing—in other words, Chain 1 is just to input the problem; Chain 2 processes data from Chain 1 into a form which the program can use; Chain 3 takes this processed data and performs the computation of Equations (1) or (2); Chain 4 is an editing chain which will (1) give a time-temperature history if requested, and (2) if the run is pulled for time, punch the current temperature distribution or decimal cards so that the run can be restarted; Chain 5 sets up change cases. A more detailed description of the program is presented in Ref. 1\*.

Figure 1 Typical S-IC Heat Shield Heating Rates & Surface Temperature As a Function of Flight Time (NASA supplied data 2-11-63)

\*Ref. 1 - Niehaus, W. R., Criss, R., Cannizzaro, R., "A Transient Heat Transfer Computer Analysis for Space Vehicle Application", Aeronaics Manufacturing Corporation, ER-638, February 1963.

A second method of heat transfer which was employed was to assemble "n" heat balance equations, one for each temperature point in the panel and for given time intervals and time dependent boundary conditions, use the Gauss-Seidel iteration method to determine the unknown temperatures.

This process is repeated for each time interval until the desired transient analysis is complete.

The general form of the heat balance equation for one point in the panel for a single time interval is given below.

$$\frac{\rho V C}{\Delta T} (T_n - T) = \sum_{n=1}^6 \left[ \frac{X_{11}}{K} + \frac{\Delta X_{11}}{h_n} + \frac{1}{h_c} \right] (T_i - T) +$$

Fluid flow input +

$$(W/W)C (T_n - T) +$$

Surface flux +

$$A_r \dot{Q}_r +$$

Solid Radiation +

$$\sum_{n=1}^3 \sum_{i=1}^6 A_h F_i \epsilon_{1/2} [T_h^4 - T_i^4]$$

Basically, the transient analysis was one of using the finite difference technique of dividing the panel geometry into a three-dimensional network of nodes. Each node had a finite volume enclosed by a maximum of six sides. Material properties and states were considered to be uniform within a given node and correspond to the temperature at the center of the node.

4

#### Design Point Analysis

##### Z-Type Edge Panel (Dwg. 30M12571):

The temperature histories at various levels throughout the panel are given in Figure 2 and are based on the effective thermal properties of the various layers as given in Table 1. The temperature histories at various points on the Z-type edge attachment are given in Figure 3.

##### Cup-Type Panel (Dwg. SK 60B20001):

The temperature histories at various levels throughout the panel are given in Figure 4 and are based on the effective thermal properties of the various layers given in Table 1.

The temperature histories at various points on the cup-type edge attachment are given in Figure 5.

##### Assumptions Made in the Preceding Analyses:

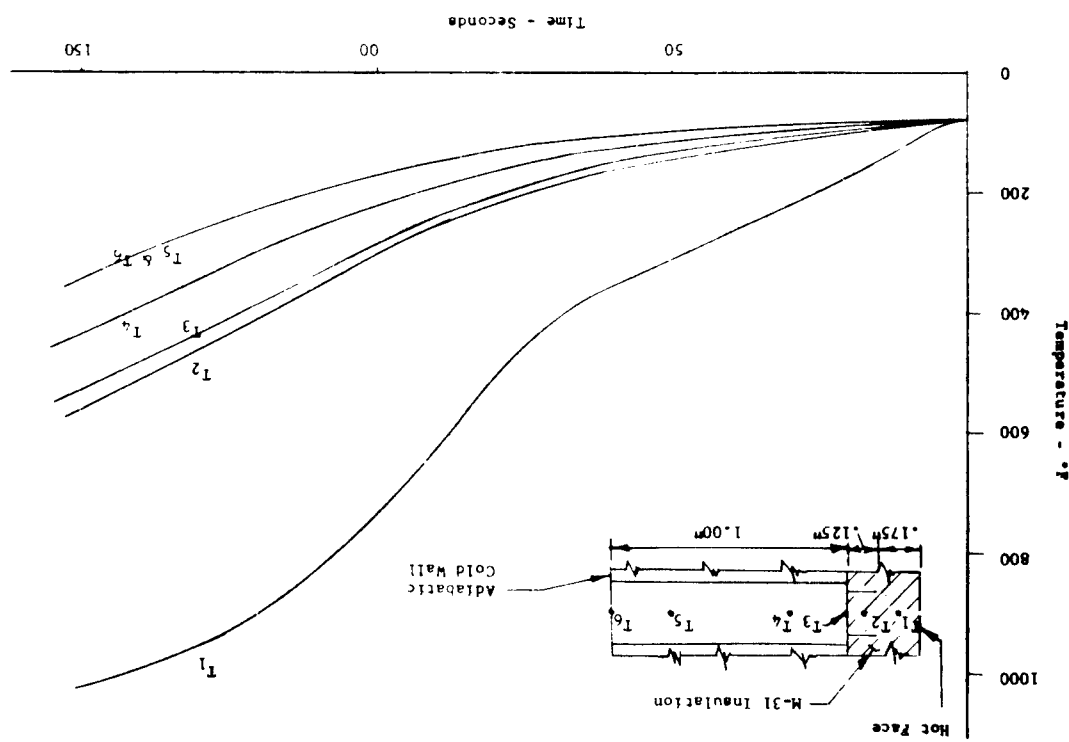
The following assumptions and/or ground rules were made and incorporated in the transient heat transfer analyses:

- When composite layers existed in the heat shields (i.e., where parallel heat transfer paths exist), an effective thermal conductivity and density were used. The effective thermal conductivity is equal to the sum of the parallel conductances divided by the total panel heat flow area.
- The temperature differential across the honeycomb support structure facing was considered small and the unit conductance ( $k/A$ ) was substituted as a contact coefficient to account for thermal conductance through them. The volumetric heating was neglected.
- Node flow was included in the thermal conductance of the honeycomb support panel. Two (2) braze nodes per honeycomb cell were considered having an effective cross sectional area equal to that of an equilateral triangle of side 0.010 inch. This dimension was based on measurements of the node flow width made from 30M12571 panel X-rays.
- The cold face surface was adiabatic.
- The radiation exchange and natural convection were both considered negligible in the honeycomb cells.
- The contact coefficients between the panel edges and the attachment bolts were based on a nominal air gap of 0.001".

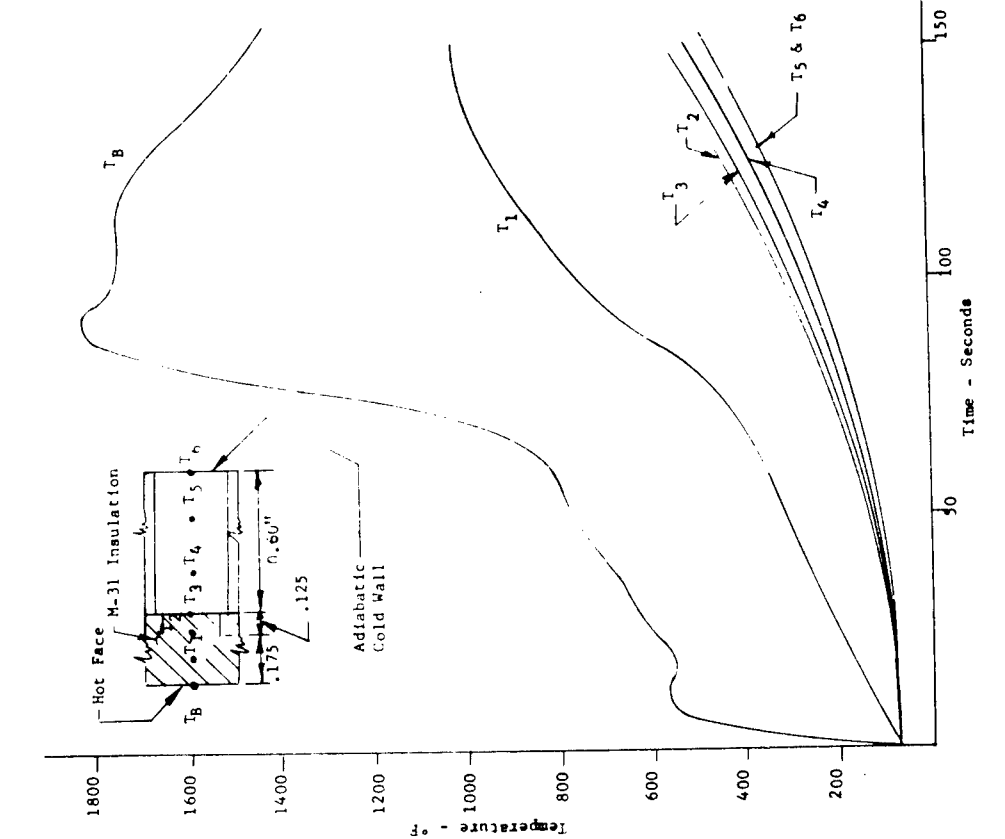
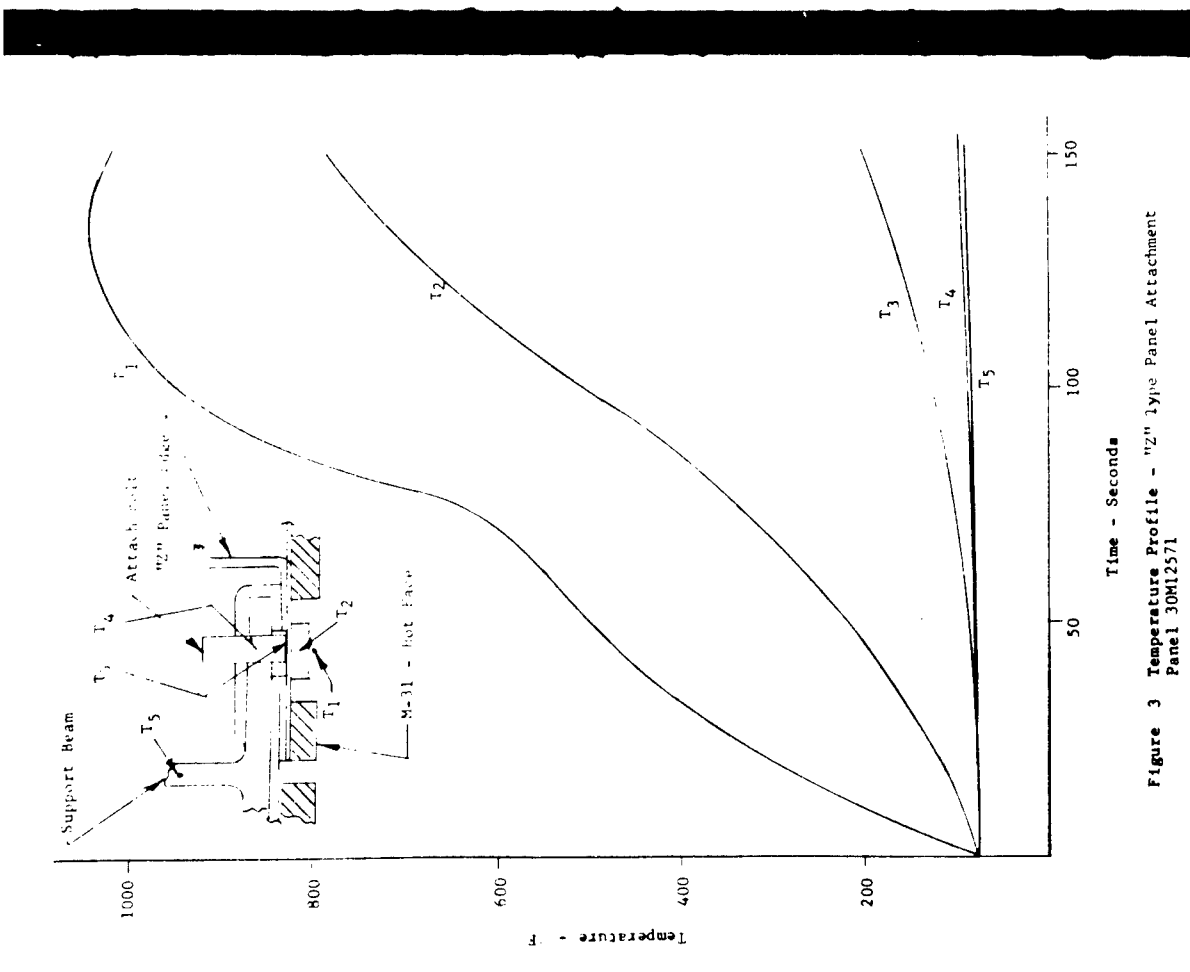
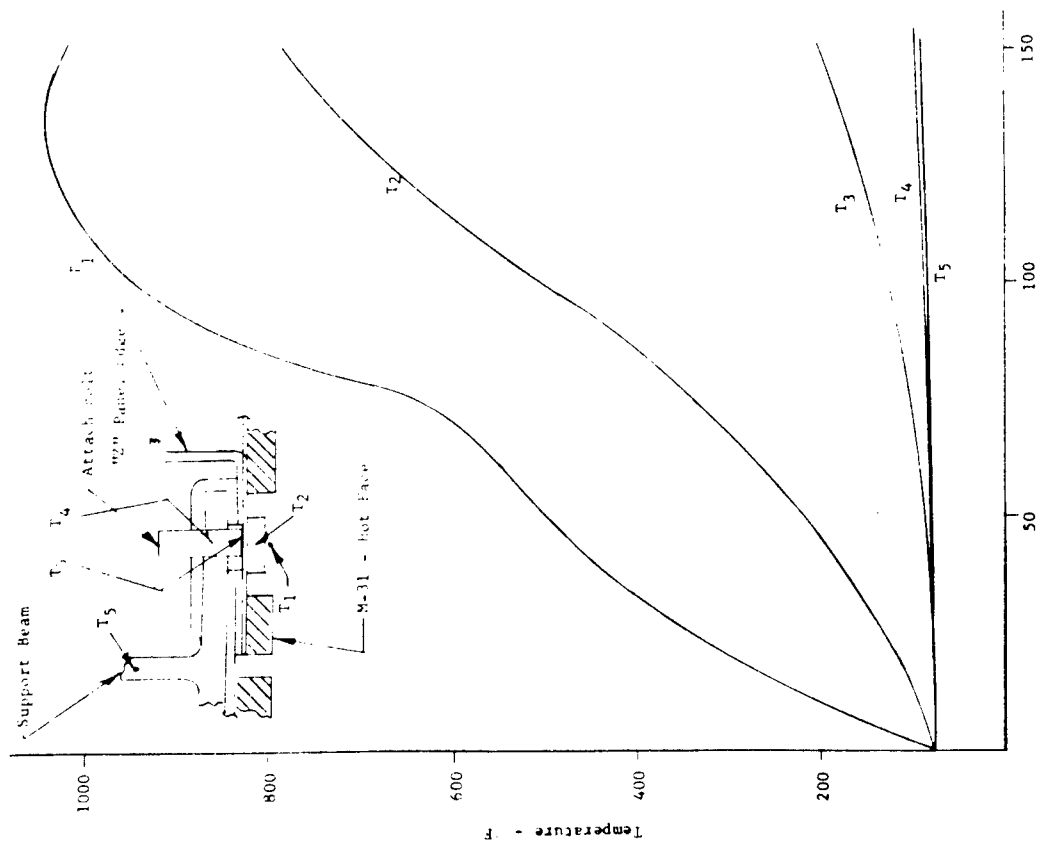
TABLE I  
THERMAL ANALYSIS,  
EFFECTIVE MATERIAL PROPERTIES  
BASED ON HOMOGENEOUS LAYERS

Material Layer	T = F	K effective		Specific Heat BTU/lb hr °F	Density - Lbs/Cu.Ft.
		Cell Size	PH15+7Mo		
1. Honeycomb Structure	0	.228	.11	.19	
	800	.265	.11	.19	
2. M-31 Plus Honeycomb Support	0	.130	.31	.50.1	
	800	.152	.31	.50.1	
3. M-31	3,000	.083	.31	.47.0	
		.083	.31	.47.0	

FIGURE 2 Temperature Profile for Heat Shield Panel 30M12571  
1000 Node Flow (.010 inch width)



19



20

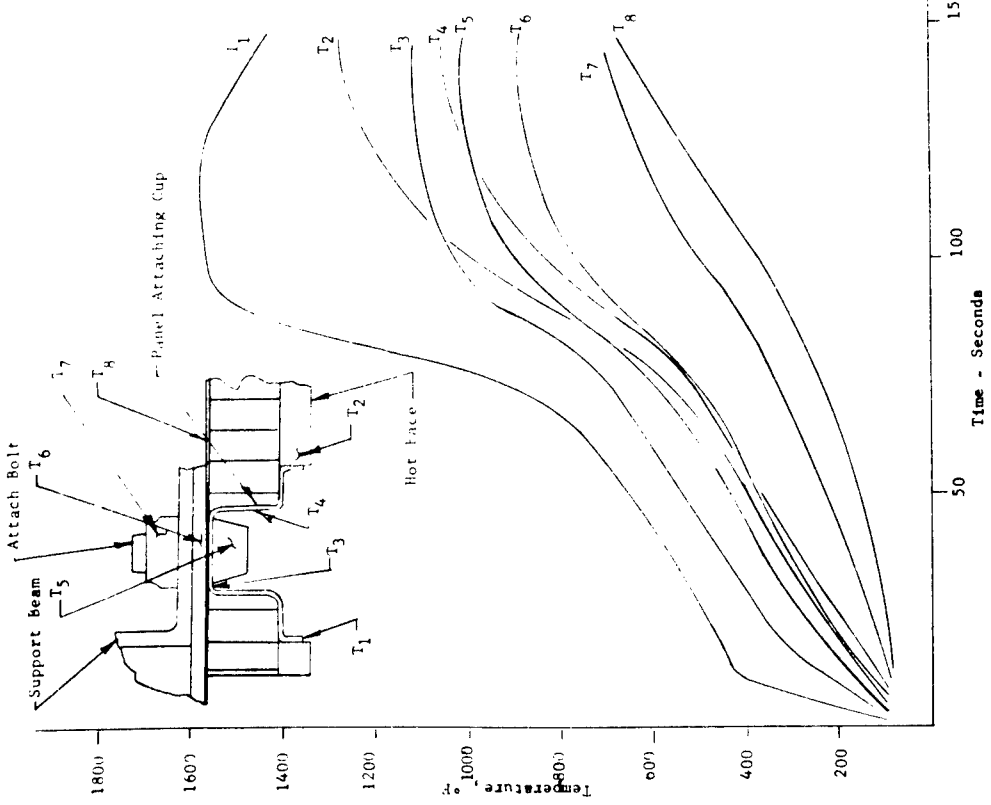


Figure 5 Temperature Profile - Cup-Type Panel Edge Attachment

#### Design Point Temperatures

The maximum temperature differentials to be used for design purposes across the brazed honeycomb sandwich panels are as follows:

Panel Configuration	Silver Brazing Alloy Node Flow Condition	$\Delta T_F$	Time Duration Second*
SK60B20001 0.6"	Complete--0.010"	80	155
Thick Core	Width		
30M12571 1.0" Thick Core	Zero	320	155
30M12571 1.0" Thick Core	Complete--0.005"	280	155
30M12571 1.0" Thick Core	Complete--0.010"	180	155
Width			

The beneficial effect of brazing alloy node flow in the lead tearing honeycomb core, reducing the temperature difference and the resultant thermal stress, is shown for the JUM12571 heat shield panel design by the above data.

#### Parametric Analysis

As a result of the thermal analysis performed on the two heat shield panel concepts, a parametric analysis was made which considered the effects of node flow width, cell dimensions, and M-31 reinforcing honeycomb effects on the transient temperature differentials across the honeycomb support structure.

A careful review of the thermal analyses of honeycomb panels in the past has indicated that the presence of good node flow with the use of high thermal conductivity brazing alloy is the probable cause of the high rate of heat conductance through honeycomb panels.

The term "node flow" refers to the phenomenon of the formation of fillets of braze alloy which connect the panel faces, in the corners of the honeycomb core cells. Such metal "bridges" offer conduction paths between the panel faces which are orders of magnitude better than that in the air gap within the cells and which, at reasonably low temperature levels, transfer considerably more thermal energy between panel faces than is transferred by thermal radiation. If the thermal conductivity of the node-flow metal approaches that of silver, which is on the order of 20 times that of a high-nickel-content brazing alloy, the node-flow conductance path will be by far the dominating factor in the transmission of heat through the panel.

Reference 2\* presents an analysis of sample test data wherein it is shown, on the basis of a reasonable set of assumptions, that of the total heat passing through the test panel, 5.2% was by radiation between the panel faces, 17.0% was by conduction through the core foil, and the remaining 77.8% was by conduction through the high-silver-content brazing alloy. While the exact magnitude of the numbers may be subject to some question on the basis of the assumptions used in calculating them, the relative magnitudes are felt to be quite correct.

The parametric analyses presented here are intended to furnish in limited way the trade-offs to be made in designing a heat shield panel from thermal considerations. The range of honeycomb cell dimension considered brackets the dimensions of the two design panels. As such the material discussed in this section and the feasible trade-offs that can be derived from the curves apply only in the neighborhood of the dimensions and environments of the previously mentioned design panels.

#### Node Flow Effect

Figures 6 to 8 show the effect of node flow width on the effective thermal conductivity of the honeycomb, the weight of the honeycomb panel, and the temperature differential across the honeycomb panel.

Figure 6 shows that in doubling the cell width the effective conductivity of the panel is reduced by a factor of from 2 - 3 for node flow widths of about 0.010". Also, it is evident that for a node flow width above 0.010" the effective conductivity increases rapidly. However, with this increase in thermal conductivity, which is desirable from a thermal stress standpoint, there is an increase in panel weight. Figure 7 shows the trade-off between effective honeycomb density and increase in effective conductivity as a function of cell width and node flow width. For a node flow width of 0.010", the percent increase in density of a honeycomb having a 3-15 cell (.188" cell width, .0015" foil width) when such a braze node flow is added is 21% of the original density with no node flow. The per cent increase in thermal conductivity, however, is 11.8%. In values of density the increase would go from 9.3 to 10.03 lb/ft<sup>3</sup> while the conductivity would increase from .136 BTU/HR-Ft-°F to .387 BTU/HR-Ft-°F.

Figure 8 gives the effect of node flow width and cell width on the temperature differential across a 1.0" thick honeycomb panel (Panel No. 30H12571). The temperature differential decreases with an increase in both cell width and node flow width. This is to be expected since an increase in either of these increases the effective thermal conductivity across the panel.

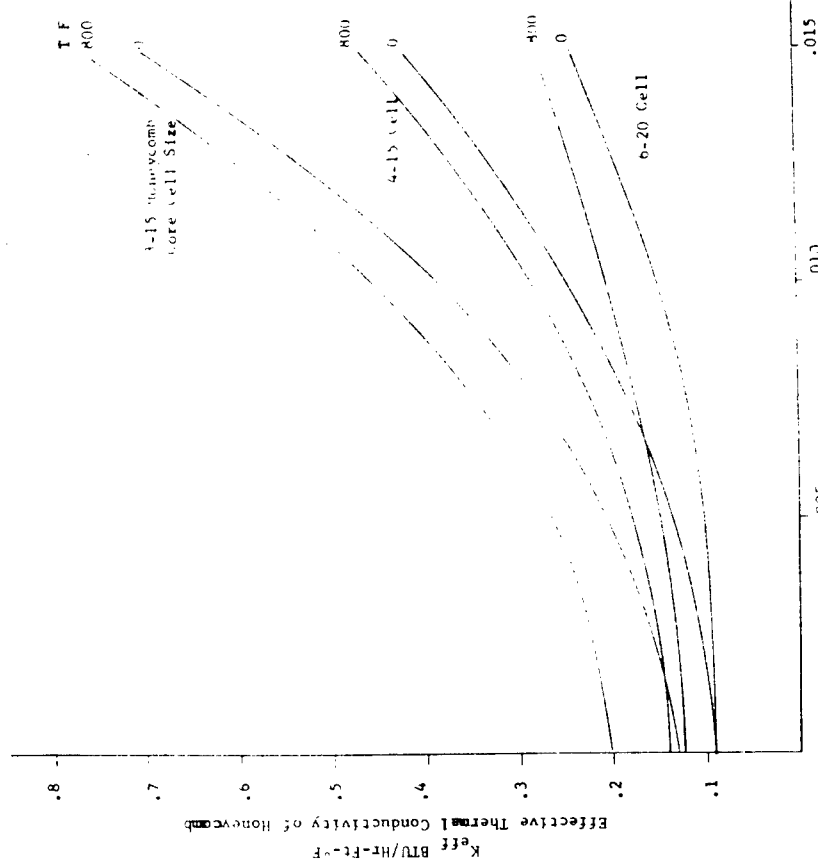


Figure 6 Thermal Conductivity of Heat Shield Panel vs.

Silver Node Flow Width - Inches  
Cell Width and Node Flow Width  
(Based on Equilateral Triangle Cross-Section)

\*Reference 2 - ASD-TR-7-845 (II) Page 367

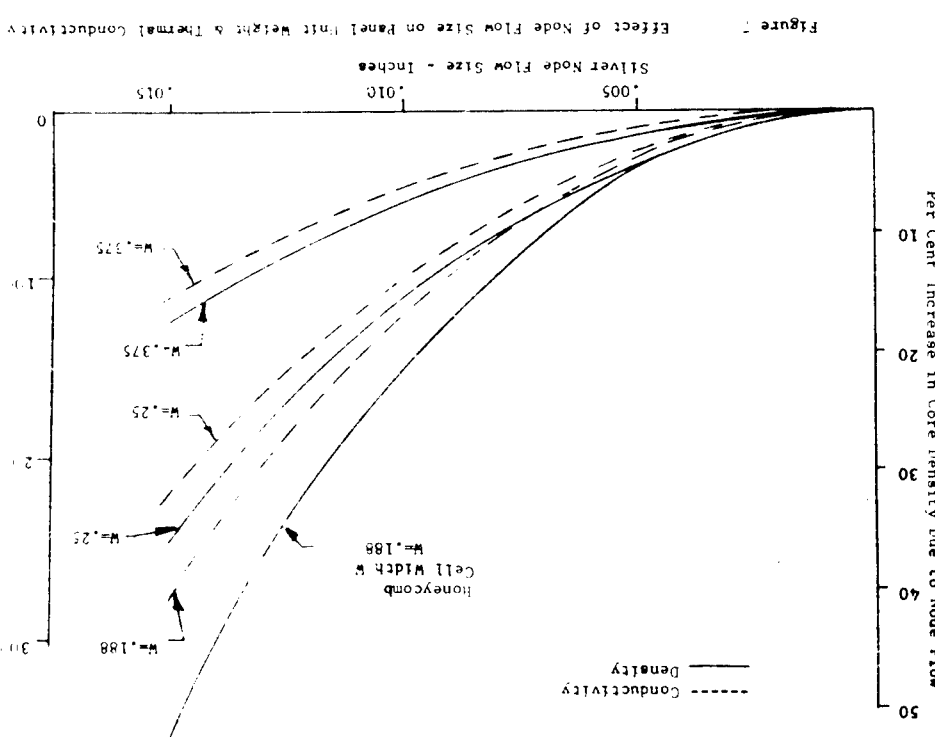
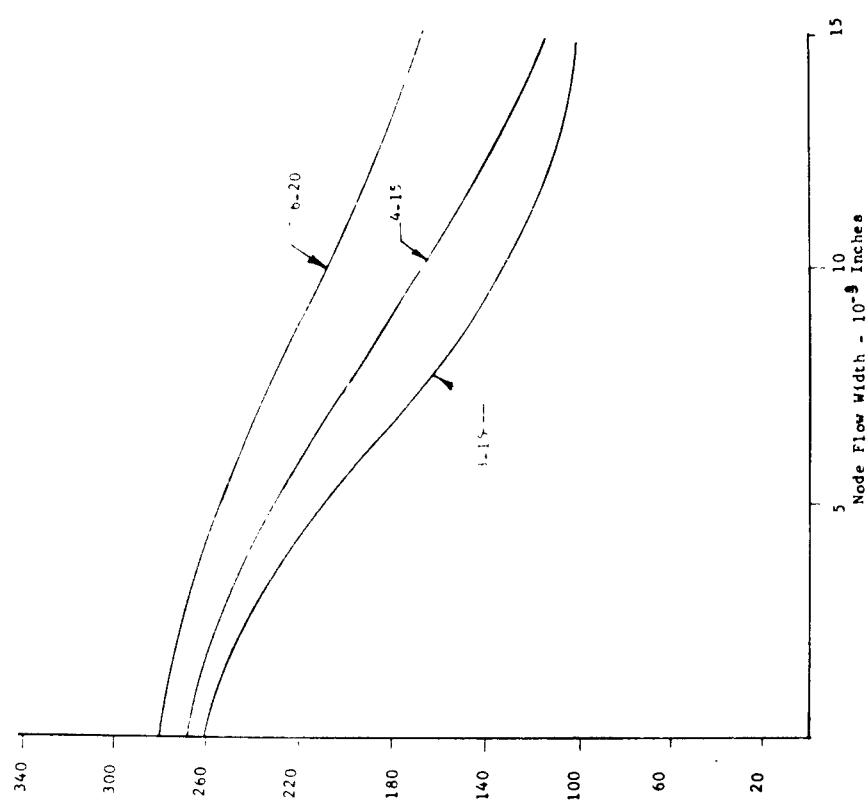


Figure 1 Effect of Node Flow Size on Panel Unit Metric as Thermal Conductivity

SILVER Node Flow Size - Inches



**Figure 8** Effect of Node Flow Width & Cell Size on Temperature Differentials Across the 30M12571 Panel Design for Three Different Load Bearing Core Sizes

Cell Depths

In Figure 9, the adiabatic temperature differentials are given across the honeycomb core as a function of cell depth and node flow width for a constant cell size of 4-15" wide and 0.15" tall thickness. It is quite evident that for any one cell depth, the temperature drop across the honeycomb decreases with an increase in node flow width. Also, for a constant node flow width with  $\Delta T \neq 0$ , the cell depth is decreased, as would be expected.

It should be pointed out here that holding all parameters constant and decreasing the cell depth increases the stack factor (cold side) temperature of the honeycomb panel. This is in contrast to the fact that the boundary conditions are the same so that there is no change in the heat transfer coefficient at all for the same amount of heat.

M-31 Reinforcing Honeycomb Effects

Figure 10 gives the temperature profiles for the heat shield panel No. 30M-12571 as a function of variable M-31 reinforcement cell width. The cell size was varied from 8-15 to 4-15, respectively. As is evident from the curves, there was no noticeable effect on the temperature distribution in the honeycomb structure. Although not shown on the curves, a slight variance was noted in the temperatures  $T_1$  and  $T_2$ , but was of such a magnitude ( $\pm 10\%$ ) as to make it negligible.

Supplementary Information Relating to Parametric Studies

The temperature profiles given in Figures 11 to 23 were the basis for the preceding parametric analyses. Table 2 shows in tabular form the characteristics of the three honeycomb panels that served as the models for the parametric analyses.

Discussion

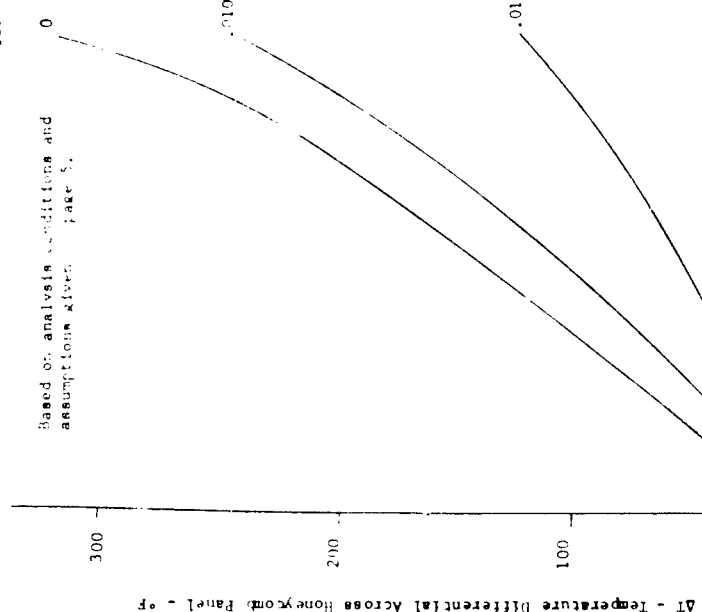
The methods of thermal analysis and the design point analysis presented here have been discussed previously (Ref. 1) and have been given to consolidate the thermal analysis and its results into a single unit for reference.

In reference to the information given in the section on the parametric analyses, it should be pointed out that the curves can be used most accurately in predicting the trend or trade-offs that occur for any one set of cell dimensions. This is especially so when predicting the effect of node flow width on temperature differentials across the honeycomb panel. It is quite evident from the curves that the node flow size is of prime consideration.

It should also be noted here that the  $\Delta T$  (160°F) for the 4-15 cell having 0.010" node flow width in Figure 8 differs from the  $\Delta T$  given in the section "Design Point Temperatures" for the design point (180°F). The difference is due to a refinement in the effective thermal conductivity of the honeycomb panel which was made for the parametric analyses. However, since the design point value was conservative, it was not changed.

Figure 9

Sliver Node Flow Width



Based on analysis conditions and assumptions given.  
Assumption given:  
1.  $\Delta T = 0$   
2.  $T_1 = 160^\circ F$   
3.  $T_2 = 180^\circ F$

$\Delta T = \text{Temperature Difference Differential Across the Honeycomb Panel} = 0$

Cell Depth = 4-15"

Core Size = 8-15"

Figure 9  
Temperature Differentials Across the Honeycomb Panel as a Function of Cell Depth and Node Flow Width.

17

29

Figure 10 Temperature Profiles in Heat Shield Panel No. 30M12571

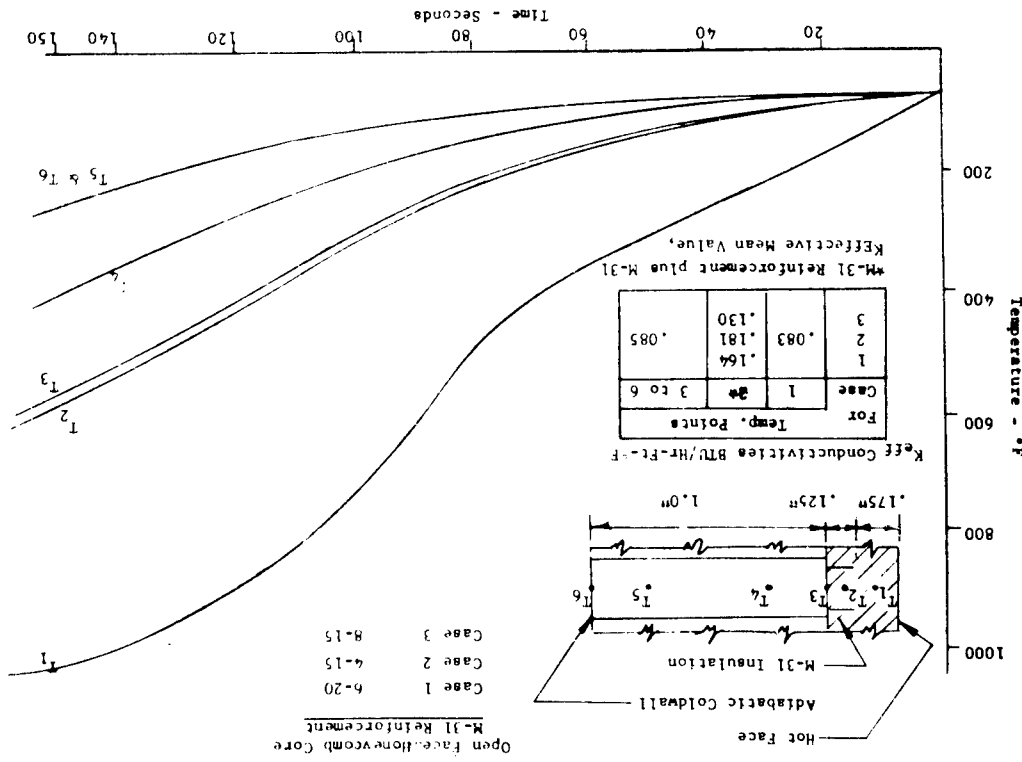
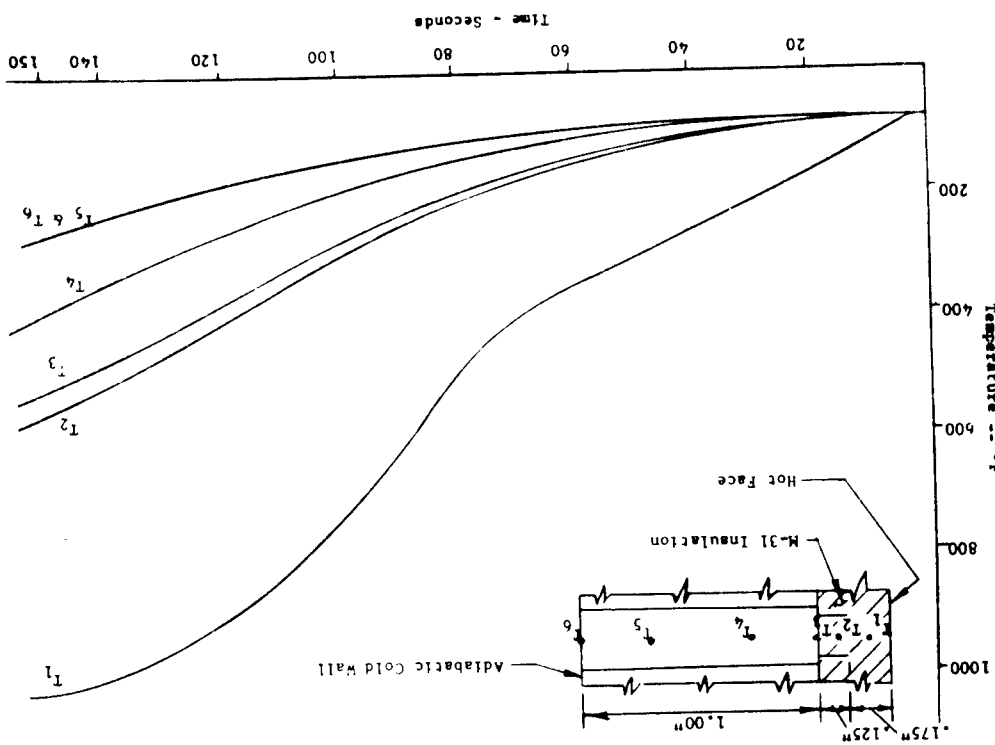


Figure 11 Temperature Profiles, Panel No. 30M12571  
Zero Node Flow - Cell Size 3-15  
Open Core Size, 8-15



30

32

Figure 13 Temperature Profiles, Panel No. 30M12571  
.010 Inch Node Pitch - Cell Size 3-15  
Open Core Size, H-15

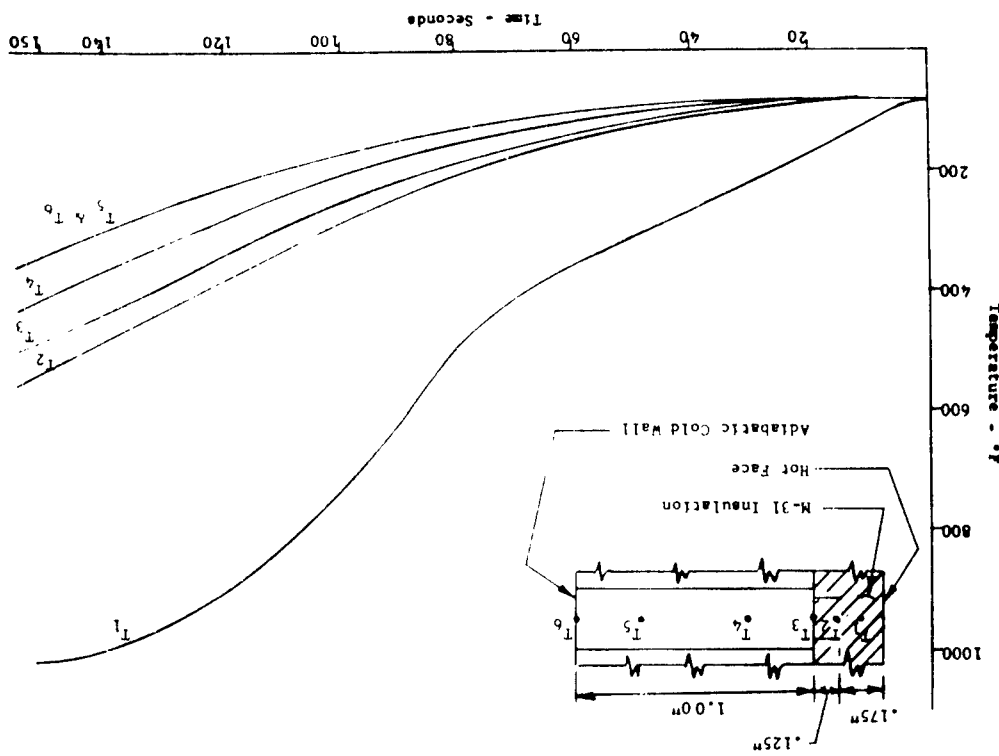
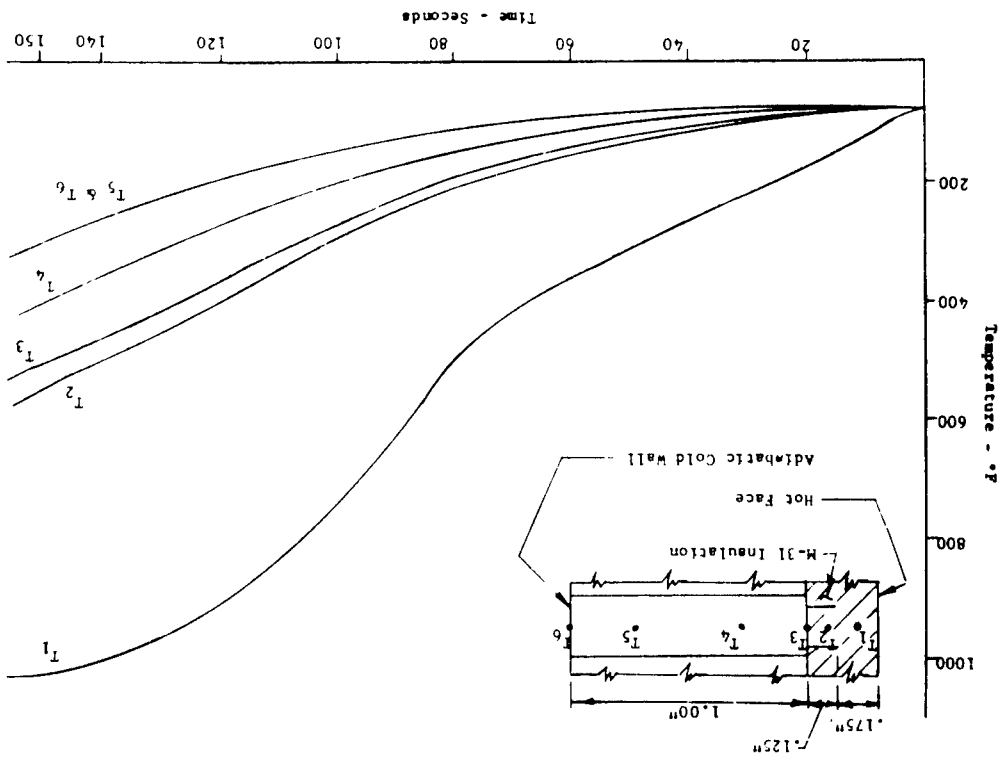


Figure 12 Temperature Profiles, Panel No. 30M12571  
.005 Inch Node Pitch - Cell Size 3-15  
Open Core Size, B-15



31

33

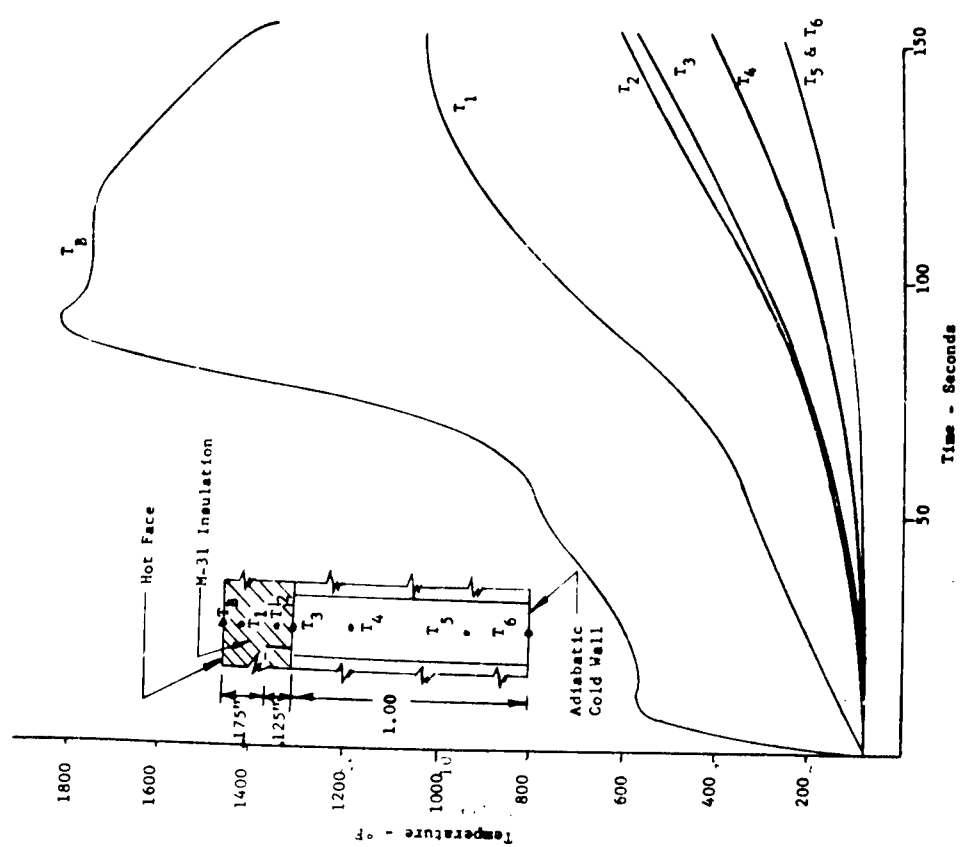
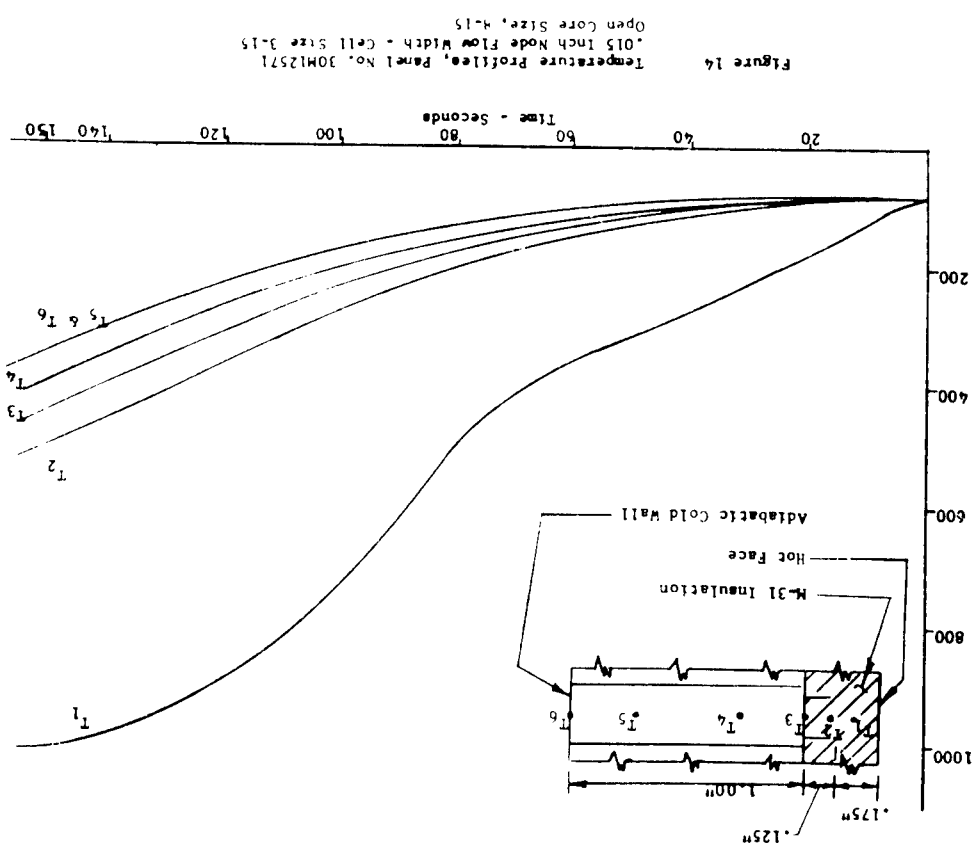


Figure 15  
Temperature Profiles - Panel No. 30M12571  
Zero Node Flow - Cell Size 4-15  
Open Core Size, H-15

34

35

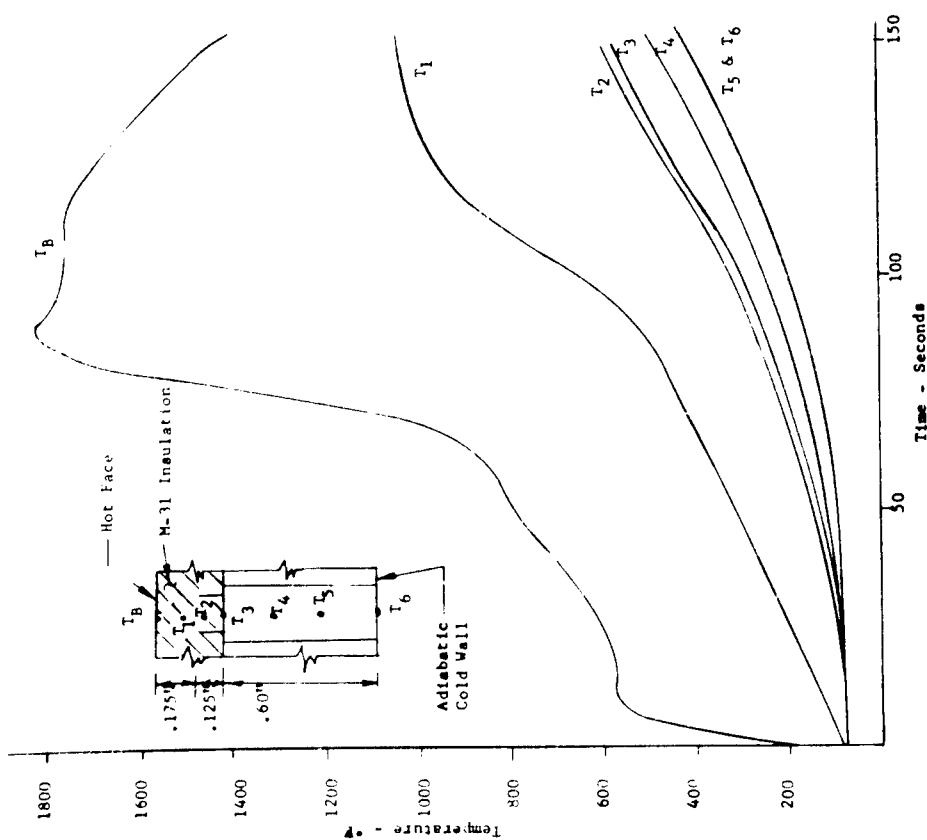


Figure 16    Temperature Profiles - Panel No. SK 60B20001  
Zero Node Flow - Cell Size 4-15  
Open Core Size, 8-15

36

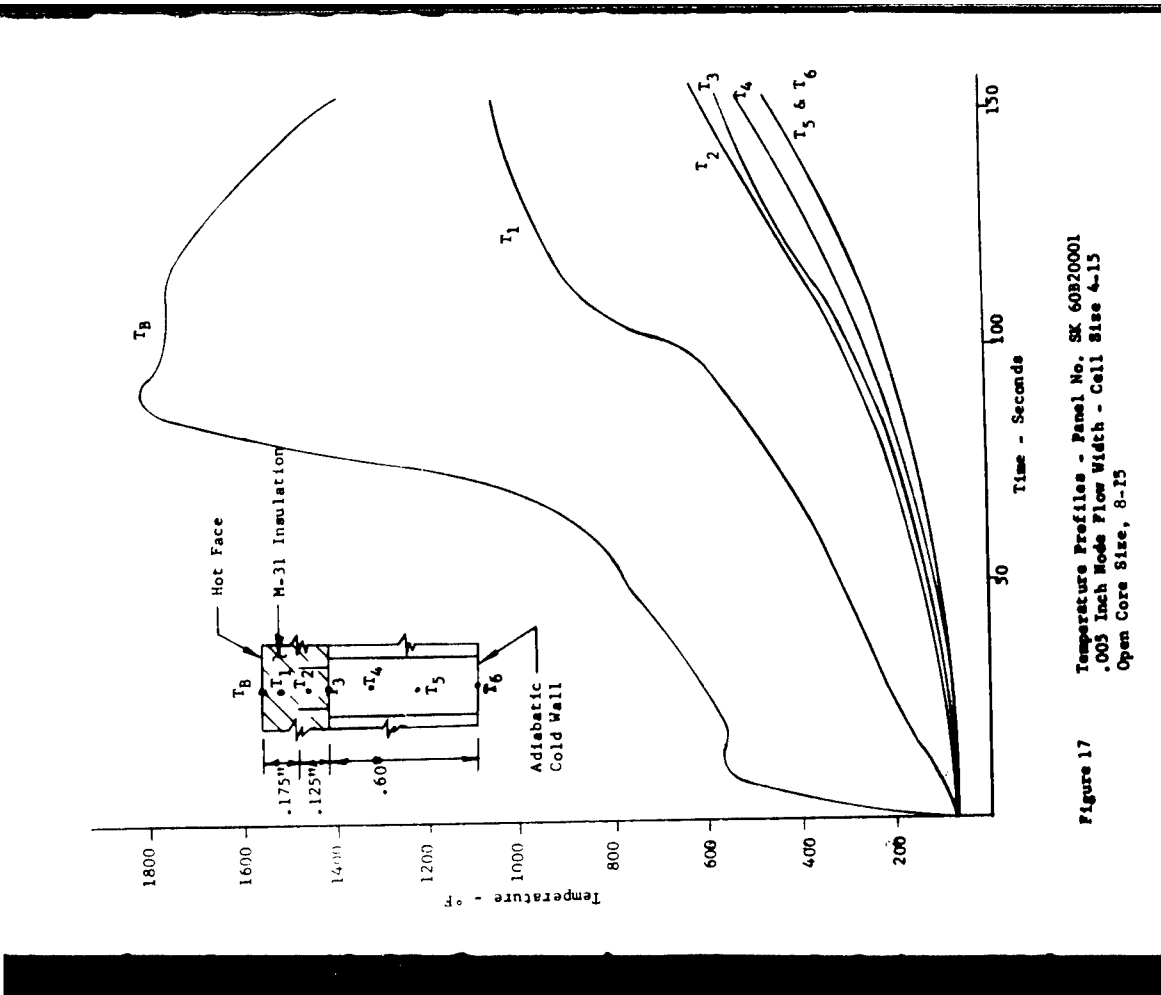
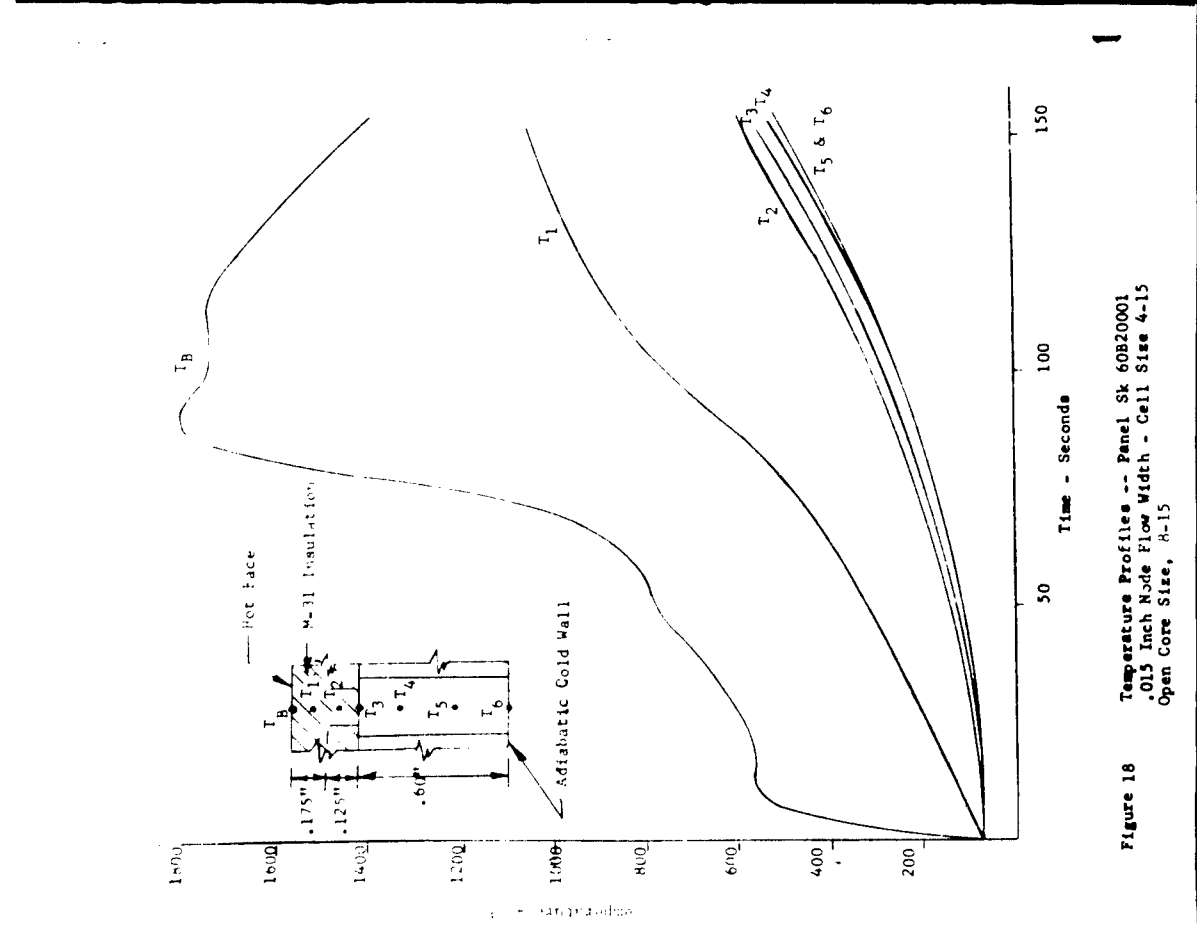
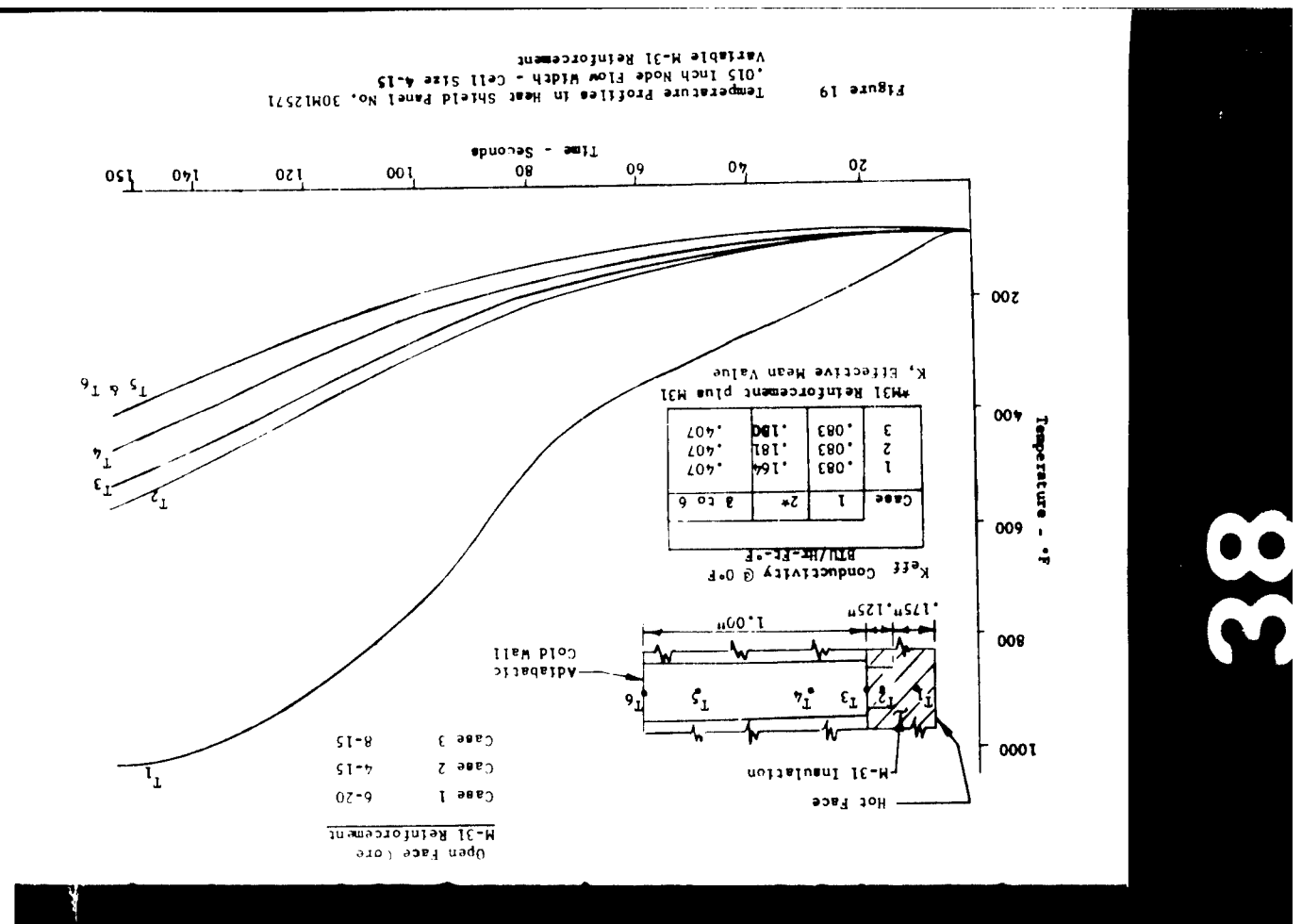


Figure 17    Temperature Profiles - Panel No. SK 60B20001  
.003 Inch Node Flow Width - Cell Size 4-15  
Open Core Size, 8-15

38



37

60

39

FIGURE 21  
Temperature Profile - Panel No. 30H12571  
Zero Node Flow - Cell Size 6-20  
Open Core Size, B-15  
.005 Inch Node Width - Cell No. 30H12571

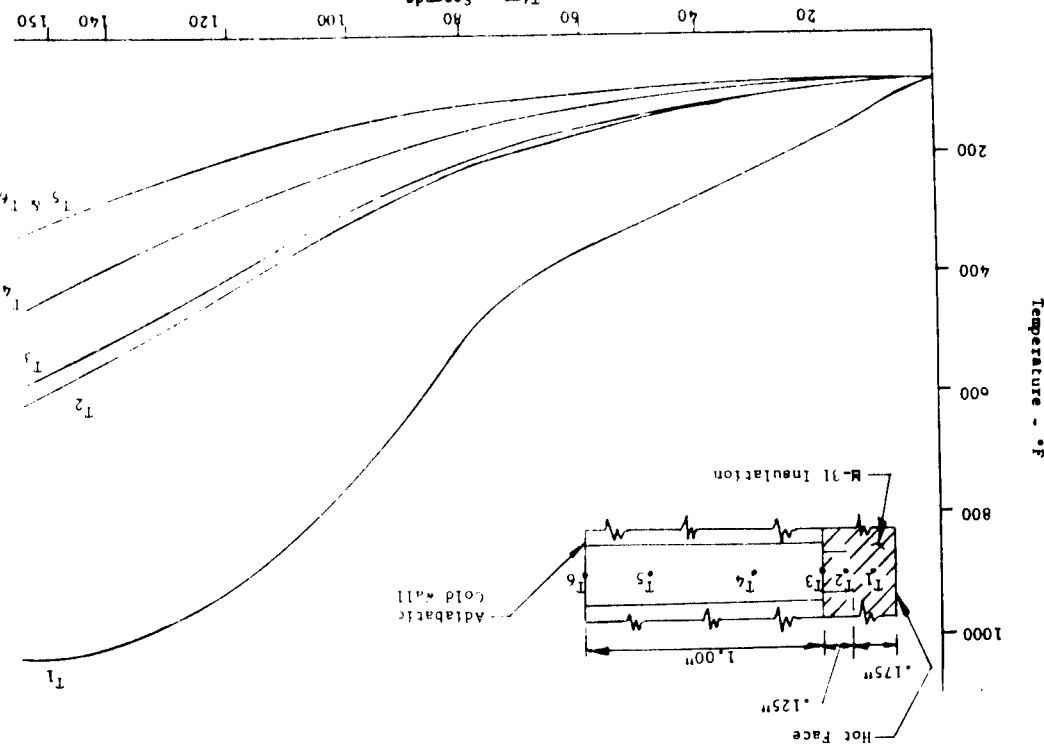
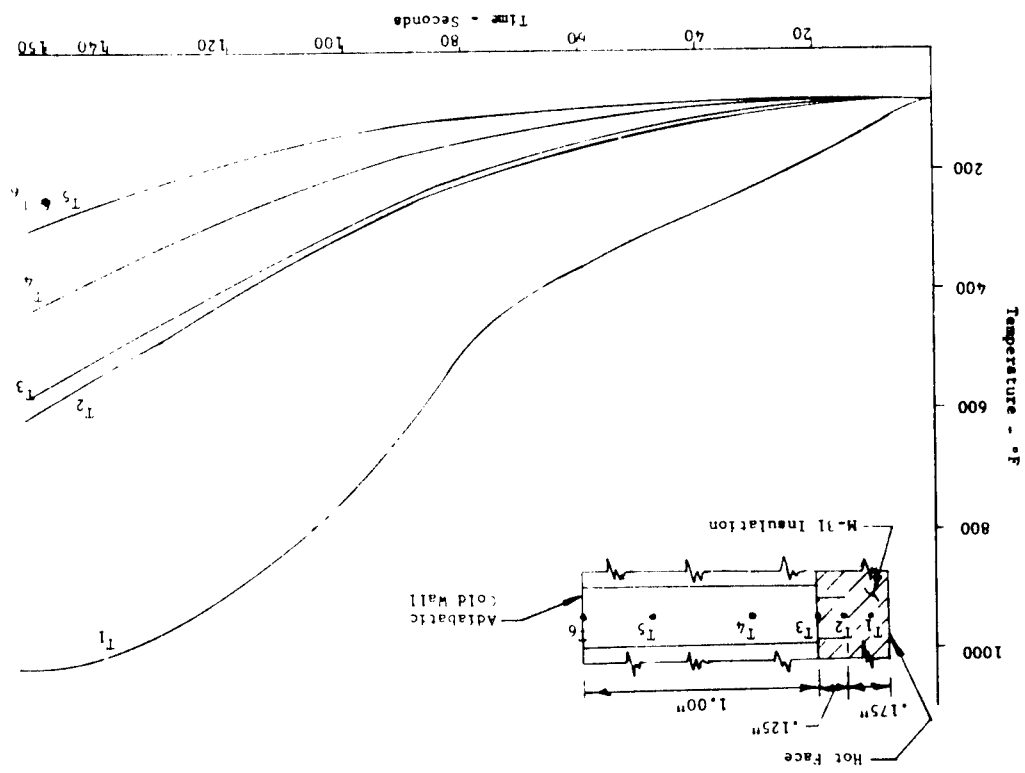


FIGURE 20  
Temperature Profile - Panel No. 30H12571  
Zero Node Flow - Cell Size 6-20  
Open Core Size, B-15



42

41

Figure 23 Temperature Profiles - Panel No. 30M12571  
.015 Inch Node Flow Width - Cell Size 6-20  
Open Core Size, 6-20

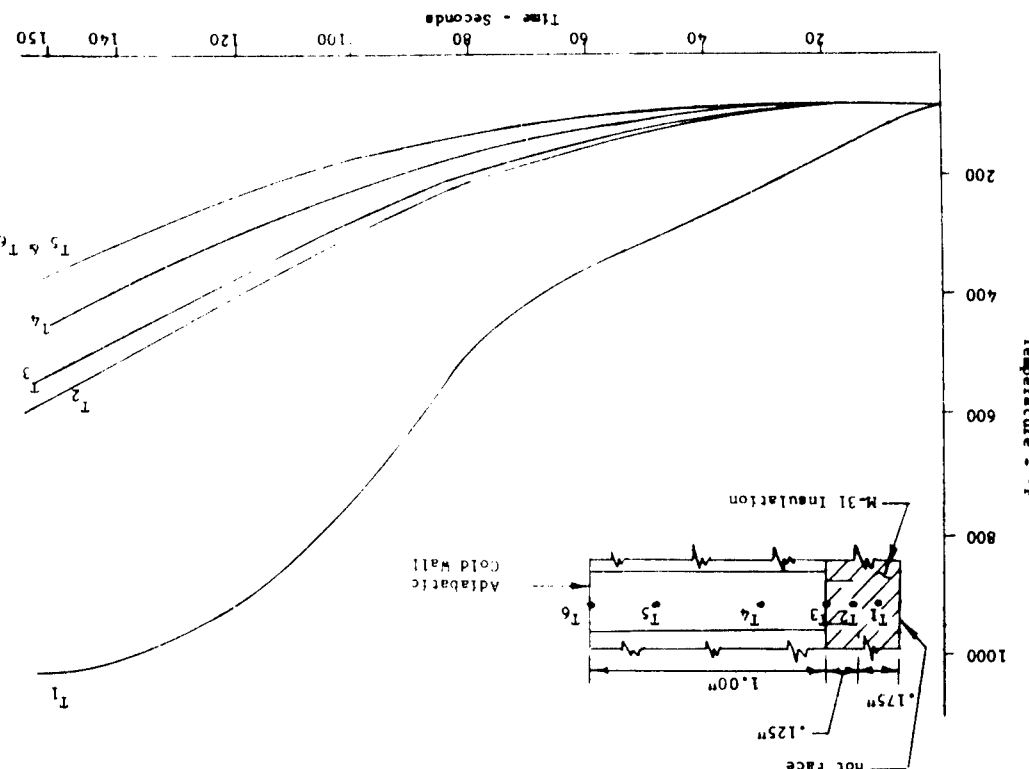
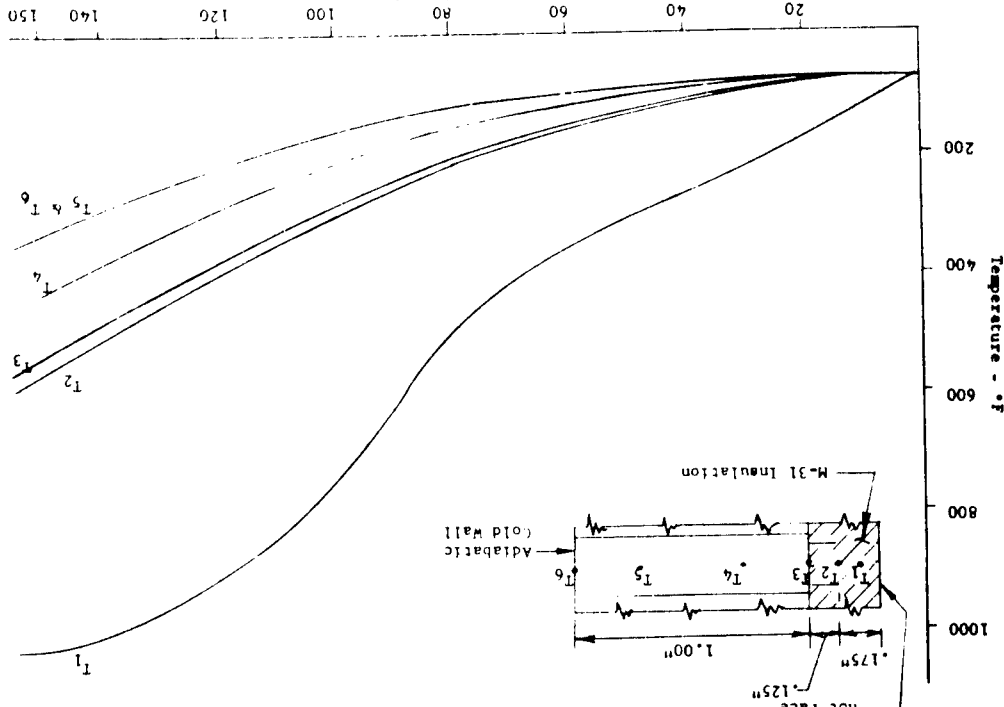


Figure 22 Temperature Profiles - Panel No. 30M12571  
.010 Inch Node Flow Width - Cell Size 6-20  
Open Core Size, 8-15



SECTION III

STRESS ANALYSIS FOR S-1C HEAT SHIELD PANELS  
30M12571 AND 60B20210

For small deflections within the elastic range, the sandwich heat shield panels behave as homogeneous plates when the proper modulus of rigidity is used. An approximate formula for  $D$  which has been used for all calculated data is:

$$D = \frac{E_1 E_2 h_f (h_c + h_f)}{(E_1 + E_2) (1 - v^2)}$$

This expression assumes both facings to be of the same material and thickness, and thin compared to the height of the core.

Three panels were considered: the see panel 30M12571,  $h_c=1.0"$ ; the two cup panels 60B20210, with  $h_c=0.6"$  and 1.0". Each panel was calculated for every reasonable combination of conditions. The results are shown in Tables 4 through 7.

Table 3 lists all the pertinent stress functions as they apply to the heat shield panels. Formulas taken from Timoshenko have had the various series in his expressions evaluated for the maximum value for a square for either the edge or center as required.

Table 4 shows the calculations for the simple support condition on the cup panels, 60B20210. The most severe loading occurs at the center for the maximum  $\Delta T$  and is 79,524 psi and 63,416 psi for the two thicknesses, respectively. Since the allowable for the maximum  $\Delta T$  is 140,000 psi\*, there is an adequate margin of safety.

Table 5 shows the fully clamped condition for the same panels. Here, the maximum stress occurs at the edge and is 97,885 psi and 81,099 psi for the two panels, respectively, at the maximum  $\Delta T$ . Again, an adequate margin of safety is indicated.

It is easily recognized that in actual practice neither of the above two edge mounting conditions represent the physical picture. The panel loading imposes a stress condition on the flange and insulation both of which are elastic materials. Table 6 considers the flexibility of the panel, flange and the JM-146 insulation as a system. The per cent of edge fixity was calculated and tabulated for the various conditions for the two panels, and presented in Table 6.

\* $f_{t,y} = 170,000$  psi at room temperature, Ref. MIL-HDBK-5

43

(TYPE 6-20 Honeycomb Core)											
Panel	Honeycomb Thickness	Honeycomb Cells	Honeycomb Node Flow Area	Node Flow Depth	#eff	Node Flow Width	Conductivity	Effective	Width	Node Flow Width	Area
.375	.002	2048	.011	.0002	.0007	.0016	5.6	.124	.43	.990	.112 .157 .237 .800
.188	.0015	4096	.016	.0007	.0028	.0064	8.3	.435	1.73	3.960	.199 .446 .768 .900
.25	.0015	2304	.012	.0004	.0016	.0036	6.2	.148	.99	2.23	.138 .245 .424 .800
(TYPE 4-15 Honeycomb Core)											
.188	.0015	4096	.016	.0007	.0028	.0064	8.3	.435	1.73	3.960	.199 .446 .768 .900
.25	.0015	2304	.012	.0004	.0016	.0036	6.2	.148	.99	2.23	.138 .245 .424 .800
(TYPE 3-15 Honeycomb Core)											
.188	.0015	4096	.016	.0007	.0028	.0064	8.3	.435	1.73	3.960	.199 .446 .768 .900
.25	.0015	2304	.012	.0004	.0016	.0036	6.2	.148	.99	2.23	.138 .245 .424 .800
(TYPE 6-20 Honeycomb Core)											
.375	.002	2048	.011	.0002	.0007	.0016	5.6	.124	.43	.990	.112 .157 .237 .800

TABLE 2 PANEL DIMENSIONS AND THERMAL CONDUCTIVITIES FOR PARAMETRIC STUDY											
Area of Honeycomb											
Cell Dimensions											
Panel	Honeycomb Thickness	Honeycomb Cells	Honeycomb Node Flow Area	Node Flow Depth	#eff	Node Flow Width	Conductivity	Effective	Width	Node Flow Width	Area
P01	Honeycomb Thickness	Honeycomb Cells	Honeycomb Node Flow Area	Node Flow Depth	#eff	Node Flow Width	Conductivity	Effective	Width	Node Flow Width	Area
	Sq. Ft.	Sq. Ft.	Sq. Ft.	in.	in.	in.	W/m-K	W/m-K	in.	in.	in.

45

Table 7 utilizes the edge fixities determined in Table 6 and tabulates the stress functions for both the edge and center conditions. The results show an appreciable reduction in maximum stresses in the center and a substantial reduction in edge stresses. It is believed that this result represents a realistic estimate of stresses to be expected in the 60B2020 panel. The 1.0" thick panel meets the maximum deflection criteria of 0.5" for all conditions under 280 °F. The maximum deflection, 1.441" inch at a  $\Delta t$  of 45° indicates that the M-31 would be cracking and probably breaking off from vibration. Since there is now relatively good indications of appreciable cooling on the back face of the heat shield, the maximum  $\Delta t$ 's are more probable for the terminal flight condition.

If the M-31 deflection values obtained for the radius of curvature at cracking for the M-31 insulation material is extrapolated, it is found that the probable cracking deflection on these panels is about 0.8". Thus, it appears that the crack would not start until the latter stages of the flight and probably would be of no actual significance.

Table 8 shows the panel calculations for the mounted 30M1251 unit 1.0" thick. The zee mounting approximates a simple support condition and all panel calculations for this table are based on the assumption of ample support for the panel edges. The maximum deflection is seen to be less than that for the comparable cup panel (the 1.0") by about a tenth of an inch.  $\Delta t = .751"$  for 450 °F. Thus, the danger of cracking and flaking off of the M-31 is lessened. Further, the maximum stresses are only nominally greater than the cup panel (elastic support) at maximum  $\Delta t$  and less at zero  $\Delta t$ . The zee mounting is better able to withstand shock than the cup panel mounting as it is essentially a cantilever spring. The damping effect of the zee mounting on vibration is significant whereas vibration loads add directly to the possibility of exceeding the core crushing load at the cup area on the 60B2020 panel.

Table 9 shows the calculations for the edge member for the zee type mounting of the 30M1251 panel. The  $h_2$  shown is the thickness of the edge member and extended facing to which it is brazed during manufacture. Although the 30M1251 design called for a combined  $h_2 = 0.050 + .010$ , it is seen that the maximum stresses do not exceed the allowable (140,000 psi  $\Delta t = 450^\circ$ ) except for  $h_2 = 0.30$  and  $0.20"$ . Thus, an appreciable weight saving could be effected by using an  $h_2 = .040"$ . This thinner edge member would also increase the vibration damping effect over the present design.

All calculations in the tables are based on the following data and procedures.

The 165 db noise level was converted to an equivalent pressure of 0.72 psf. This noise loading was used (for both ignition and flight) as an equivalent moment of 102.8 inch pounds per inch. It was assumed to be uniformly distributed over the panel surface for the fully clamped condition; a maximum at the center and zero at the edge for the simply supported condition.

\* Ref: NASA memorandum M-P&VE-PH 217-63, Aug. 16, 1963, Figure 5.  
\*\* Ref: S-IC Base Heat Shield Design Criteria

\*Ref: NASA correspondence M-P&VE-SB 3/15/63.

46

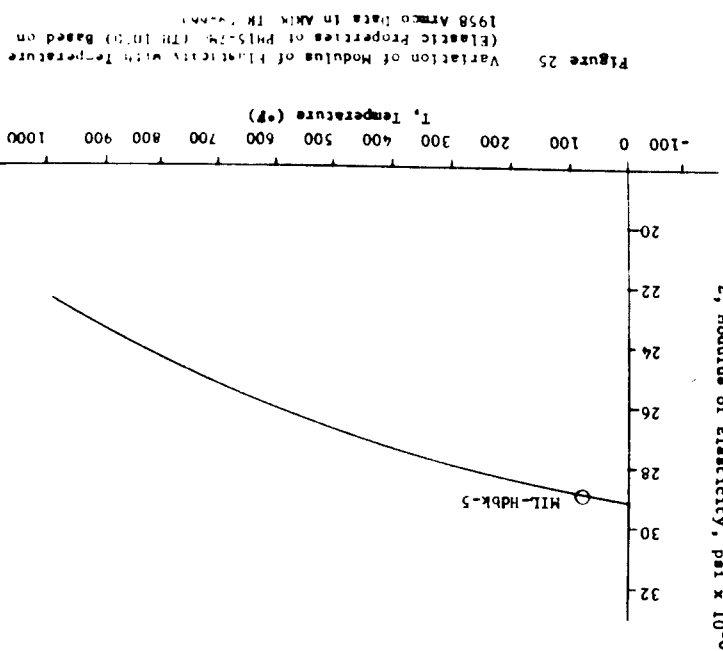
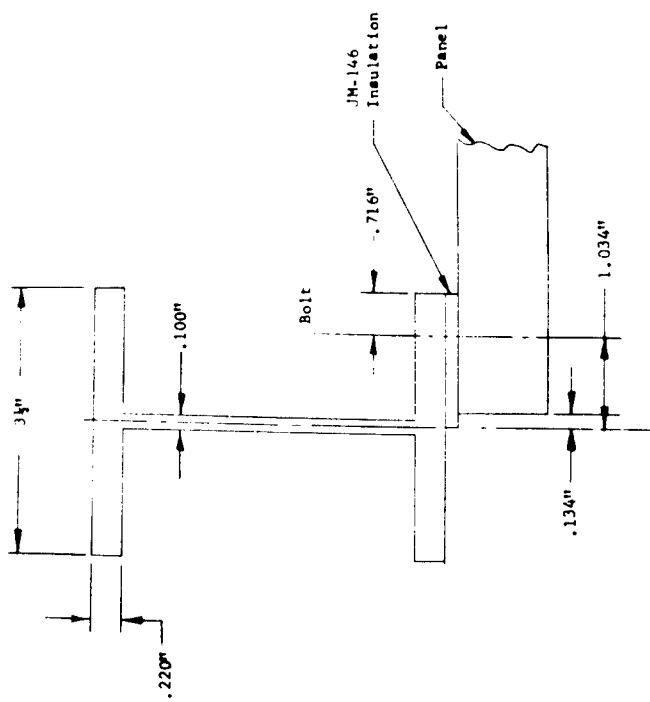
NOMENCLATURE SYMBOLS AND UNITSNOMENCLATURE SYMBOLS AND UNITS (Cont'd)

A	Area, square inches	RT	Room Temperature
a	Panel width, inches	T	Temperature - $^{\circ}$ F
b	Panel length, inches	$\Delta T$	Temperature difference, $^{\circ}$ F; subscript, temperature difference, F
C	Center	V	Edge reaction force, pounds per inch
c	subscript, core	w	Deflection, inches
D	Modulus of rigidity, inch pounds	x	Axis
E	Young's Modulus, psi	y	Axis
$E_m$	Average of two values of Young's modulus	z	Subscript, zee edge member
E.F.	Edge Fixity	$\alpha$	Temperature coefficient of expansion, in/in/ $^{\circ}$ F
F	Flange, subscript	$\epsilon$	Strain, microinches per inch
f	Stress, psi; subscript, facing	$\theta$	Rotation of panel edge, Radians
$f_{tu}$	Tensile ultimate strength, psi	$\Delta\theta$	Differential rotation of zee edge member, $\Delta\theta = \theta_1 - \theta_2$
$f_y$	Tensile yield strength, psi	$\nu$	Poisson's Ratio
h	Thickness, inches; corr height, inches	$\sigma$	Stress, psi
I	Moment of inertia; insulation; subscript, insulation		
K	Spring constant, in-pounds/ $^{\circ}$ rotation		
L	Length, inches		
M	Moment, in-pounds/in.		
$M_{\Delta\theta}$	Differential moment due to $\Delta\theta$		
P	Subscript, panel		
q	Unit pressure loading, psi; subscript, unit pressure loading, psi		
Q	Shear, lbs/in		
R	Corner reaction force, pounds; radius, inches		

49

50

Figure 24 Mounting System for 60520210 Panel  
Showing Calculation Dimensions Only



MAXIMUM VALUES FOR 60820210 PANEL  
SIMPLY SUPPORTED EDGE CONDITION

54

35

TABLE 5

Iteration

TABLE 5

Iteration

9 TIME



## TABLE Q

MAXIMUM BENDING STRESSES IN ZEE MEMBER  
FOR 30R12571 PANEL, ZEE EDGE MEMBER 1.0" CORE THICKNESS

$q_p$	Ignition Condition					$h_z = .020$
	$h_z = .060$	$h_z = .050$	$h_z = .045$	$h_z = .040$	$h_z = .030$	
$l_z$	18-6	10.42-6	7.59-6	5.34-6	2.25-6	$h_z = .020$
$q_p$	.0254	.0503	.0870	.1192	.1694	$h_z = .020$
$\Delta\theta$	-0.0249	-0.0616	-0.0938	-0.1440	-0.3768	-1.3580
$M_q$	52.58	52.58	52.58	52.58	52.58	52.58
$M_{\Delta\theta}$	13.58	19.45	21.57	23.30	25.70	26.40
$M_{total}$	39.00	33.13	31.01	29.28	26.88	25.68
$c_2$	65,000	79,486	91,927	109,663	179,200	385,200
Flight Condition						
$q_p$	.0203	.0363	.0510	.0708	.1680	.5670
$h_z$	21.23	21.23	21.23	21.23	21.23	21.23
$\Delta\theta = 0^\circ \Delta T$	.0103	-.0100	-.0260	-.0605	-.1577	-.5567
$180^\circ$	.0268	+.0065	-.0095	-.0242	-.0440	-.1412
$280^\circ$	.0360	+.0157	-.0003	-.0150	-.0148	-.1320
$320^\circ$	.0397	+.0194	+.0034	-.0113	-.0111	-.1283
$450^\circ$	.0516	+.0153	+.0006	+.0006	-.0192	-.1164
$M_{total}$	-5.45	-8.21	-9.36	-9.79	-10.75	-11.25
$M_{total} \Delta T$	+3.54	-3.00	-5.59	-7.12	-9.63	-10.91
$180^\circ$	8.56	-0.56	-3.45	-5.63	-9.00	-10.93
$280^\circ$	10.58	+1.07	-2.60	-5.03	-8.75	*10.65
$320^\circ$	17.07	4.83	+0.14	-3.11	-7.94	-10.41
$450^\circ$						
$M_{total} \Delta T$	15.78	13.02	11.87	11.44	10.48	9.98
$180^\circ$	24.77	18.23	15.66	14.11	11.60	10.32
$280^\circ$	29.79	21.14	17.78	15.60	12.23	10.50
$320^\circ$	31.81	22.30	18.63	16.20	12.48	10.58
$450^\circ$	38.30	26.06	21.37	18.12	13.29	10.82
$\Delta\theta = 0^\circ \Delta T$	26,289	31,235	35,183	42,343	69,860	149,700
$180^\circ$	41,267	43,734	46,416	52,844	77,326	154,800
$280^\circ$	49,630	50,715	52,700	58,422	81,525	159,500
$320^\circ$	52,995	53,498	55,219	60,669	83,192	158,700
$450^\circ$	63,808	62,518	63,341	67,859	88,591	162,300

NOTE: The value of the moment arm  $a$  used for the zee calculations was 0.057m, the distance from center line of mounting hole to the vertical leg of the zee.

## SECTION III

DESIGN PARAMETERS FOR BRAZED HONEYCOMB HEAT SHIELD PANELS  
WITH SIMPLY SUPPORTED EDGES

## Air Load Deflection

Figure 26 shows the deflection at the center of panel versus core thickness for an air load  $q$  of 2.7 psf, for the ignition condition. This graph can be used for determining the face sheet thickness and core thickness for a given deflection.

## Thermal Deflection

Figure 27 shows thermal deflection at center of panel versus height of panel for various temperature differences. This graph shows the thermal deflection pattern for constant temperature differences. The lower panel height gives the greater influence on deflection.

## Combined Deflection

Figures 28 and 29 show the combined thermal and air deflections versus height of panel for constant temperature difference, air load, and face sheet thickness, and also give deflection for constant air load without temperature differences.

Figure 30 shows the same information as Figures 28 and 29, but is plotted in a different form to show the pattern of the temperature difference.

60

FIGURE 27 Thermal Deflection at Center of Panel vs. Height of Panel for Constant Temperature Differences

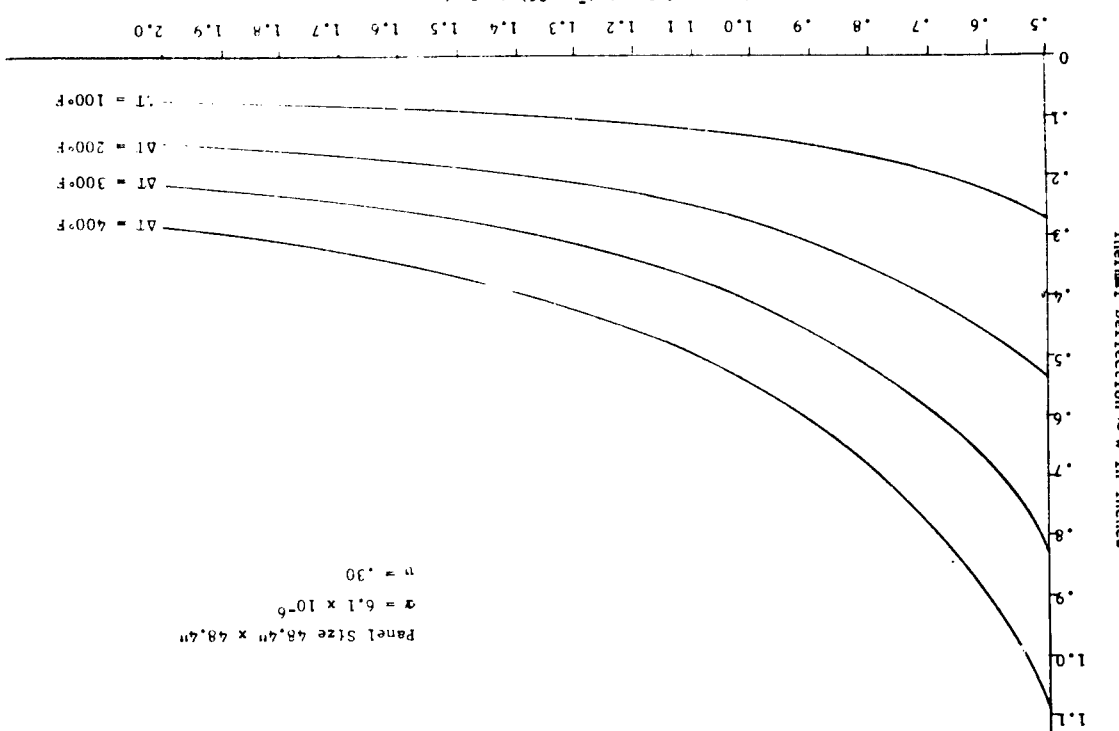
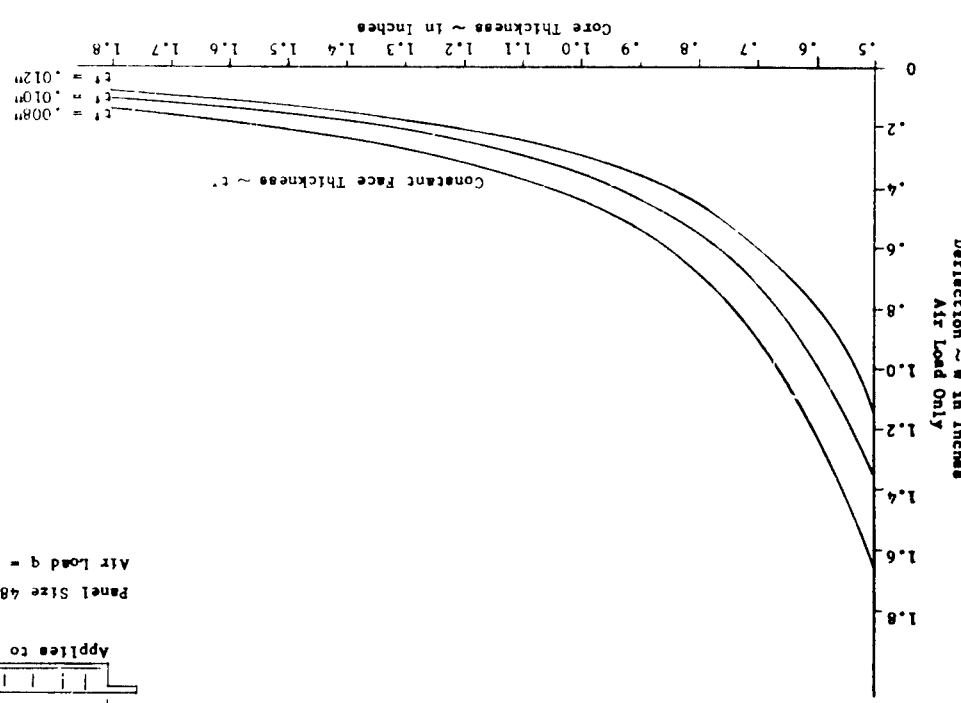
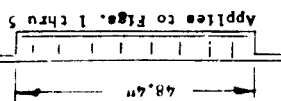


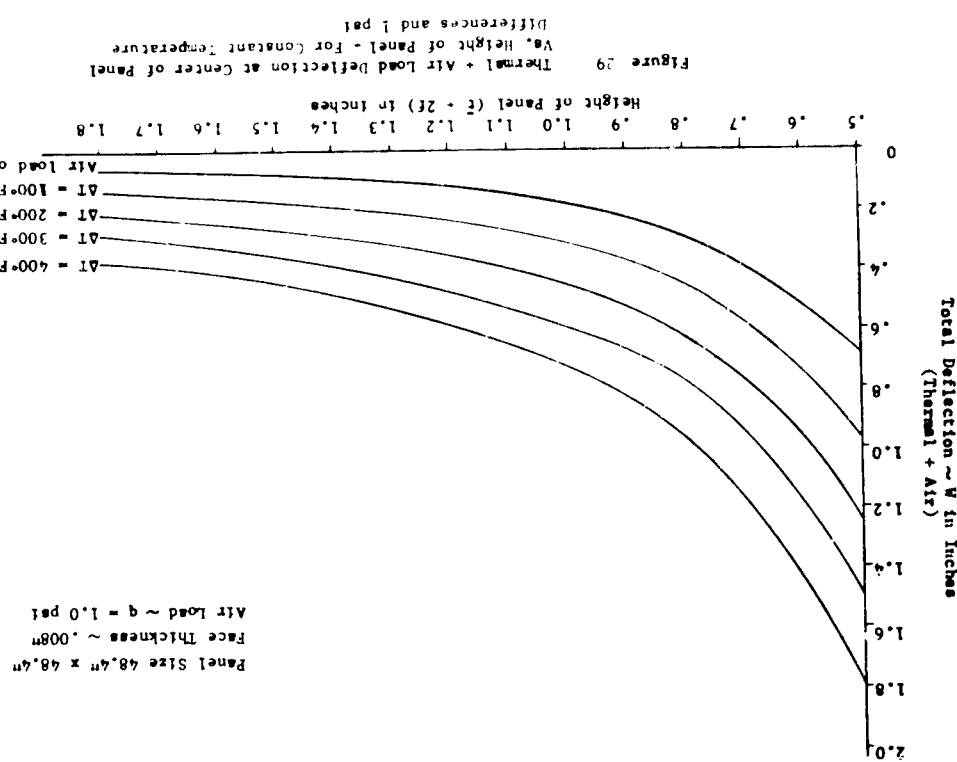
FIGURE 26 Deflection at Center of Panel vs. Core Thickness



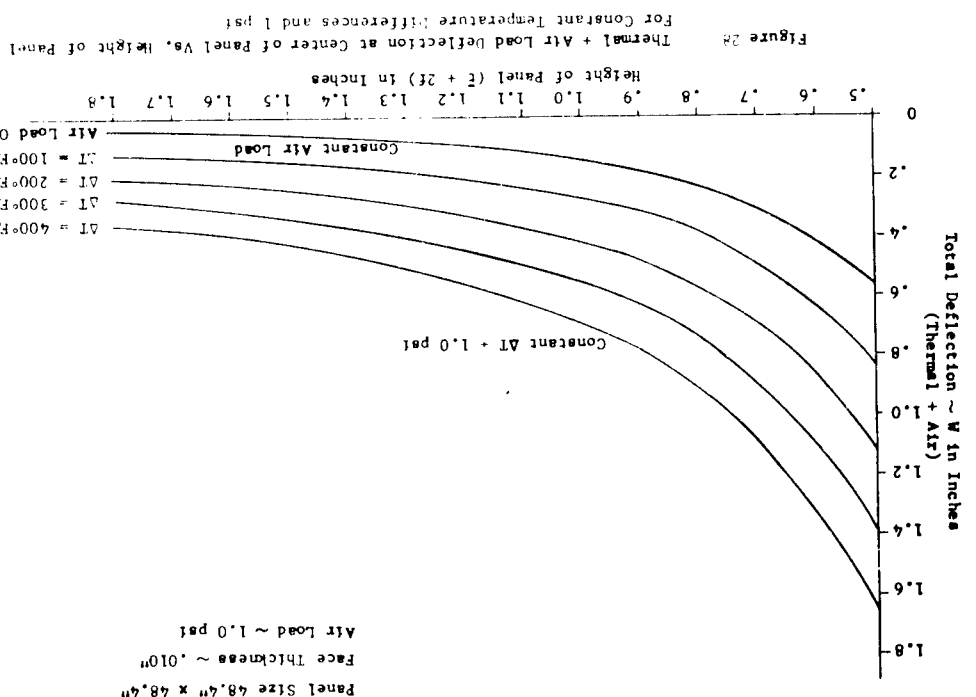
59



62



61



SECTION IVAPPLICATION OF BERYLLIUM TO HEAT SHIELD PANELSPreliminary Analysis of Zee Section Edge Member  
Heat Shield Panel with Beryllium Facing and Edge Members

The use of cross rolled beryllium sheet components for facings and edge members were evaluated for potential heat shield panel application using the JOK12571 panel design as a basis.

Panel stresses, deflections and margins for the ignition and flight conditions are given in Table 10. The critical item from a stress view point is the relatively high stress in the zee section edge member which would require a minimum thickness of .08".

The allowables for silver braze beryllium sheet employed were:

$$f_{t_u} = 50,000 \text{ psi}$$

$$f_{t_y} = 35,000 \text{ psi}$$

$$\% \text{ Elongation} = 1.2\%$$

and reflect our experience in beryllium brazing and fabrication\*. These values for .04" gauge material are substantially less than the allowables for unbrazed beryllium sheet, which presently are:

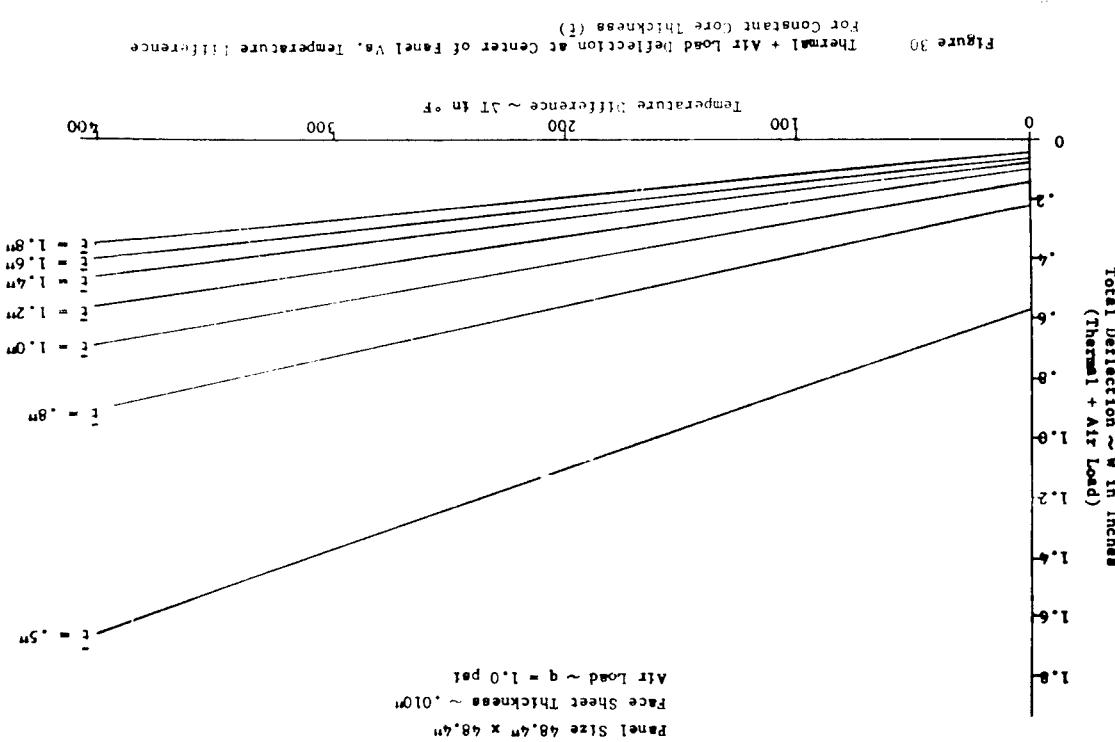
$$f_{t_u} = 70,000 \text{ psi}$$

$$f_{t_y} = 50,000 \text{ psi}$$

$$\% \text{ Elongation} = 5\%$$

The reduction in strength and loss of ductility results principally from the reaction between the beryllium and the silver brazing alloy (99.5Ag-5Li) and cannot be eliminated or further minimized with presently available braising methods or brazing alloys within the current state of art. Current studies being conducted at Aeroneca are aimed at the development of low melting braze alloys for beryllium. A reduction of braze temperatures below recrystallization and diffusion temperatures would overcome many of the problems which cause embrittlement and loss of strength. The braze alloy compositions which show the greatest promise in this regard would either be zinc base or aluminum base with zinc additions.

\*Contract AF 33(657)-715;  
Sheet Beryllium Composite Structures



65

66

TABLE 10  
DEFLECTION AND STRESS CHARACTERISTICS OF THE 30M12571 PANEL DESIGN  
WITH BERYLLIUM EFFECTS AND EDGE MEMBERS

Load Condition	Panel Configuration	at Centre	Packing Stress	Thickness Stress	Stress $\sigma_{xy}$	M.S.*
<b>WEDGE</b>						
1.0m Core 0.23m 0.370 part E (edge)	13,816 part C (center)	.02 47,260 813 -.33	20,187 part E 0.216m 0.096m	12,791 part C 0.071m 0.071m	.02 42,100 11,063 -.24	.02 44,860 0.286 -.22
1.0m Core .03m Be Faces .6m Edge Members	39,930 1.069 -.26	.03 43,130 1.069 -.26	38,935 1.060 -.18	.03 36,450 1.060 -.18	.03 35,210 1.066 -.18	.03 33,260 2.310 -.04
1.0m Core .03m Be Faces .6m Edge Members	37,350 1.067 -.20	.04 39,930 1.067 -.20	37,350 1.067 -.20	.04 36,450 1.067 -.20	.04 35,210 1.066 -.18	.04 33,260 2.310 -.04
1.0m Core 0.23m 0.370 part E (edge)	31,850 2.654 +.00	.08 31,080 2.590 +.02	32,590 2.245 -.02	.05 34,350 1.917 -.07	.05 35,210 1.917 -.10	.05 36,450 1.917 -.13
1.0m Core 0.216m 0.096m	31,850 2.654 +.00	.07 31,080 2.590 +.02	32,590 2.245 -.02	.06 32,590 2.245 -.02	.06 33,430 0.579 -.10	.06 35,210 0.579 -.16
1.0m Core .03m Be Faces .6m Edge Members	33,430 0.579 -.10	.03 40,950 0.376 -.223	35,210 0.376 -.223	.03 35,210 0.376 -.223	.03 33,430 0.579 -.10	.03 31,720 0.809 +.002
1.0m Core 0.071m 0.071m	35,210 0.376 -.223	.02 35,110 .322 -.09	32,590 -.23 +.23	.02 32,590 -.23 +.02	.02 32,590 -.23 +.02	.02 31,720 0.809 +.002
<b>IGNITION</b>						
2.7 part, Zero AT	9,806 part C (center)	.02	44,860 0.286 -.22	44,860 0.286 -.22	44,860 0.286 -.22	44,860 0.286 -.22
1.0m Core .03m Be Faces .6m Edge Members	40,950 0.376 -.223	.03	40,950 0.376 -.223	40,950 0.376 -.223	40,950 0.376 -.223	40,950 0.376 -.223
1.0m Core 0.071m 0.071m	44,860 0.286 -.22	.02	44,860 0.286 -.22	44,860 0.286 -.22	44,860 0.286 -.22	44,860 0.286 -.22

TABLE 11

DEFLECTION AND STRESS CHARACTERISTICS OF THE 30M12571 PANEL DESIGN  
WITH BERYLLIUM EFFECTS AND EDGE MEMBERS

Load Condition	Panel Configuration	at Centre	Packing Stress	Thickness Stress	Stress $\sigma_{xy}$	M.S.*
<b>WEDGE</b>						
1.0m Core 0.23m 0.370 part E (edge)	13,816 part C (center)	.02 47,260 813 -.33	20,187 part E 0.216m 0.096m	12,791 part C 0.071m 0.071m	.02 42,100 11,063 -.24	.02 44,860 0.286 -.22
1.0m Core .03m Be Faces .6m Edge Members	39,930 1.069 -.26	.04 39,930 1.069 -.26	37,350 1.067 -.20	.04 36,450 1.067 -.20	.04 35,210 1.066 -.18	.04 33,260 2.310 -.04
1.0m Core 0.216m 0.096m	31,850 2.654 +.00	.08 31,080 2.590 +.02	32,590 2.245 -.02	.05 34,350 1.917 -.07	.05 35,210 1.917 -.10	.05 36,450 1.917 -.13
1.0m Core 0.216m 0.096m	31,850 2.654 +.00	.07 31,080 2.590 +.02	32,590 2.245 -.02	.06 32,590 2.245 -.02	.06 33,430 0.579 -.10	.06 35,210 0.579 -.16
1.0m Core 0.071m 0.071m	35,210 0.376 -.223	.02 35,110 .322 -.09	32,590 -.23 +.23	.02 32,590 -.23 +.02	.02 32,590 -.23 +.02	.02 31,720 0.809 +.002
<b>IGNITION</b>						
2.7 part, Zero AT	9,806 part C (center)	.02	44,860 0.286 -.22	44,860 0.286 -.22	44,860 0.286 -.22	44,860 0.286 -.22
1.0m Core .03m Be Faces .6m Edge Members	40,950 0.376 -.223	.03	40,950 0.376 -.223	40,950 0.376 -.223	40,950 0.376 -.223	40,950 0.376 -.223
1.0m Core 0.071m 0.071m	44,860 0.286 -.22	.02	44,860 0.286 -.22	44,860 0.286 -.22	44,860 0.286 -.22	44,860 0.286 -.22

TABLE 10

DEFLECTION AND STRESS CHARACTERISTICS OF THE 30M12571 PANEL DESIGN  
WITH BERYLLIUM EFFECTS AND EDGE MEMBERS

Other characteristics of beryllium which make it undesirable for braced heat shield panels are:

1. The high modulus, 43,000,000 psi, while desirable for stiffness is undesirable for thermal loads which produce a high thermal moment. The high moment along with the relatively low strength of beryllium soon produces stresses comparable to the yield or ultimate of the material.
2. The highly directional tensile properties of beryllium sheet, with low ductility in the short transverse direction, results in sharply limited and unpredictable capacity to accept multi-axial loads without catastrophic failure. Consequently, an extensive test program would be required to support a production design.
3. The maximum width sheet at present is .36" which would require a load carrying splice. The poor welding characteristics of beryllium and erratic joint properties preclude the use of fusion welding; consequently, the facing sheet splices would have to be accomplished during the panel braising and would consist of a butt joined sheet with a braised on doubler reinforcement. For the open faced core side of the panel, the reinforcing doubler would probably have to be located in a rabbit machined in the load bearing honeycomb core (at increased cost).
4. The susceptibility of beryllium sheet in the large sizes required and in gages less than .04" to breakage during shop handling imposes additional fabrication problems.
5. An experimental program to determine the material allowances for braced beryllium sheet for a range of thicknesses would be required as well as an optimum braising cycle for beryllium panels of this size (.53" x .53").

As a consequence of the foregoing considerations, the use of beryllium sheet is not recommended for braced, honeycomb sandwich heat shield panels within the present state of art.

Preliminary Analysis of Heat Shield Panel with  
Beryllium Facings and Cup Type Edge Attachment  
per drawing 60B20210

The use of cross rolled beryllium sheet facings was evaluated for potential use in the cup type edge heat shield panel design shown in NASA drawing No. 60B20210 based on the following assumptions:

1. A facing gage of .030" beryllium sheet, load bearing core Type 4-15 PH 15-7 Mo 1.0" thick

2. Allowables for brazed beryllium sheet using a brazing alloy of fine silver with 0.5" lithium.

$$f_{t_u} = 50,000 \text{ psi}$$

$$f_{t_y} = 35,000 \text{ psi}$$

$$\% \text{ Elongation in } 2^{\text{in}} = 1.24\%$$

$$E = 43 \times 10^6 \text{ psi at R.T.}$$

$$E = 37 \times 10^6 \text{ psi at } 600^{\circ}\text{F}$$

$$v = 0.1$$

Panel stresses, deflections and margins were calculated for the flight conditions at four levels of edge fixity and are given in Tables 1, and 13. The compressive stresses in the honeycomb core area under the cup flange were also calculated for the same loading conditions and three levels of edge fixity (Tables 14 and 15).

Based on any degree of edge fixity and 180° ΔT representative of the 100°F node flow condition this panel design shows positive margins for .030" beryllium sheet facings. As the thermal gradient increases, the margins decrease rapidly as shown in Table 13 for a 320°F ΔT representative of the zero node flow condition; however, small positive margins exist for most of the edge fixity conditions. Consequently, the use of beryllium facings of cross rolled beryllium sheet .030" thick appear feasible from a stress viewpoint for this panel design. However, the use of beryllium sheet facings in this application is subject to the same qualifications (Items 1 thru 5) previously noted and is not considered to be a suitable material for braided honeycomb sandwich heat shield panels.

Compression load on insulation (JH-146)

$$\frac{P}{A} = \frac{M}{G \cdot I \cdot W} = \frac{16}{.6 \times .9 \times 1} = 30 \text{ psi}$$

Simply Supported Edge Condition

$$W_A = \frac{.00006 \times 1.0 \times 30.978}{624,018} = .00447$$

$$W_T = \frac{.017(1+\eta)^{4.2}}{\pi h} = \frac{6.0 \times 10^{-6} \times 1.0 \times 30.978 \times .5708}{32.86654}$$

$$W_T = .2147$$

$$W_{TOTAL} = .2587$$

69

70

OF THE 60B20210 PANEL DESIGN WITH BERYLLIUM, PAGE 13  
DEFLECTION AND STRESS CHARACTERISTICS

TABLE 12

Load Condition - Flange 10 psi + 180°. AT

	Deflection	W (inches)	Deflection Moment M (in-lb)	Bearing Stress $f_b$ (psi)	Margin of Safety	M, S.
100%	.012	832E	26,926E	+0,18		
94.91	0,172	286C	9,256	+2,44		
*1.927	0,253C	431C	13,948	+1,28		
		168	19,968	+0,59		
		617E	14,207	+1,24		
0%	0,258C	439C	20,356	+0,56		

Materials: Beryllium, Room Temperature, After Brazing  
(Facning) (Cu 50,000 psi  
Flange 35,000 psi  
Margin of safety is normal to panel surface.

M.S. based on a load factor of 1.1 and yield strength.

\* Beam flanges, flange insulation and panel rotate.

Core: PH13-TM0 Material

(Cu 50,000 psi  
Flange 35,000 psi  
Margin of safety is normal to panel surface.

Materials: Beryllium, Room Temperature, After Brazing  
(Facning) (Cu 50,000 psi  
Flange 35,000 psi  
Margin of safety is normal to panel surface.

M.S. based on a load factor of 1.1 and yield strength.

\* Beam flanges, flange insulation and panel rotate.

OF THE 60B20210 PANEL DESIGN WITH BERYLLIUM, PAGE 13  
DEFLECTION AND STRESS CHARACTERISTICS

TABLE 13

Load Condition - Flange 10 psi + 1.15 psi dynamic (C.15 psi) plus 320° AT

	Deflection	W (inches)	Deflection Moment M (in-lb)	Bearing Stress $f_b$ (psi)	Margin of safety is normal to panel surface.	M, S.
100%	0,027	1530E	49,515E	-0,36		
34.91%	0,319	539C	17,443C	+0,82		
*2.514%	0,464	807C	26,117C	+0,22		
		38E	1,230E	+Very large		
		1091E	35,307E	-0,10		
0%	0,475	828C	26,796C	+0,19		

M.S. based on a load factor of 1.1 and yield strength.  
\* Beam flange, flange insulation and panel rotate.

Core: PH13-TM0 Material

(Cu 50,000 psi

Material: Beryllium, Room Temperature, After Brazing  
(Facning)

Moment is normal to panel surface.

M.S. based on a load factor of 1.1 and yield strength.

72

卷之三

5

8

1. Edge Fixity	Core	Compressive Stress	Core	Loadings Condition
in core area under edge fixity	alloimable stresses	(PH15-7M) Mortar(1)	100% beam flange	1.00 psi + 180° LAT
cup flange (psi)	(PH15-7M) Mortar(1)	7,371 psi	panel and flange tensile	100% mode follow
cup flange (psi)	(PH15-7M) Mortar(1)	7,371 psi	100% beam flange	1.00 psi + 180° LAT
alloimable stresses	alloimable stresses	(PH15-7M) Mortar(1)	panel and flange tensile	1.00% mode follow
Core	Core	RT-760 psi	RT-760 psi	RT-760 psi
600° - 675 psi	600° - 722 psi	600° - 722 psi	600° - 722 psi	600° - 722 psi
fur Type 4-15	core Ref. NASA	core Ref. NASA	core Ref. NASA	core Ref. NASA
Structural Design	Structural Design	Structural Design	Structural Design	Structural Design
Manufacture	Manufacture	Manufacture	Manufacture	Manufacture

$$M_A = .0479 q^2 = .0479 \times 1.0 \times \frac{50.978^2}{1.06} = 124.68 \text{ in-lbs/in at center of panel}$$

$$M_T = \frac{2 M(1-q^2)D}{h} = \frac{180 \times 1.0 \times 10^{-6} \times .50 \times 624.018}{1.06} = 629.43 \text{ in-lbs/in at edge of panel}$$

#### Clamped Edge Condition

$$W_A = \frac{.0137 \times Q \times a^4}{12 \times D(1-q^2)} = \frac{.0137 \times 1.0 \times 50.978^4}{12 \times 624.018 \times .99} = .012"$$

$$M_A = .0513 q a^2 = .0513 \times 1.0 \times 50.978^2 = 133 \text{ in-lbs/in at edge of panel}$$

$$M_T = \frac{2 \Delta T D (1-q^2)}{h} = \frac{6.0 \times 10^{-5} \times 180 \times 624.018 \times 1.0}{1.06} = 699 \text{ in-lbs/in at edge of panel}$$

$$M_{\text{total}} = 832 \text{ in-lbs/in at edge}$$

Then the edge moment of panel with 34.91% fixity is:

$$M = 832 \times .3491 = 290 \text{ in-lbs/in.}$$

Load reacted by cup:

$$P = \frac{290 \times 7.463}{.9} = 2405 \text{ lbs/cup}$$

Compression load on panel core:

$$\frac{2405}{.93593} = \underline{\underline{2570 \text{ psi}}}$$

Assume retention of panel, flange and insulation

Use  $K_F = .60^r$   $lb/in \cdot in^2$  (25-50 psi)

$$C = .60^r \quad l = .90^r \\ K_L = \frac{C k L^2}{2} = \frac{.6 \times 3086 \times .9^2}{2} = 750 \text{ in-lbs/in/Rad.}$$

$$K_F = .50 \text{ in-lbs/in/radian}$$

$$K_F = 19.11 \text{ in-lbs/in/radian}$$

$$K_1 = .50 \text{ in-lbs/in/radian}$$

$$Edge Fixity = \frac{36.753}{750} \cdot \frac{1}{19.711} = \frac{1}{51.47859} = 1.927.$$

$$M = K_F \times .01927 = 1.6 \text{ in-lbs/in}$$

Load reacted by cup:

$$P = \frac{16}{9} \times \frac{7.463}{.9} = 133 \text{ lbs/cup}$$

compression load on panel core:

$$\frac{133}{.93593} = 142 \text{ psi}$$

Detail calculation

<sup>(1)</sup> 100% survival factor and flight condition:  $T = 150^r$ ,  $q = 1.0 \text{ psi}$   
panel 50.928"  $\times$  1" of fasteners.

$$f_{t,y} = 35,000 \text{ psi}$$

$$f_{t,u} = 50,000 \text{ psi}$$

$$\alpha = 6.0 \times 10^{-6} (\text{RT}=500)$$

$$E = 4.3 \times 10^5 \text{ RT psi}$$

$$E = 37 \times 10^5 \text{ 6000°F psi}$$

$$\nu = .1$$

$$M = .94736 \text{ in-lbs/in} \\ D = \left[ \frac{1.032}{1.04736} \right] \left[ \frac{37.8 \times 10^6 \times .030}{1 - t^2} \right] \\ D = 624,018 \text{ in/lb.}$$

Assume no rotation:

$$M_T = \frac{6.0 \times 10^{-6} \times 1.30 \times 624,018}{1.06} (1.1) = 699 \text{ in-lbs/in}$$

$$M_A = .0513 \times 1.0 \times \frac{50.978^2}{2} = 133 \text{ in-lbs/in}$$

$$M_{\text{total}} = 832 \text{ in-lbs/in}$$

Load reacted at cup:

$$P = \frac{832 \times 7.463}{.9} = 6,895 \text{ lbs/cup}$$

Compression load on panel core:

$$\frac{6899}{.93593} = 7,371 \text{ lb/in}^2$$

Assume the insulation to be incompressible and allow the flange and panel rotate.

Assume the spring rate of the panel is the average of the pressure and thermal condition.

Thermal

$$K_p = \frac{M_{\text{clamp}}}{\theta_{\text{Free}}} = \frac{\alpha \Delta T \cdot J(1+\nu)}{h a \alpha \Delta T} \frac{2h}{a} = \frac{2D(1+\nu)}{a}$$

$$K_p = \frac{2 \times 624,018 \times 1.1}{50.978} = 26,930 \text{ in-lbs/in/Radian}$$

Pressure

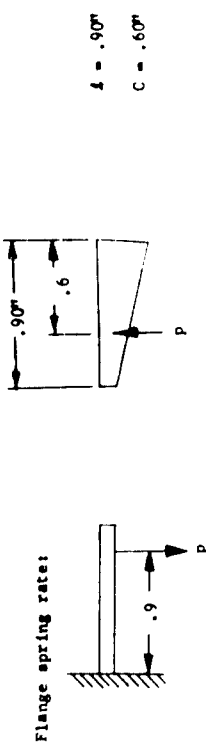
$$K_p = \frac{M_{\text{clamp}}}{\theta_{\text{S.S.}}} = \frac{.0513 \times \pi^4 \times D}{1.31330 \times .9} = \frac{.0513 \times \pi^4 \times 624,018}{1.31330 \times 50.978} = 1243 \text{ in-lbs/in}$$

$$K_p = 46,576 \text{ in-lb/in/Radian}$$

Use average spring rate:

$$K_p = \frac{46,576 + 26,930}{2} = 36,753 \text{ in-lb/in/Radian}$$

Flange spring rate:



$\delta = .90"$

$C = .60"$

$$M_T = \frac{M}{\theta_F} = \frac{M \cdot 2EI}{MI} = \frac{2 \times 10 \times 10^6 \times .9 \times 687 \times 10^{-6}}{.9} = 19,711 \text{ in-lb/in. Rad.}$$

$$E.F. = \frac{\theta_p}{\theta_{\text{total}}} = \frac{\frac{6}{K_F}}{\theta_p (\frac{K_p}{K_F} + 1)} = \frac{1}{\frac{K_p}{K_F} + 1}$$

$$E.F. = \frac{1}{\frac{16,753}{19,711} + 1} = \frac{1}{2.86459} = 34.911$$

Flight Condition:

$$q = 2.15 \quad \Delta T = 320^\circ F$$

.030 Beryllium Facing

Panel size 50.978 in of bolts

$$D = 624,018$$

Assume no rotation:

$$M_T = \frac{6.0 \times 10^{-6} \times 320 \times 624,018 \times 1.1}{1.06} = 1243 \text{ in-lbs/in}$$

$$M_A = .0513 \times 2.15 \times \frac{50.978^2}{.9} = 286 \text{ in-lbs/in.}$$

$$M_{\text{total}} = 1529 \text{ in-lbs/in}$$

$$\text{Load reacted at cup: } P = \frac{1529 \times 7.463}{.9} = 12,679 \text{ lbs/cup}$$

Compression load on panel core:

$$\frac{12,679}{.93593} = 13,347 \text{ lb/in}^2$$

Assume the insulation to be incompressible and allow the flange and panel to rotate.

Assume the spring rate of the panel is the average of the pressure and thermal condition.

Thermal

$$K_p = \frac{M}{\theta} = \frac{2D(1+\nu)}{a}$$

$$K_p = \frac{2 \times 624,016 \times 1.1}{50,978} = 26,930 \text{ in-lb/in/Radian}$$

Pressure

$$K_p = \frac{0513 \times \pi^4 \times 624,016}{1.31330 \times 50,978} = 46,576 \text{ in-lb/in/Radian.}$$

$$\text{Average: } K_p = \frac{46,576 + 26,930}{2} = 36,753 \text{ in-lb/in/Radian}$$

Flange spring rate:

$$K_F = 19,711 \text{ in-lb/in/Radian}$$

$$E.F. = 34.91\% \text{ same as above (page 65)}$$

Then the edge moment of panel with 34.91% fixity is:

$$M = 1529 \times 34.91\% = 534 \text{ in-lb/in.}$$

Load reacted by cup:

$$P = \frac{536 \times 7,463}{.9} = 4,428 \text{ lb/cup}$$

Compression load on panel core:

$$\frac{4428}{.93593} = 4,731 \text{ psi}$$

Assume rotation of panel, flange, and insulation.

$$\text{Use } K = 4098 \quad (50-75 \text{ psi}) \text{ Ref.}$$

$$C = .6^n \quad I = .90^n$$

$$K_I = \frac{CI^2}{2} = \frac{.6 \times 4098 \times .9^2}{2} = 996 \text{ in-lb/in Radians}$$

$$K_p = 36,753 \text{ in-lb/in. Radians}$$

$$K_F = 19,711 \text{ in-lb/in. Radians}$$

$$K_I = 996 \text{ in-lb/in. Radians}$$

$$\text{E.F.} = \frac{36,753}{996} + \frac{36,753}{19,711} + 1 = \frac{1}{39,76519} = 2.514\%$$

$$M = 1529 \times .02514 = 38.4 \text{ in-lb/in.}$$

Load reacted by cup:

$$P = \frac{38.4 \times 7,463}{.9} = 318 \text{ lbs/cup}$$

Compression load on panel core:

$$\frac{318}{.93593} = 340 \text{ psi}$$

Compression load on insulation (JM-146)

$$\frac{P}{A} = \frac{M}{C \cdot I \cdot W} = \frac{38.4}{.6 \times .9 \times 1} = 71 \text{ psi}$$

which is within the limits (50-75 psi) assumed above.

Simply Supported Edge Condition:

$$\begin{aligned} q &= 2.15 \text{ psi} & \Delta T &= 320^\circ F \\ W_A &= \frac{.00406 \times 2.15 \times 50.978^4}{624,018} = .094^n \\ W_T &= \frac{\alpha \Delta T (+\nu)}{\pi^3 h} 4\pi^2 \cdot 5708 = \frac{6.0 \times 10^{-6} \times 320 \times 1.1 \times 4 \times 50.978^2 \times .5708}{32,86654} \end{aligned}$$

$$W_T = .381^n$$

$$W_{total} = .475^n$$

77

78

$$M_A = .0479 q \cdot a^2 = .0479 \times 2.15 \times \frac{50.978}{2} = 268 \text{ in-lb/in center of panel}$$

$$M_T = \frac{\alpha \Delta T (1-\beta)^2 D}{h} = \frac{6.0 \times 10^{-6} \times .99 \times 320 \times 624,018}{1.06} = 1119 \text{ in-lb/in at edge of panel.}$$

#### Clamped Edge Condition:

$$q = 2.1, \text{ per } F$$

$$\Delta T = 120^\circ F$$

$$M_A = \frac{.0137 \times 2.15 \times \frac{50.978}{2}}{12 \times 624,018 \times .99} = .0277$$

$$M_A = .0513 \times 2.15 \times \frac{50.978}{2} = 287 \text{ in-lb. edge}$$

$$M_T = \frac{6.0 \times 10^{-6} \times 320 \times 624,018 \times 1.1}{1.06} = 1243 \text{ in-lb. edge}$$

$$M_{\text{total}} = 1530 \text{ in-lb/in.}$$

#### Preliminary Design Considerations for Beryllium Faced Honeycomb Heat Shield Panels

Based on the previously indicated feasibility of using beryllium facings for the cup type edge design heat shield panel, and assuming that none of the previously described undesirable characteristics of beryllium sheet is applicable, the following design considerations are recommended.

Using the cup type edge design, per drawing 60B20210, with the changes noted below:

1. 0.03m beryllium facing
2. Cup 0.063m Ti-13V-11Cr-3Al

The weight reduction would be 5.69 lbs., or 9.2%, compared with the all-stainless steel configuration having a calculated weight per drawing of 61.75 lbs.

#### Cost Considerations for Beryllium Faced Heat Shield Panels

The principal item of additional cost in a brazed honeycomb sandwich heat shield panel with beryllium facing for the 60B20210 design compared with the all-stainless steel design is the material cost for the beryllium sheet since the fabricating and/or brazing operations are essentially unchanged. The experience factor of considerable importance in handling and fabricating beryllium is also significant but is not readily determinable from a cost viewpoint and will not be evaluated.

The material cost of the 0.03" thick cross rolled beryllium sheet for one (1) heat shield panel per 60B20210 design is \$5677 (Table 16). This compares with a cost of \$240 for two (2) 0.01" x 52" x 56" PH 15-7 Mo facing having one fusion weld splice, roll planished and radiographically inspected.

SECTION V

DEFLECTION CHARACTERISTICS OF M-31 INSULATION  
WITH STAINLESS STEEL HONEYCOMB REINFORCEMENT

An important consideration in the use of ceramic materials for heat shield panel applications is the deflection allowable; i.e., the amount of bending the composite panel can withstand before failure of the ceramic occurs from the resultant tensile stresses. The deflection characteristics of M-31 were recently determined by Aeroneos as part of the S-1B heat shield panel program (Contract NAS8-4016) and are included as pertinent design information.

The test arrangement employed, shown in Figures 1 and 2, utilized a 3x15 specimen with two point loading. Specimen configuration was a 1.02" thick load bearing panel with 0.250" thick H-15 open faced core deformed to about 0.2" in height; M-31 thickness was 0.3". The test data is given in Table 17.

The radius of curvature for the deflection at which failure occurred may be calculated by

$$R = \frac{(C/2)^2}{2H} \quad \text{where } C = \text{chord length}$$

$$H = \text{deflection}$$

$$R = \frac{(7.2)^2}{.029} = 418 \text{ inches}$$

For the 30M12571 panel using the  $\frac{1}{4}$ " deflection allowable, the corresponding radius of curvature is:

$$R = \frac{(48.3/2)^2}{1} = 583 \text{ inches}$$

Therefore, the safety factor with regard to the deflection produced cracking of the M-31 is approximately 583/418 or 1.38.

The requirement for deformed honeycomb core to insure adherence of the M-31 insulation was established by the NASA S-1C Heat Shield Panel Test Program. These tests showed conclusively that deformation of the open faced honeycomb core was necessary to prevent separation of the M-31 under a simulated S-1C acoustic and thermal environment.

during the panel brazing.

Note: The doubler strips are required for the brazed facing sheet splice accomplishment

Material Cost for Beeryllium Faced Heat Shield Panel			
(60B20210 Design)			
Size	Quantity	Cost	Beeryllium Sheet
53" x 36"	2	\$3816	2. Doubler strips - .03" cross rolled beeryllium sheet
53" x 17"	2	1802	1. Facing - .03" cross rolled beeryllium sheet
53" x 15"	2	159	
		55877	for one (1) panel

83

84

\*Ref: Aeroforce Test Report TR-50-63

Dial Gauge	Load lbs.	Deflection in.	Match Keypoint To Load Points - inches
.0105	.012	.100	.0104
.0185	.02	.200	.0195
.026	.027	.300	.0274
.033	.034	.400	.0357
.0405	.0405	.500	.0440
.047	.047	.600	.0524
.054	.054	.700	.06
.061	.061	.800	.0688
.0685	.0685	.900	.0784
.076	.075	1000	.0875
.093	.096	.250	.09
.1085	.1065	.1310	.122
			.0145 (.122 - .1075)

Fallout of M-31 occurred at this point. Future constisted of a slight crack extending the full length of the M-31. Separation of panel which had thorough the entire depth of the M-31. Separation of the M-31 from the panel failing not occur.

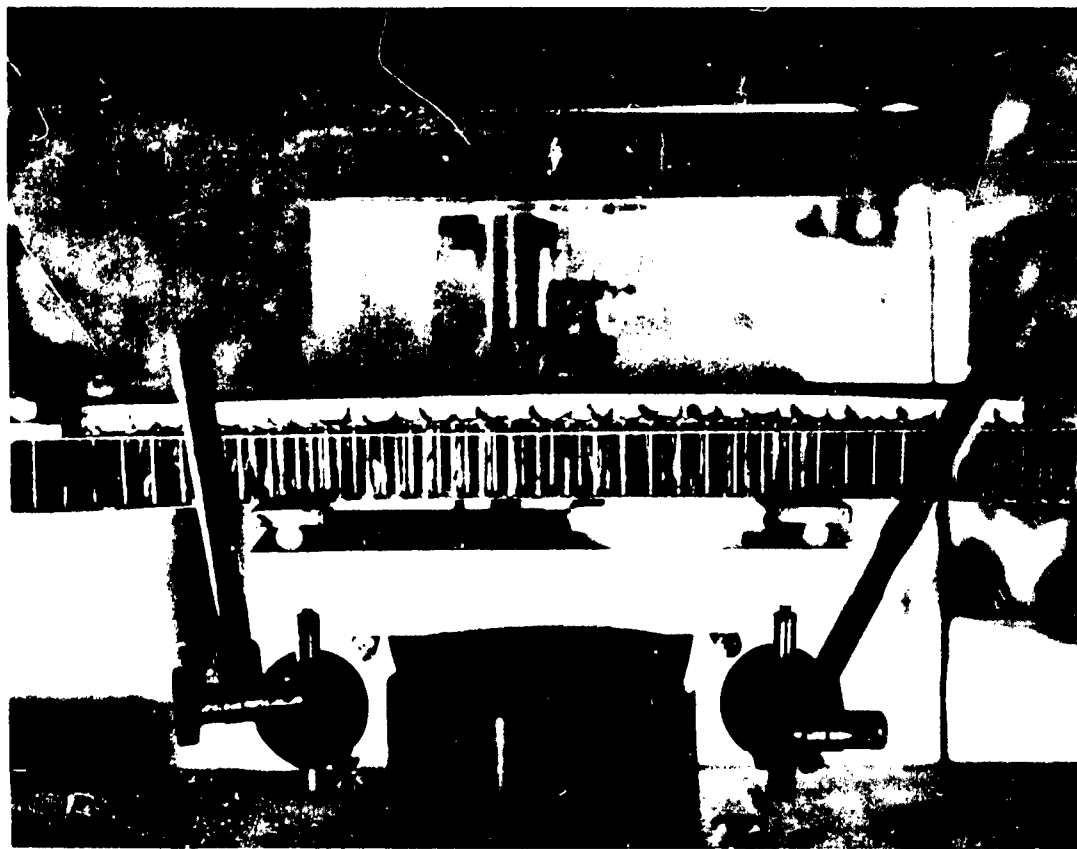


FIGURE 11 - FLEXURE TEST OF STANDARD SHEET METAL SAMPLE

SECTION V

ANALYSIS OF BRAZE EFFECTS  
QUALITY STANDARDS AND REPAIR METHODS

Heat Shield Panel Braze Quality

The types and sizes of typical braze discrepancies that are acceptable for heat shield panels of the 30M12571 design produced by Aeroneca for NASA or contract NASB-6976 are shown in Figures 3- through 7. The discrepancies include:

1. Core to facing braze light fillets (LFF).
2. Core to facing braze cell wall voids (C-WV).
3. Core to facing braze gross voids (G-V).
4. Metal to metal or facing surface braze voids (FSV).
5. Core to metal or shear tie braze voids.

Examination of these radiographic inspection reports shows the discrepancies to be principally confined to the metal to metal braze area in the edge members. The core to facing braze imperfections were confined to light fillet areas and small isolated cell wall void areas.

An unacceptable level of braze quality is shown in Figure 3<sup>17</sup>. Note the large area containing cell wall voids and light fillets which also contains a large gross void on both panel faces. These conditions resulted from rework leakage during brazing caused by failure of welded joints in the rework which results in contamination (oxidation) of the protective atmosphere. The net result of oxidized surfaces on the panel components during brazing is inability of the brazing alloy to properly wet the panel surfaces resulting in either very poor fillet formation or none at all.

It should be noted that the core to facing braze quality exhibited in Figures 3 through 5 is typical of acceptable braze quality by airframe brazed panel standards. The metal to metal and core to metal braze is likewise acceptable.

The following sections contain a detailed analysis of the effect of these five types of braze discrepancies on heat shield panels typical of the 30M12571 design and repair methods where applicable for these conditions.

FIGURE 3 - Radiographic test of standard braze with metal insulation at 100%.

75

85

86

87

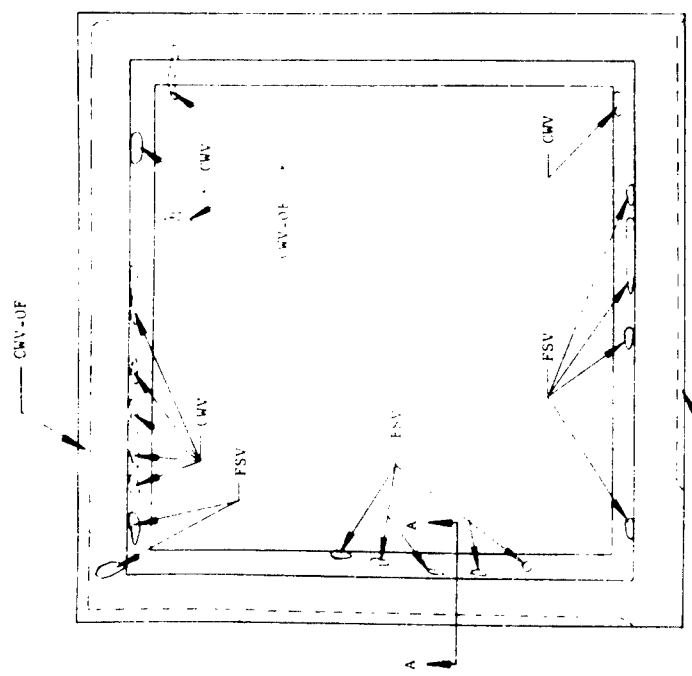


Figure 33 Quality Modifying Conditions Revealed  
By Radiographic Examination

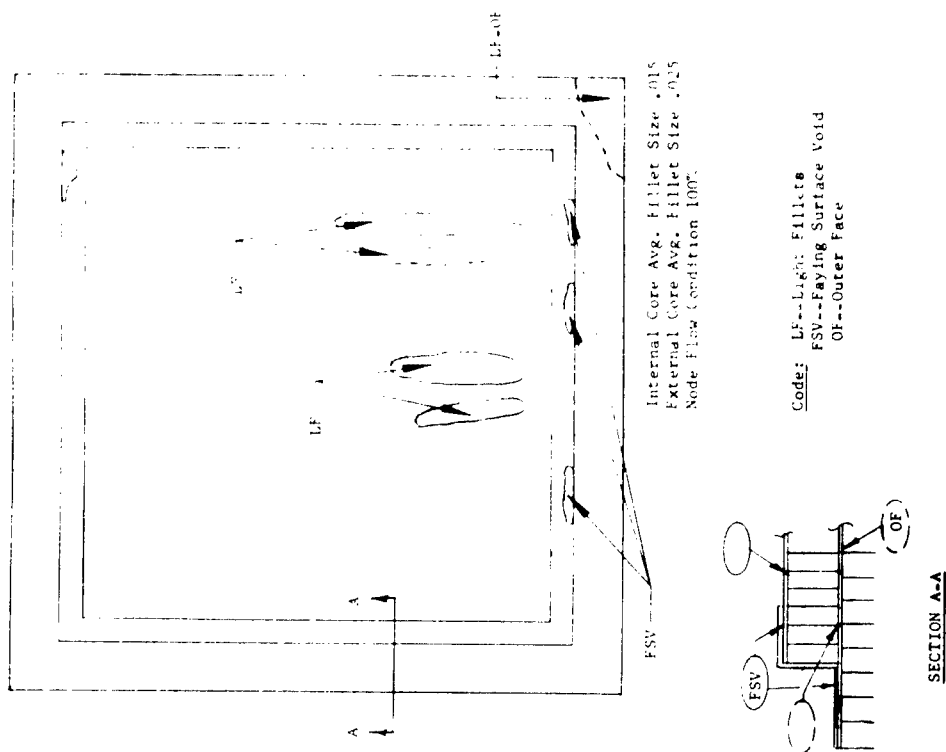


Figure 34 Quality Modifying Conditions Revealed  
By Radiographic Examination

88

90

89

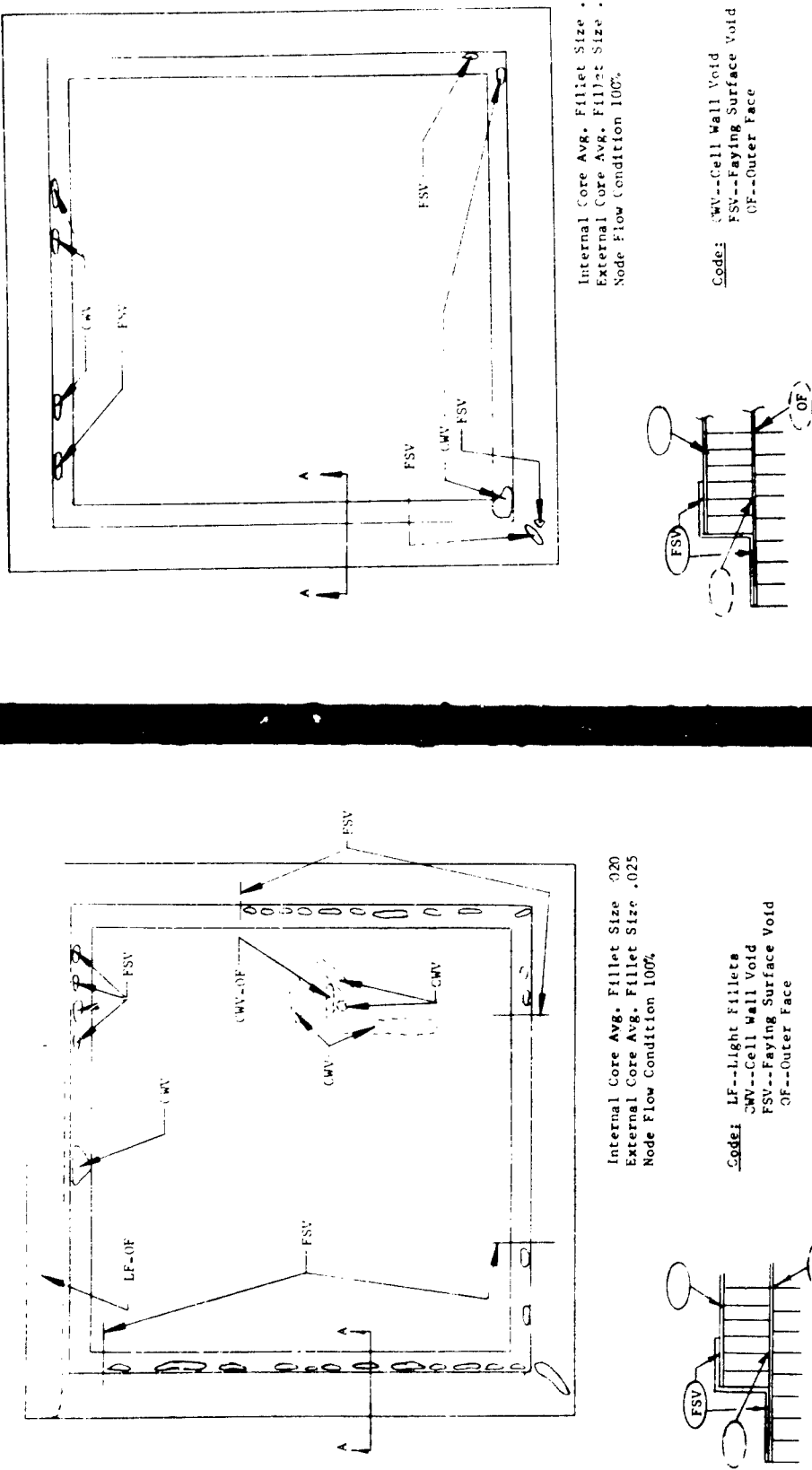


Figure 35 Quality Modifying Conditions Revealed by Radiographic Examination

Figure 36 Quality Modifying Conditions Revealed by Radiographic Examination

**91**

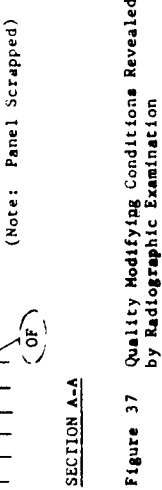
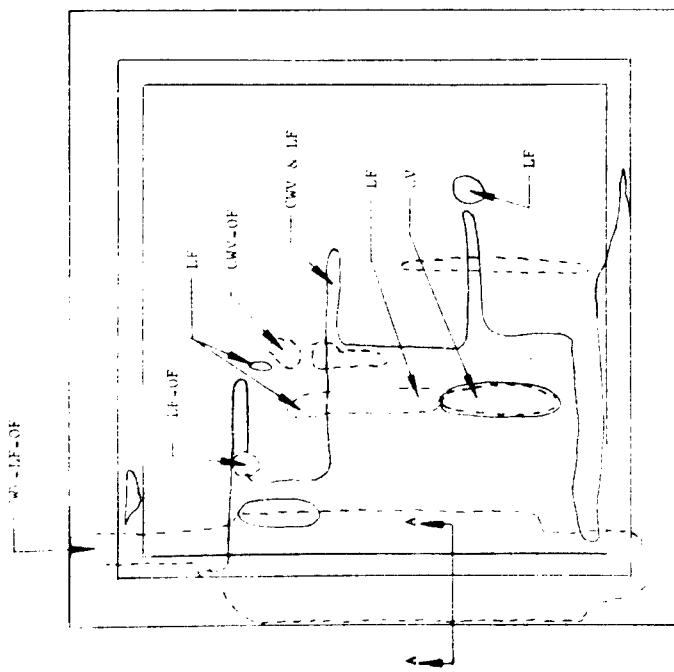


Figure 37 Quality Modifying Conditions Revealed by Radiographic Examination

— GV

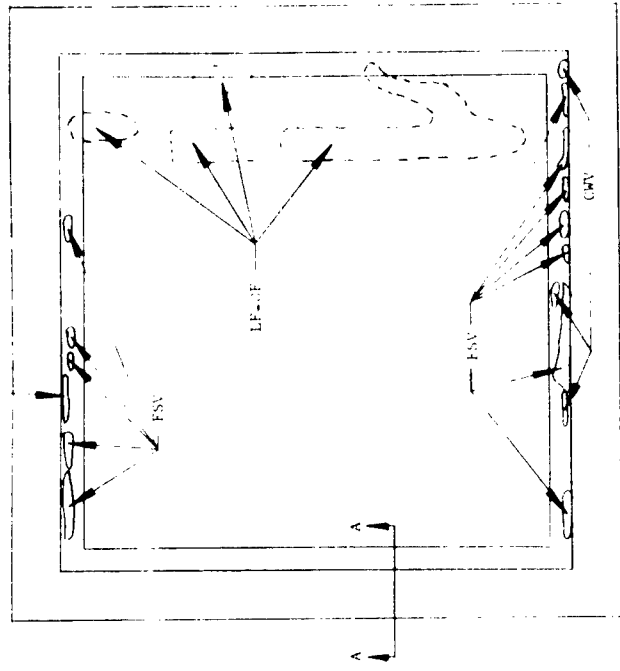


Figure 38 Quality Modifying Conditions Revealed by Radiographic Examination

**92**

Core to Facing Voids

A core to facing void is an area showing partial or total lack of braze attachment between the honeycomb core and facing sheet. This type of discrepancy is commonly encountered in brazed honeycomb sandwich panels and in numerous variations of size and shape. The effect of such unbrazed or unattached areas is a function of size and the type of loading; i.e., tension or compression. Since any sandwich panel subjected to a bending load has one facing in compression while the opposite facing is in tension, the stability of the facing(s) under compression load in voided or unbrazed areas is of critical importance. Consequently, the analysis of core to facing voids is based on the local buckling strength of the unattached facing sheet under a compression load.

Two types of core to facing voids are commonly encountered. These are:

- a. Cell Wall Void (CWV)--The condition where the cell walls are unattached to the face sheet but where attachment is present at the cell nodes. This condition may be continuous or intermittent.
- b. Gross Void (GV)--A gross void is a condition where at least one node is unattached to the facing sheet.

Circular Gross Voids

For the condition shown in Figure 39A, the critical dimension b, unattached area is given by

$$\frac{F_{cr}}{T} = .9E \left[ \frac{t_f}{d} \right]^{1.5} \quad (1)$$

where  $\gamma$  = plasticity correction factor =  $\frac{2E\gamma}{E+E\gamma}$

$E$  = Modulus of elasticity of facing material.

$E_T$  = Tangent modulus of facing material from compression stress-strain curve.

Rectangular Gross Voids (Line or Rectangular)

For the condition shown in Figure 39B where dimension b is the loaded edge, the facing behaves as a uniaxially loaded wide plate column. Tests indicate that when the void is surrounded by good braze attachment, the end restraint condition approaches 100% fixity. The local allowable buckling stress for this condition is given by,

$$\frac{F_{cr}}{\eta_1} = \frac{2.62E}{1-\nu^2} \left[ \frac{t_f}{h} \right]^2 \quad (2)$$

$\nu$  = Poisson's Ratio

where  $\eta_1 = \frac{E_T}{E}$  the plasticity correction factor for b the loaded edge.

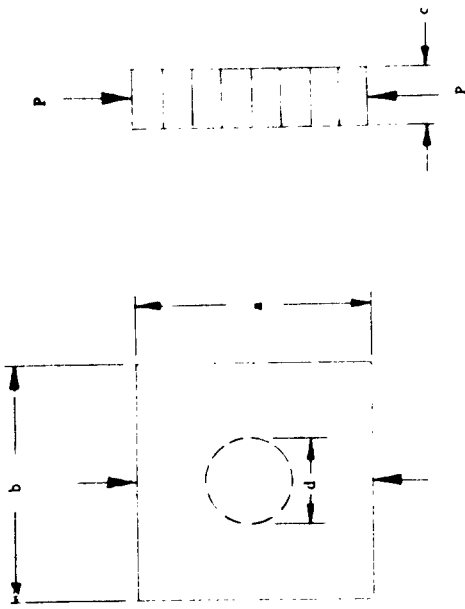


Figure 39A Circular Void

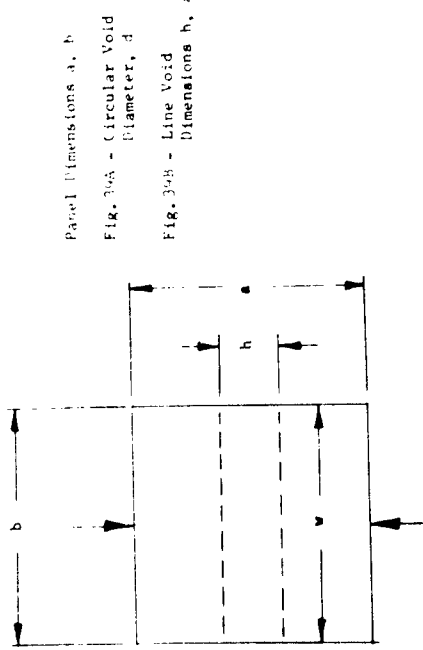


Figure 39B Line Void

Figure 39 Basic Void and Buckling Configurations

Where dimension  $a$  is the loaded edge, the rectangular void is considered a long plate elastically restrained on the unloaded edges with intermediate fixity. The buckling stress for this condition is:

$$\frac{t_{cr}}{d} = \frac{4.5E}{(1-\nu^2)} \left[ \frac{t_f}{h} \right]^2 \quad (3)$$

$\eta_2 \frac{t_f}{h} = [\varepsilon_S + 0.352 + 0.348 \sqrt{\frac{2.5 + 3\varepsilon_T}{4\varepsilon_S}}]$  where  $\varepsilon_2$  is the plasticity correction factor for the loaded edge.

Curves for the preceding equations (1), (2), (3) are shown in Figure 40 and allow ready assessment of the buckling stress for these three core to facing void conditions. Since the maximum stress condition for the 30HL2571 panel is 35,644 psi\*, all voids must be stable to this minimum buckling allowable. Voids exhibiting for values below 15,644 psi would be unacceptable and would require suitable repair. From Figure 40 the maximum circular void size acceptable is 1.87" without repair should re:

$$\frac{d}{d} = .012$$

$d = 0.83"$  diameter

For the line void conditions in Figure 30, the comparable values for  $h$  are (Fig. 40): 0.59" (curve 2) and 0.66" (curve 3).

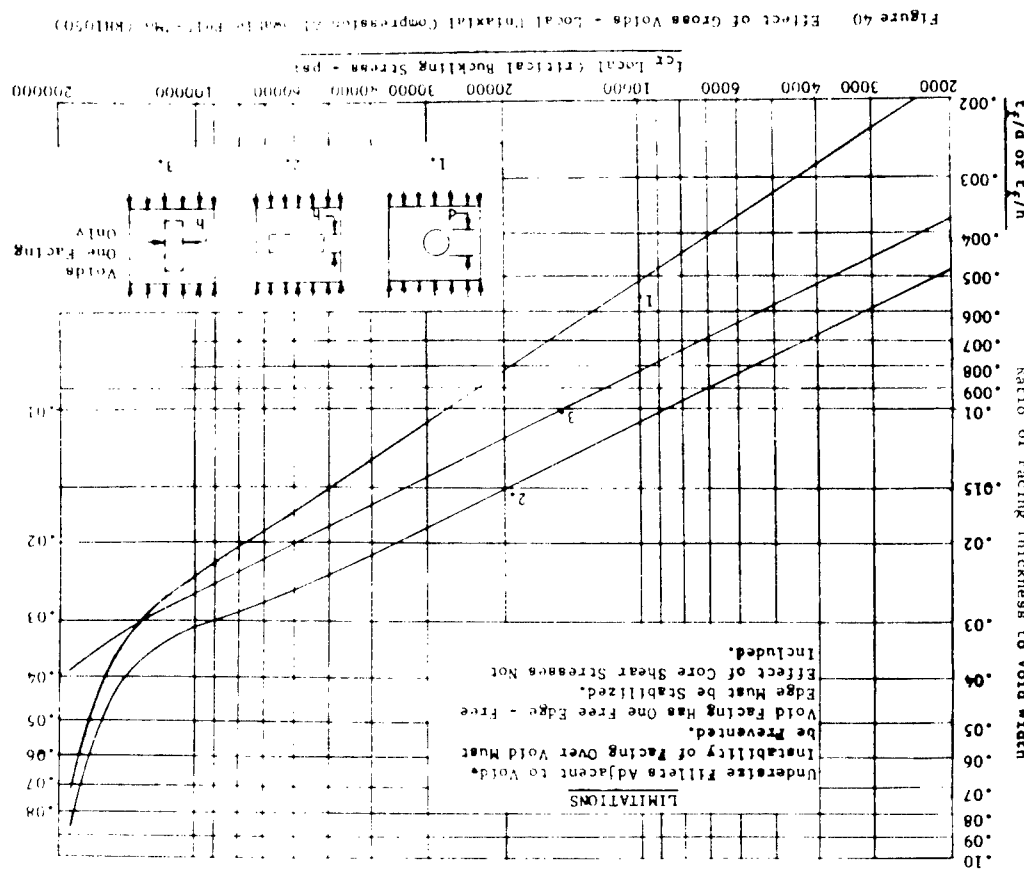
#### Cell Wall Voids

Two conditions of this type of void may be present, a (connected) row of cell wall voids or an area with intermittent cell wall voids. The former case may be treated by the use of formulas (2) or (3) for Gross line voids. For the latter case (area with intermittent cell wall voids), the following empirical equation for the local buckling stress is used:

$$f_{cr} = \frac{2.958 + \log_{10} \frac{f_f}{f_{allowable}}}{1.34}$$

$f_{allowable}$  = compression wrinkling stress in facing  
(177,000 psi for 4-15 core)

$$\frac{t_f}{d} = .025$$



98

The curve for this equation is shown in Figure 41. For a buckling stress of cr of 35,644 psi, the maximum cell wall void acceptable "is" would be:

$$\frac{35,644}{177,000} = .2 \text{ and } \frac{t_f}{d} = .002$$

for  $t = .01"$     $d = 5"$  diameter and  $h = 5"$ .

(Ref. NAA Structural Repair Manual /buckling equations and curves/).

#### Fillet Size

For in plane loads a certain minimum fillet size is required to permit development of the face shear allowable in compression loading which in turn subjected the braze fillet to a tensile load. This critical tension stress may be calculated by the following empirical equation:

$$f = \frac{1.75N_f}{S} S$$

$N_f$  = actual braze fillet width at base, inches

$S$  = honeycomb core cell size

$f$  = braze lap shear allowable, p.s.i.

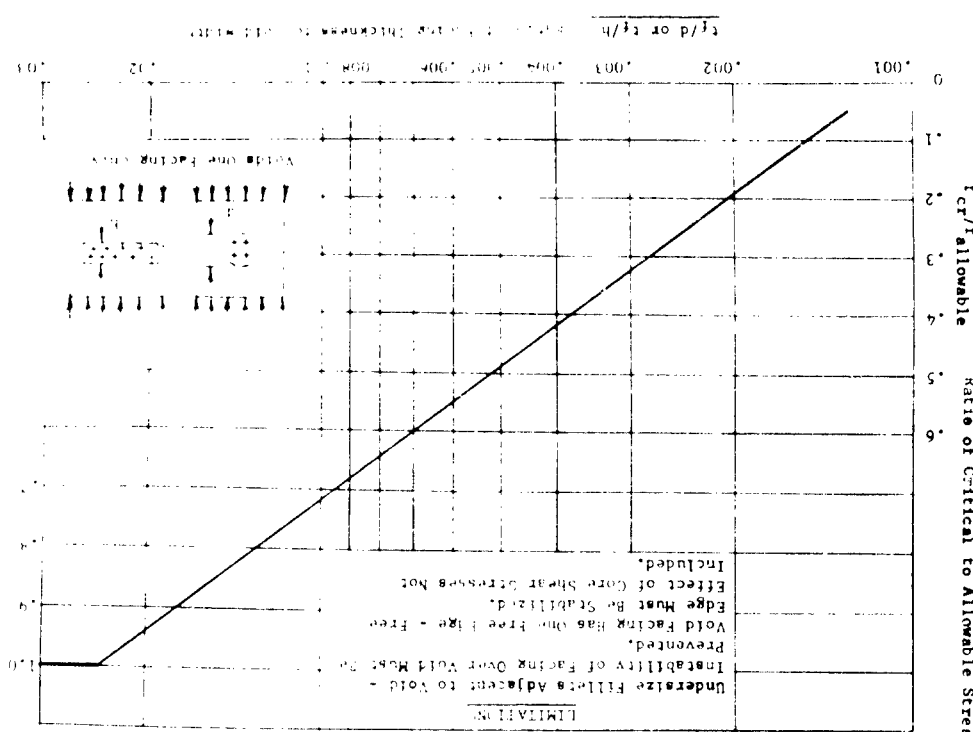
For type 4-15 core and the sterling lithium braze alloy  $f_{S} = 15,000$  psi\*,  $f$  is 0.40 psi for the minimum fillet size requirement (0.008") recommended for this application. Typical fillet size for the 30M12574 panels was 0.015". The effect of underside fillets on face sheet stability is shown in Figure 42.

#### Node Flow Requirements

For the SJC heat shield panel applications in question, brazing alloy node flow in the load bearing core is desirable from the standpoint of minimizing the thermal gradient ( $\Delta T$ ), resulting panel deflection and facing stresses rather than providing increased core shear properties.

\*Ref. Convair Spec. FZS-4-162A

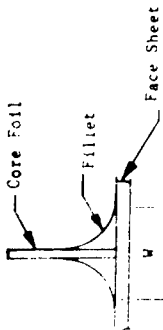
FIGURE 41 Effect of Cell Wall Void on Critical Shear Stress



97

99

100



#### Size and Spacing Requirements for Core to Face Sheet Joint

However, since the combined facing stresses for a flight condition are quite low (25,238 psi) for the zero net skin loading (AT) condition with a N.S. of .01 in. node flow is not considered a mandatory requirement for heat shield panel acceptance.

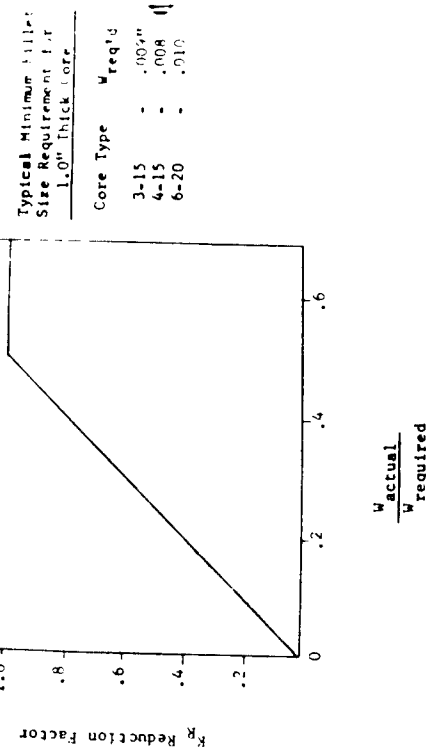


Figure 42 Effect of Undersize Fillet on Face Sheet Stability

Ref: NAA Structural Repair Manual

The maximum sizes of core to facing voids recommended for acceptance was 1 in (unprepared) are given in Tables 1 and 2, which also include the minimum recommended spacing requirements. The spacing requirements essentially represent the minimum distance necessary to prevent catastrophic propagation of adjacent voids and are based on empirical standards used for brazed honeycomb sandwich air frame panels. Because of the large M.S. associated with the maximum panel stress (35,644 psi), the maximum permissible acceptable thickness void has been defined as 1.0 in rather than 0.5 in.

Repair Procedure:

- a. Adhesive bonding using a high temperature epoxy
- b. Spot brazing--A method which employs a lower melting point braze alloy than the sterling lithium braze alloy used for the panel braze. Localized braze attachment in the form of spots  $\frac{1}{16}$  in.,  $\frac{1}{32}$  in., or  $\frac{5}{64}$  in. in diameter is accomplished by electrical resistance heating using a single electrode run applied to one side of the part only. The brazing alloy recommended for this application is the silver-copper eutectic plus 0.2-5% lithium with a melting and flow point of approximately 1400°F.
- c. Area Brazing--A method using a lower melting point brazing alloy as in item b. with heat applied either locally by means of an indirectly heated copper block or by heating the entire panel using the original brazing tooling. The latter method gives very good results but requires specialized manufacturing facilities and is relatively expensive. The local heating method is highly dependent on operator skill, limited to small size or areas, and frequently results in excessive panel warpage.

\*Ref: Monthly Report No. 3, Page 37

102

101

SIZE AND SHAPE OF GORE TO FACILITATE PANEL QUALITY

TABLE I-A

\* Concentricous Cell Wall Voids are included in this category.

MINIMUM SPACING REQUIREMENT FOR ABOVE DEFECTS FROM EDGE OF PANEL				
Defect	Line Defect	Minimum Distance to Next Defect	Line Defect	Defect
0.26 to 0.50m	0.26 to 0.75m	6 inches	0.51 to 1.0m	10 inches
up to 0.25m	up to 0.25m	1 inch	0.26 to 0.50m	3 inches
up to 0.25m	up to 0.25m	5 inches	0.51 to 1.0m	5 inches

SIZE AND SHAPE OF GORE TO FACILITATE PANEL QUALITY

TABLE I-B

\* Concentricous Cell Wall Voids are included in this category.

Diameter of Circular Defects  
Maximum Permissible  
Number of Cell Wall Voids  
Area Containing Defects

up to 1.50m	7	1.51m to 3.0m	25	3.01m to 5m	50
-------------	---	---------------	----	-------------	----

103

d. Mechanical fasteners-Limited use may be made of blind mechanical fasteners such as Inconel L-Nickel noiseless explosive rivets of the jacketed head type (PN-134A)  $0.134n \pm .001n$  in diameter. The rivet holes must be located in the center of the core cells in the sound braze area to avoid unsatisfactory core to facing braze damage.

Of the foregoing methods, the adhesive bonding, spot brazing and blind panel facing (cold side); the hot side facing bearing the open face honeycomb core effectively prevents repairs from being accomplished. Welding as a means of doubler attachment, either directly as along the doubler edge or ... a fusion spot, burn down welds of pins passing through a doubler and top and bottom facings, is likewise not feasible with conventional TIG welding equipment on panels with  $0.010n$  facings essentially because of inadequate control resulting in burn through.

Mechanical fasteners are directly applicable for heat shield panel repairs. In any case, however, doublet repairs are only practical for the forward panel facing (cold side); the hot side facing bearing the open face honeycomb core effectively prevents repairs from being accomplished. Welding as a means of doubler attachment, either directly as along the doubler edge or ... a fusion spot, burn down welds of pins passing through a doubler and top and bottom facings, is likewise not feasible with conventional TIG welding equipment on panels with  $0.010n$  facings essentially because of inadequate control resulting in burn through.

#### Analysis of Metal to metal and Core to Metal Voids in 30mil2571 Heat Shield Panel

##### Core to Metal Voids:

The core to metal joint is assumed to carry the entire load. Since the vertical leg of the Zee is  $1n$ , the total shear area for the panel is  $4 \text{ sq. in.}$ ; where  $a$  is the length of the core ( $48.3 \text{ in.}$ ). The shear load per inch of perimeter then becomes  $qa/4n$  or  $qa/4 \text{ psi}$  of wall area. The core to metal attachment area for Type 4.15 core per square inch of surface would be  $4 \times .005 = .020 \text{ in}^2$  of shear area\*. The shear stress on the braze attachment is:

$$f_a = \frac{qa}{4 \times .02} = \frac{48.3 q}{.08} = 603q \text{ psi}$$

The shear strength allowable for the silver-copper-lithium braze alloy is  $15,000 \text{ psi}$  at R.T. and  $12,750 \text{ at } 500^\circ\text{F}$ \*\*.

For  $q = 2.7$  air load plus  $0.72 \text{ psi}$  dynamic load (noise and vibration)

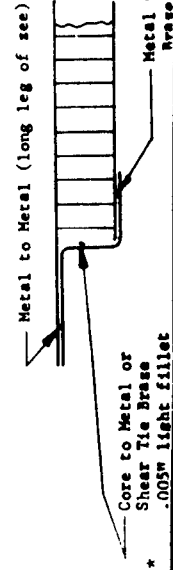
$q = 1.0$  air load plus  $0.72 \text{ psi}$  dynamic load (noise and vibration)

$f_a = 2050 \text{ and } 1025 \text{ psi}$ , respectively.

Thus for the worst condition, the maximum void allowable is

$$1 = \frac{2050}{15000} \times 100 = 8\%$$

With the panel edge secured by means of bolts to the support beam flanges



\*Ref: Convair Spec. FMS-0036  
\*\* .005n light fillet

#### Metal to Metal Voids--Short Leg of Zee Member:

Assume the short leg of the zee must carry the entire panel load as a tensile loading on the facing to short leg zee braze. The width of this braze area is  $0.875n$  and the total width of the zee is  $1.125n$ . The panel load is  $qa/2$  with the tensile stress in the braze given by  $\sigma_{braze} = 3.5 \times 12.3q \text{ psi}$ . Applying the worst loading condition, The stress in the braze is  $42 \text{ psi}$ . The braze tensile allowable is approximately  $25,000 \text{ psi}$ ,  $(13000/\sqrt{2})$  consequently a very large margin is present for this loading condition.

#### Metal Voids--Long Leg of Zee Member:

When the composite edge member (long leg of zee) and facing is bent by a shear load at point P the edge P



rotation is given by:

$$\theta = \frac{PL^2}{2EI} - \frac{ML}{EI} = \frac{41.4 \times (.897)^2}{2 \times 29 \times 10^6 \times 1.84 \times 10^{-6}} = .03125 \text{ radians}$$

Where  $P = \frac{1}{2}q \text{ lbs/inch}$

$a = 48.3"$

$$q = (2.7 + 0.72) = 3.42 \text{ psi}$$

The stress in the braze is:

$$f = \frac{MC}{I} \quad \text{where } M = \frac{2EI\theta}{L}$$

$$f = \frac{2EBC}{L} = \frac{2 \times 10.2 \times 10^6 \times .03125 \times .019}{.897} = 18,500 \text{ psi}$$

Since the braze must withstand the shearing force resulting from bending, the  $13,500 \text{ psi}$  value may be compared with the braze shear allowable namely,  $15,000 \text{ psi}$ . Actual values, however, for the silver-copper-lithium braze alloy are  $19,600 \text{ psi}$  (R.T.)\*\*.

With the panel edge secured by means of bolts to the support beam flanges the principal concern with voids between the facing and see occurs when the facing experiences a compression loading resulting from bending of the .061" flange

\*Ref: Convair Spec. FMS-0036

104

105

thick composite edge member (flight condition loading). As a result, the facing would tend to buckle in unbrazed areas so that voids might propagate into the core to facing areas, particularly if core to facing voids near the edge members were present. Where no core to facing voids near the panel edge are present, metal to metal void propagation is unlikely since the panel edge rotation is very small. As a consequence, the compressive force required for extensive buckling in metal to metal voided areas will not be produced.

Repair Methods for Metal to Metal Voids

Repair methods applicable to metal to metal braze voids include:

- a. Mechanical Fasteners.—Either blind or countersunk rivet fasteners depending on the void location and interference requirements may be used. A recommended fastener is the DuPont Aircraft Blind Expansion Rivet (PN series) of low carbon nickel alloy. This fastener is available with either a modified braizer head or 100% flush head. Expansion of the rivet shank is accomplished by applying a heated tool to the rivet head which activates the sealed internal chemical charge. This type of rivet has been widely used for applicable braised panel repairs with complete success. Certain NASA test panels produced on Contract NAS-6976 were repaired using this type rivet, as shown in Figure 43. Repairs to voids in either the short or long leg of see member can be readily accomplished with this fastening system both in the field as well as by the panel fabricator.
- b. Spot Welder.—This joining method has been used for metal to metal repairs where the area to be repaired is accessible; i.e., the long legs of the see and the faying surfaces are sufficiently clean (unoxidized) so a sound nugget can be formed. As a consequence, this method is limited with respect to void location and equipment availability.
- c. Fusion Welding.—This is applicable to metal voids between long legs of see and facing that extend the full width (edge to edge). Essentially a burndown weld is performed which joins the facing and edge member. The presence of silver brazing alloy in the fusion zone is not detrimental to the joint; however, it does cause some difficulty because of the tendency to "blow out". Consequently, a complete void condition is preferred for this type of repair.

Repair Methods for Core to Metal (Shear Tie) Voids

Repair for core to metal or shear tie voids consists of injection of a foam type adhesive through holes drilled in the vertical leg of the see, curing the adhesive and plugging the drilled holes with a sealer or potting compound.

94



Figure 43. Typical metal to metal voids prior to repair (left) and after repair (right).

106

The detail requirements are:

- a. Clean surface (MEK) and lay out hole pattern using 1.0" hole spacing and drill holes (No. 50 drill).
- b. Inject with a lever type gun (thermofoam 7), type I (Hexcel Products). Cover holes with one layer masking tape, reopen holes and add another layer of tape so there are two layers. This provides an expansion area for adhesive overflow during the curing.

c. Attach thermocouple(s) to the area to be repaired and cure in oven at:

180°-190° F for 25-30 min. followed by

225°-240° F for 50-60 min. followed by

325°-350° F for 45-55 min.

d. Reopen holes used for injection to a depth of approximately 0.1" and seal with Silastic RTV.

Braze Quality Standards for Metal to Metal and Core to Metal Joints

The maximum sizes of metal to metal and core to metal braze voids recommended for acceptance has 1/8" are given in Table V. These size and spacing requirements are based on empirical standards modified for the S-1C heat shield panel requirements.

METAL TO METAL AND CORE TO METAL BRAZE REQUIREMENTS

TABLE

Metal to Metal	(Faying surface void)
Core to Metal	(shear tie void)
Any vertical shear tie 50% or more brazed is acceptable. The maximum number of unbrazed or completely void shear ties shall be not more than 3 in any 5 consecutive shear ties.	
edge to edge.	
metal to metal void shall not be continuous from metal to metal void each joint inch of braze joint. A	
The voided area shall not exceed 25% of the joint area for each joint inch of braze joint. A	
metal to metal void shall not be continuous from	
edge to edge to edge.	

## ANALYSIS OF HOLES IN REACTOR BULLET PANELS

Methods for calculation of stress concentration factors around holes in sandwich panels are outlined in AS/NZS Part 1, Section 3, 1981, Clause 3.7152, 3.7153. See Figure 3.7152 and 3.7153. The parametric equations describing the boundary of the hole (with no doubler) are:

$$A = A \cos \theta + i \sin \theta$$

$$B = B \cos \theta - i \sin \theta$$

$$\text{where } \tan \theta = \frac{B}{A}$$

The stress in the facing at the edge of the hole in a tangent direction is given by

$$\begin{aligned} & \left[ (\mathbf{A}^2 + \mathbf{B}^2) \sin^2 \theta + (\mathbf{B}^2 - \mathbf{A}^2) \cos^2 \theta \right] + \frac{\left\{ \mathbf{f}_x^2 + \mathbf{f}_y^2 \right\}}{\mathbf{A} + \mathbf{B}} \\ & \left( \mathbf{f}_x^2 + \mathbf{f}_y^2 \right) (\mathbf{A}^2 + \mathbf{B}^2) \sin^2 \theta + \mathbf{B}^2 \cos^2 \theta - \frac{\left\{ \mathbf{f}_x^2 + \mathbf{f}_y^2 \right\}}{\mathbf{A} + \mathbf{B}} \left[ \frac{(\mathbf{A}^2 + \mathbf{B}^2) (\mathbf{f}_x^2 + \mathbf{f}_y^2) - (\mathbf{A}^2 - \mathbf{B}^2) (\mathbf{f}_x^2 - \mathbf{f}_y^2)}{\mathbf{A} + \mathbf{B} - 2\mathbf{f}_z^2} \right] \end{aligned}$$

卷之三

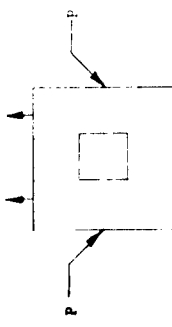
$$\begin{aligned} f_t &= (f_x + f_y) - 4f_{xy} \sin 2\theta - 2(f_x - f_y) \cos 2\theta \\ f_r &= (1 - 2 \cos \theta) f_x + (1 + 2 \cos 2\theta) f_y - 4f_{xy} \sin 2\theta \end{aligned}$$

For an assumed uniaxial condition where  $f_y = 0$ , we have a maximum value for  $f_x$  at  $\theta = \pi/2$ . Thus  $f_t(\pi/2) = 3f_x$ .

Thus the maximum stress concentration factor for a round hole in a plate subjected to a uniaxial stress is 3 and is independent of the hole size and the distance of the point of interest from the hole.

The recent analytical work by W. Griffell<sup>\*</sup> indicates a factor of 3.1 for a square hole always considered to be adjacent to the edge of a plate. At distances of less than one hole diameter from the hole, the stress concentration factors for the points of interest will be equal to the ratio of 3.1 to 1. Subsequently, available results are considered to be the more accurate.

For a square hole theory indicates  $\sqrt{2}$  as the stress concentration factor at the center (p) of a side parallel to the applied stress.



At the corners the stress concentration factor is a function of the corner radius to side length ratio,  $\frac{r}{d}$ .

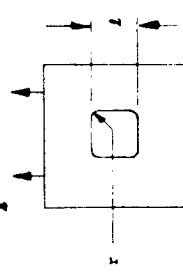


Figure 45 shows a plot of  $K \times \frac{r}{d}$  for square and diamond holes taken from Savin's data. Table 2 and Figure 44 show the stress concentration factors for different hole shapes and locations.

For the case of a round hole near a boundary edge of the panel for the case where (distance of hole center from edge/hole radius = 2) the stress at the panel edge adjacent to the hole will be zero; at the hole boundary adjacent to the panel edge  $K = 3.3$ ; at the hole boundary opposite to the panel edge  $K = 3.1$ .

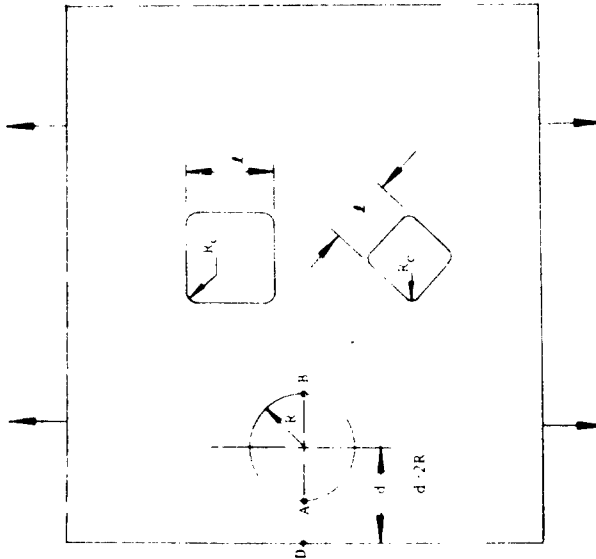


Figure 44  
Hole Diagrams, Typical  
(See discussion of Stress Concentration  
Factors, pages 9a-10a)

113

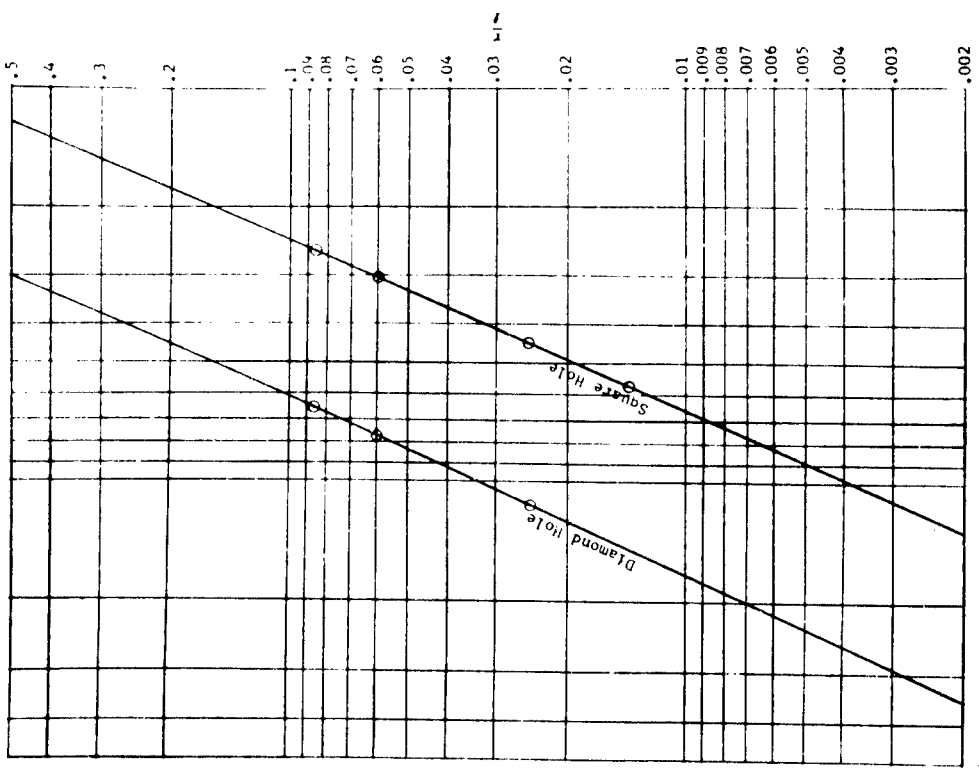


Figure 45 Stress Concentration Factor,  $K$  at  $\theta=\pi/4$  for Square and Diamond Holes

\*These values are 2.6; 3.1; and 4.5, respectively, at  $\theta = \pi/4$ ;  $r = a$  shown in Figure 45.

114

TABLE 2  
VALUES OF  $K$  AT  $\theta = \pi/4$  FOR HOLE DIAMETER,  $d$ , EQUAL TO ONE-THIRD OF THE PLATE THICKNESS  
SHADED VALUES WHICH ARE GREATEST IN A UNIFORM SERIES

	$K$ at $\theta=0$	$r$ at $\theta = \frac{\pi}{2}$	$K$ Value
Round Hole (per A.N.C.23)	-1	3	3
Round Hole (per G. H. Savin)	-1	3	3
Round Hole ( $d=2R$ )	-1	3.3 at A 0 at D 3.1 at B	3.3
Near Edge per G. H. Savin			
$R_C = .006L$ per G. H. Savin	-0.828	1.645	3.3
Square Hole per G. H. Savin			
$R_C = .006L$	-.86	1.4	2.8 at 50°*
$R_C = .008L$	-.8	1.6	3.9 at 50°*
$R_C = .025L$	-.95	1.8	4.5 at 50°*
$R_C = .014L$	+1.4	-.9	5.8 at 45°
Diamond Hole per G. H. Savin			
$R_C = .006L$	+.35	+.35	6.5 at 45°
$R_C = .008L$	+.4	+.4	7.8 at 45°
$R_C = .007$	+.5	+.5	11.6 at 45°
$R_C = .006$			
$R_C = .005$			
$R_C = .004$			
$R_C = .003$			
$R_C = .002$			

When biaxial stresses are present as will be the case with the heat shield panels and the test samples, the factor for the tangential stress at the boundary of a round hole is a maximum of 4 when  $f_x = f_y$ , for steady state load conditions.

For dynamic loads (noise and vibration) the stress concentration factor for a round hole is approximately 2.8.

Accordingly, the maximum stress at the boundary of a round hole with no doubler in a heat shield panel is given by:

$$f_t = 4.79 \times (4 \times 2.7 \text{ psi} + 2.8 \times 0.72 \text{ psi}) \times (48.3)^2 = 142,313 \text{ psi}$$

Since this value is well below the yield strength minimum of 170,000 psi and assuming 100% core to facing brace attachment in the panel area surrounding the hole, a positive margin is indicated. If the hole was located in an area of light fillets or voids, the addition of a doubler around the hole would be necessary.

#### Holes with Doubler Reinforcement

The stress in the facing at the boundary of a round hole with a doubler on one facing where  $\frac{R_D}{H} = \frac{3}{2}$  and  $\frac{R_1}{R_2} = \frac{1}{4}$  is:

$$f_{t_1} = (f_1 + f_2) C - 4(f_1 - f_2) \left[ \frac{B + 3P}{R_2} \cos 2\theta \right] \quad (1)$$

$H$  = extensional stiffness of panel,  $2tfE$

$R_D$  = extensional stiffness of panel in doubler area,  $3tf^2E$

$R_1$  = radius of hole, inches

$R_2$  = outside radius of doubler, inches

$f_1, f_2$  = thickness of facing and doubler, respectively, inches

The stress in the facing at the junction of the doubler is given by:

$$f_{t_2} = \frac{(f_1 + f_2)}{2} \frac{(1-A)}{2} \frac{(f_1 - f_2)}{2} (6J-1) \cos 2\theta \quad (2)$$

The values of the parameters A - J for the conditions set forth above are:

\*Ref: Dynamical Stress Concentrations in An Elastic Plate, J. of Applied Mechanics, June 1962, Pg. 304.

$$A = \frac{3(1 - \frac{R_1^2}{R_2^2}) \frac{R_D}{H} - 5 \frac{R_1^2}{R_2^2} \cdot J}{5(1 - \frac{R_1^2}{R_2^2}) \frac{R_D}{H} + 5 \frac{R_1^2}{R_2^2} \cdot J} = -0.886$$

$$C = \frac{\frac{8}{R_1^2} \frac{R_D}{H} + 5 \frac{R_1^2}{R_2^2} \cdot J}{5(1 - \frac{R_1^2}{R_2^2}) \frac{R_D}{H} + 5 \frac{R_1^2}{R_2^2} \cdot J} = +0.81$$

$$D = +0.228$$

$$F = -0.5 / 97$$

$$J = +0.5272$$

$$B = -0.423$$

Fig. 6.

$$f_{t_1} = (f_1 + f_2) \cdot 81 - 4(f_1 - f_2) \left[ .423 - 3 \times \frac{-587}{4} \right] \cos 2\theta$$

$$\text{or} \quad f_{t_1} = .88 f_1 \text{ at } \theta = 0; f_{t_1} = .74 f_1 \text{ at } \theta = \frac{\pi}{2}; \text{ (for } f_2 = 0)$$

$$f_{t_1} = 1.62 f_1 \text{ for all values of } \theta \text{ when } f_1 = f_2$$

For the stress in the facing at the edge of the doubler from Equation (2):

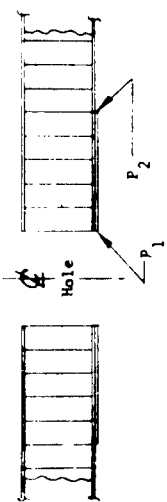
$$f_{t_2} = -1.023 f_1 \text{ at } \theta = 0; f_{t_2} = -1.137 f_1 \text{ at } \theta = \frac{\pi}{2} \text{ (for } f_2 = 0)$$

$$f_{t_2} = 0.114 f_1 \text{ at all } \theta \text{ for } f_1 = f_2; f_{t_2} = 1.08 \text{ at } \theta = \frac{\pi}{2} \text{ (for } f_2 = -f_1)$$

Consequently, the maximum stress concentration factors tangentially for a hole with a doublet axial stress conditions are:

$K_{facin}$  = edge of the hole  $P_1$  for a biaxial stress condition; and

$K_{facin}$  = the edge of the hole  $P_2$  for a biaxial stress condition.



Since the biaxial factor without a doubler was 4, these results indicate the substantial reduction in peak stress values for round holes produced by the addition of a doubler framing the panel opening.

Predicted Values of Stress, Deflection, Moment, Shear Edge Loading, and Corner Reaction for the Test Panels and Heat Shield Panels (3OM12571)

#### Test Panel Configuration:

Size...20" x 30" x 1.02" thick  
Facing...0.010 PH15-7Mo Alloy  
Core...Type 4.15 1.0m thick Ph15-7Mo Alloy  
Brace Alloy--Silver-Copper-Lithium

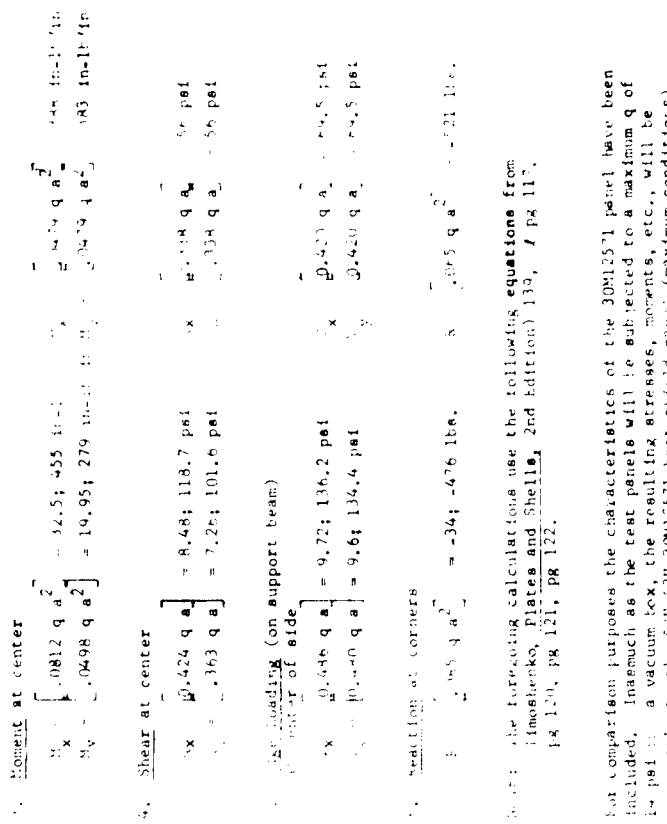
- Deflection at center of test panel  
for  $q = \frac{1}{4}$  and 14 psi  
 $W = (.00772 q a^4/D) = .00767, .1663"$

- Stress at center  

$$\frac{N_x = (0.12 q a^2)}{N_y = (4.98 q a^2)} = 3250, 45,300 \text{ psi}$$

$$\frac{N_x = (4.79 q a^2)}{N_y = (4.79 q a^2)} = 36,350 \text{ psi}$$

$$\frac{N_x = (4.79 q a^2)}{N_y = (4.79 q a^2)} = 36,350 \text{ psi}$$



In Fig. 1, the foregoing calculations use the following equations from Timoshenko, Plates and Shells, 2nd edition) 130, p 117, for 1.20, PR 121, PR 122.

For comparison purposes the characteristics of the 3OM12571 panel have been included. Inasmuch as the test panels will be subjected to a maximum  $q$  of 14 psi in a vacuum box, the resulting stresses, moment, etc., will be comparable to the 3OM12571 heat shield panel (maximum conditions).

EXPERIMENTAL MEASUREMENT OF  
STRESS CONCENTRATIONS AT HOLE BOUNDARIES

Two identical sample panels were fabricated of the same materials, cire type, facing gage and panel thickness at the heat shield panels. Size of the panels was  $20 \times 30 \times 1.02$  thick. A vacuum box (see Fig. 46) to simulate simple support conditions was made with the centerline of support  $19 \times 29$ . It was believed that the use of corner reaction forces would overcome the slight compressibility of the support ridges around the fixture edge and thus offset the tendency of the panel to curl. Had this been successful, the calculations would have been made much simpler as the face edges would lie in a plane and the formulas and expressions for simple support edge condition would apply. However, no amount of corner reaction force would hold the edges to a straight line. This necessitated considering the deflection of the panel with all four edges elastically supported.

Panel No. 1 was drilled to provide a  $2\frac{3}{8}$ " hole through the center. Deflection data was recorded and a second  $2\frac{3}{8}$ " hole placed near a corner with the center distant from the edge,  $d/R = 2$ . Stresscoat and deflection data were obtained. This test was repeated again with strain gage data also being taken. The center round hole was then cut out to make a square of the same size. A stresscoat pattern was obtained in the vicinity of the square hole, then deflection and strain gage data were recorded. No edge reinforcement doublers around the holes were employed. The test arrangement is shown in Figures 47 and 48. No failures of any nature in the vicinity of the holes occurred during the panel tests.

Table 22 shows the summary of the dial indicator deflection data. Dial indicator locations appear in Figure 49. The deflections tabulated for each test have been adjusted to a common value of  $28.5^{\circ}$  of mercury. The two corner indicators (No. 1 and No. 7) were used as a reference plane and the mean deflection of the five tests at the other positions on the panel were listed as the observed deflection of the panel. The value of  $\sigma$  was then computed for each of the indicator positions other than the corners 1 and 7 for a panel aspect ratio of 1.5 with elastically supported edges. These are tabulated. The value of  $Q_{a/D}$  is 13.768. The tabulated values of  $W_{calc}$  are thus  $13.768\sigma$ . A comparison of the observed and calculated deflections shows in general good agreement in the central panel area of greatest deflection.

The strain patterns for each condition are clearly shown in Figures 50 through 54 and particularly the areas of stress concentrations around the holes. Figures 51, 52 and 53. Stress concentration factors were determined by the comparative strains at the same points and for the same loading for the panel with holes versus the panel with no holes. Consequently, the simple ratios of hole strain

\* See Theory of Plates and Shells,  
2nd Ed., Page 218, by Timoshenko.

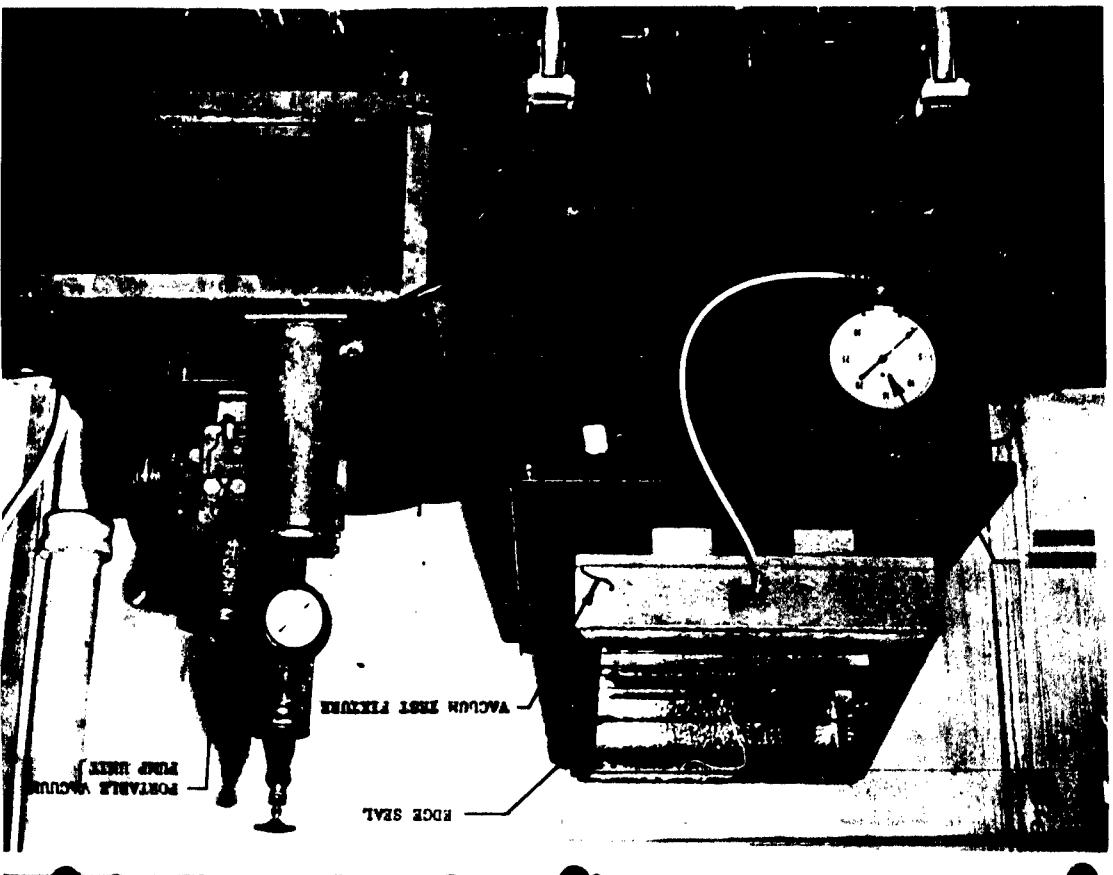
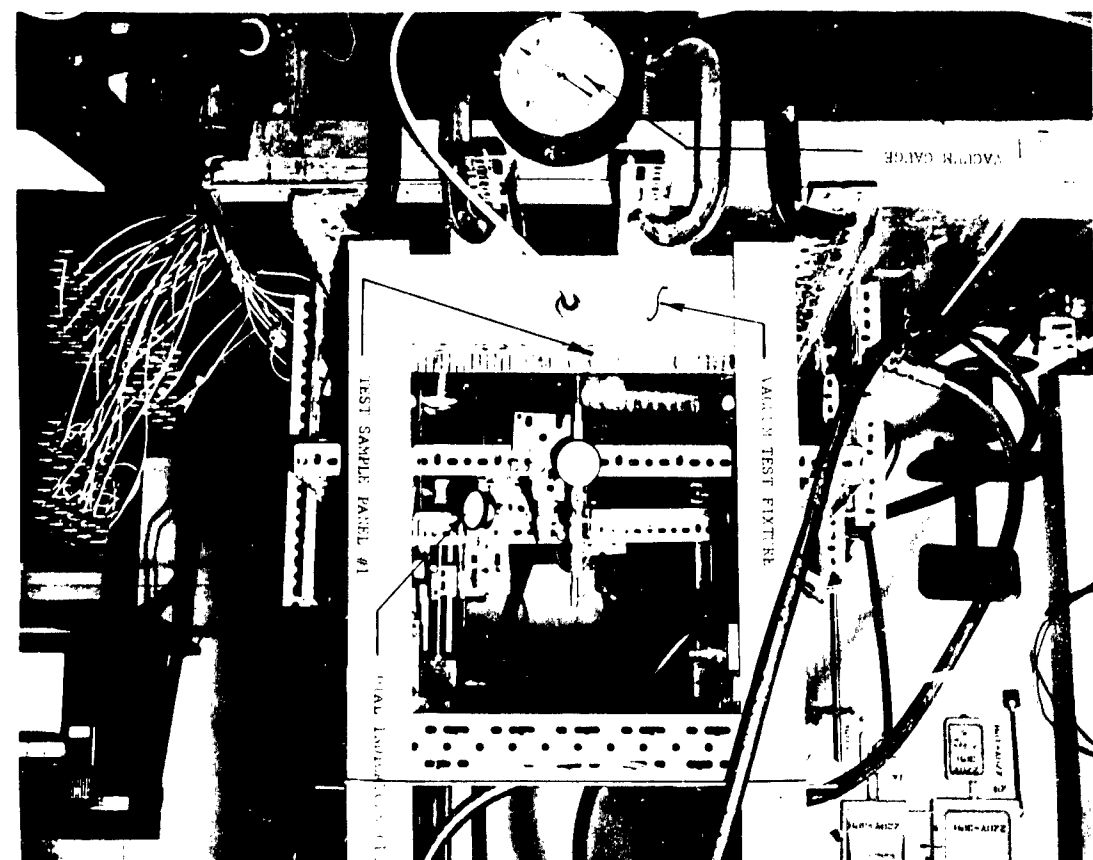


FIGURE 46 Vacuum Box Fixture

122



121

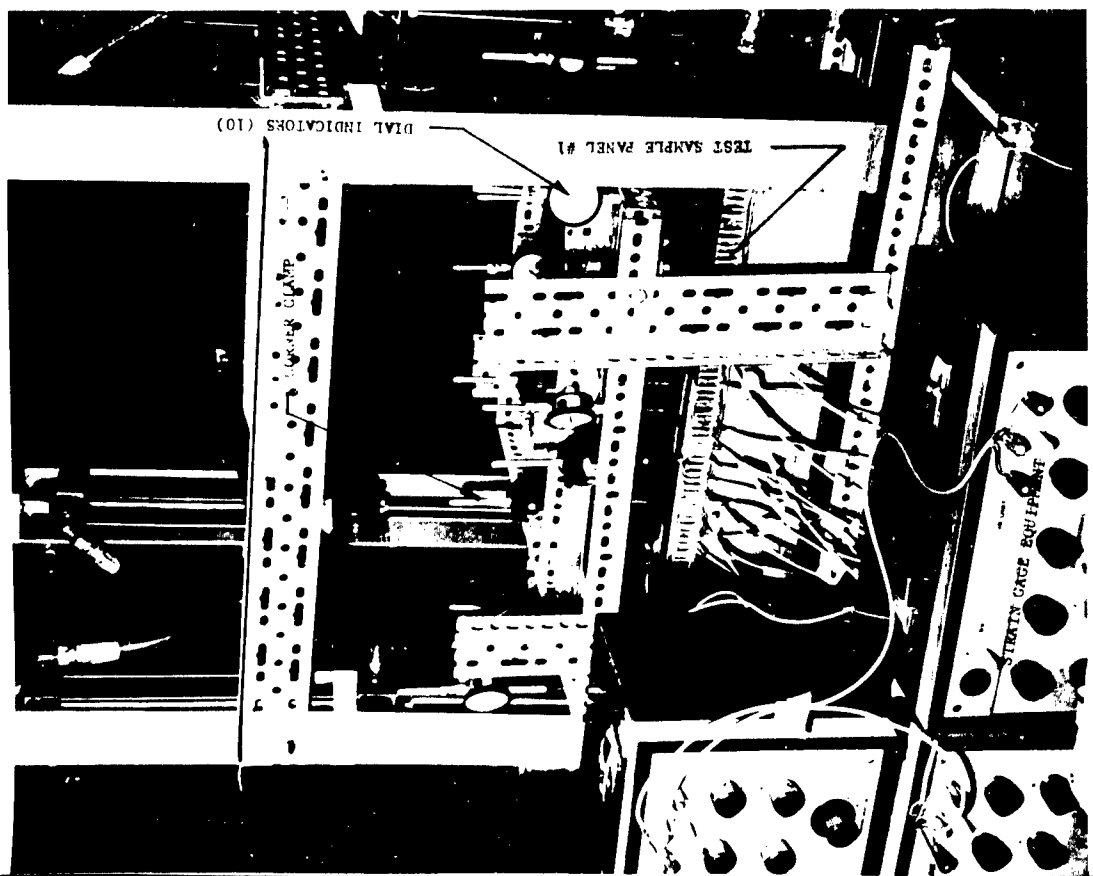


Figure 47. Strain Gages, Test Article No. Panel 1, Item 1.

123

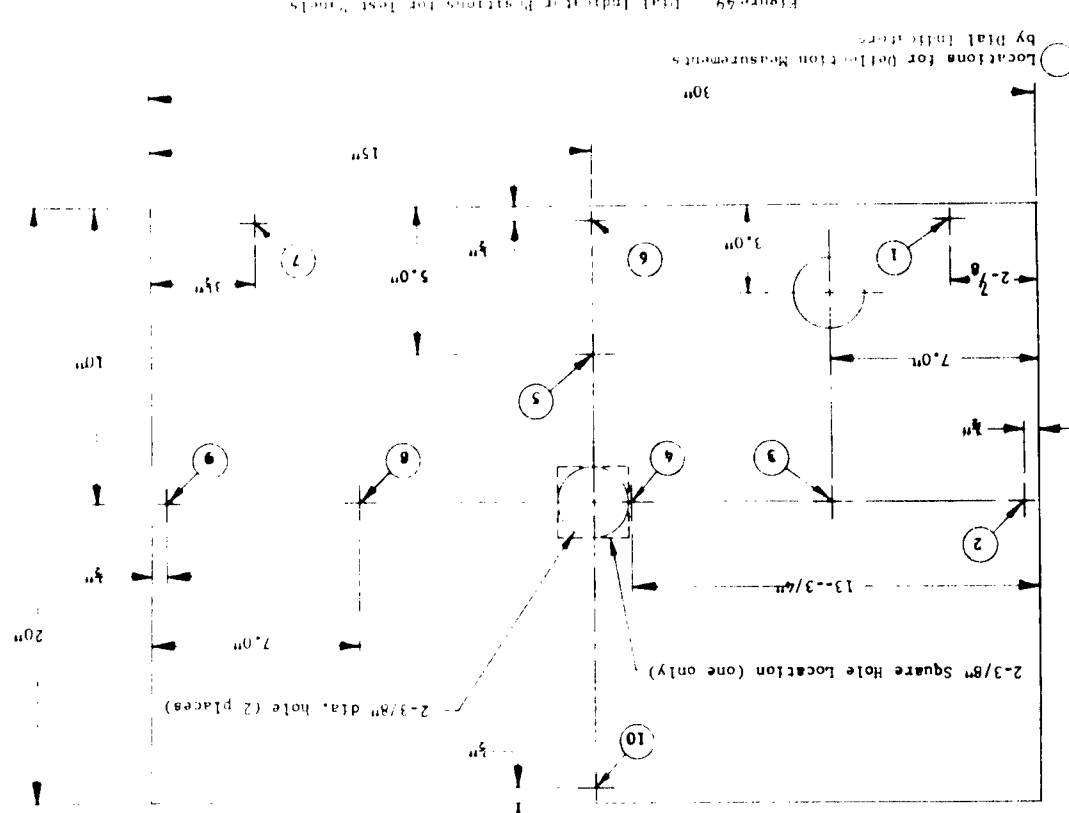
124

TEST PANEL DEFLECTION DATA

TABLE 2

Detail	Indicator	Panel No. 1										Panel No. 2										
		Panel No. 1 One Hole	Panel No. 1 Two Round	Panel No. 1 Two Round	Panel No. 1 One Square	Panel No. 1 One Round	Panel No. 1 Two Round	Panel No. 1 One Round	Panel No. 1 One Hole	Panel No. 1 Two Round	Panel No. 1 Two Round	Panel No. 1 One Square	Panel No. 1 One Round	Panel No. 1 Two Round	Panel No. 1 One Round	Panel No. 1 One Hole	Panel No. 1 Two Round	Panel No. 1 One Round	Panel No. 1 One Hole	Panel No. 1 Two Round	Panel No. 1 One Round	
1	.150	.190	.211	.197	.194	.194	.188	0	--	--	--	.027	.0026	.039	.137	.187	.161	.187	.161	.122	.122	.122
2	.205	.196	.220	.220	.233	.220	.215	.027	--	--	--	.305	.327	.331	.325	.319	.136	.00996	.137	.187	.161	.187
3	.306	.305	.347	.380	.379	.383	.367	.187	.187	.187	.187	.322	.330	.332	.313	.133	.01026	.141	.187	.161	.187	.161
4	.347	.347	.380	.379	.383	.383	.367	.187	.187	.187	.187	.228	.243	.239	.239	.239	.056	.009484	.122	.187	.161	.187
5	.268	.315	.322	.330	.332	.332	.313	.187	.187	.187	.187	.165	.180	.186	.173	0	--	--	--	--	.157	.180
6	.222	.250	.228	.228	.228	.228	.228	.228	.228	.228	.228	.165	.180	.186	.173	.173	.0	--	--	--	--	.190
7	.157	.180	.180	.180	.180	.180	.180	.180	.180	.180	.180	.165	.174	.174	.174	.174	.146	.000996	.137	.187	.161	.180
8	.306	.296	.324	.317	.328	.328	.314	.146	.146	.146	.146	.165	.180	.186	.173	.173	.0	--	--	--	--	.190
9	.220	.190	.211	.197	.194	.194	.188	0	--	--	--	.203	.201	.201	.194	.194	.030	.0028	.039	.122	.187	.161
10	.356	.267	.267	.267	.267	.267	.267	.267	.267	.267	.267	.165	.180	.186	.173	.173	.0	.00084	.122	.187	.161	.180

All cases to provide a common reference value. Data was reduced to this value for inches of mercury vacuum on test fixture. Data was reduced to the value for calculated from  $\frac{D}{D_0} = 1.00$ .



BRUNO 69

Locations by detail

126

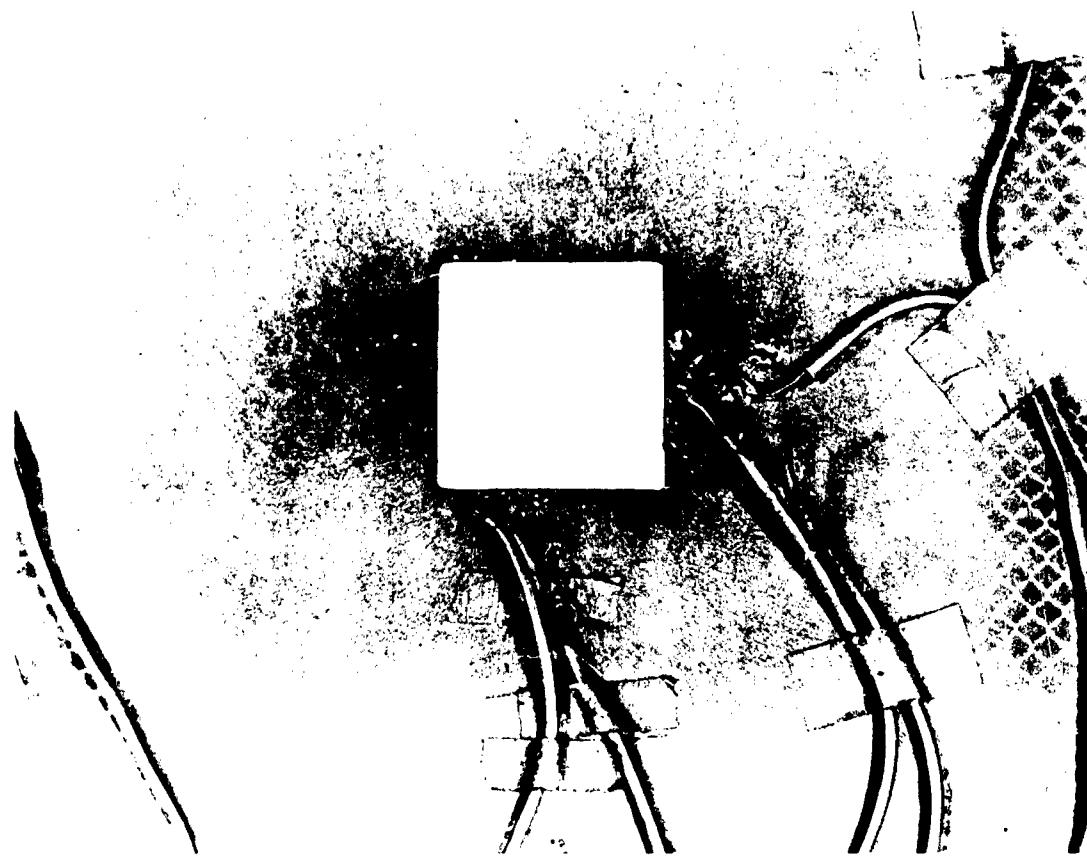


125

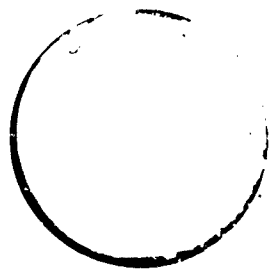


128

Figure 53 Center hole stress area (lose-up, front) at hole pattern



127



130

129

Figure 54 Panel No. 2, Stresscoat Pattern,

to no hole strain at the hole boundary gives the corrected stress concentration factors for biaxial loading. Theoretical values for the same hole conditions were obtained from published data. The observed and theoretical values are given in Table 2 and the agreement appears satisfactory. The desirability of round holes versus square holes is clearly shown.

Since only steady state loading conditions were evaluated while practical application includes a sizeable thermal and acoustic load, the addition of a factor equal in thickness to the factor is recommended for all instrumentation holes. Simulated environment testing under combined air, thermal and noise loads on a full size heat shield panel having multiple hole patterns accomplished after panel fabrication is recommended.

131

TABLE 2:

SUMMARY OF EXPERIMENTAL AND THEORETICAL VALUES FOR BIAXIAL LOADING

Strain Gage Position**	First Test, Panel No. 1 Two Round Holes		Second Test, Panel No. 1 Square Center Hole Round Corner Hole	
	K <sub>theory*</sub>	K <sub>obs.</sub>	K <sub>theory*</sub>	K <sub>obs.</sub>
A	2.4	2.38C 2.41T	.9	.69C .85T
B	3.9	4.1 T	2.4	2.34T
C			4.5	4.7 T
D			4.5	4.25T
E			6.0	6.20T
F	3.8	3.66T		
G	3.8	3.25T		
H	2.3	1.9T	2.3	2.13T
J	3.4	3.13T	3.4	3.25T

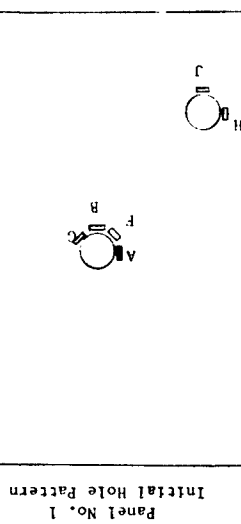
T, Tension Side of Panel

C, Compression Side of Panel

\* Theoretical values for biaxial loading from Stresses Around Holes,  
W. Griffel, Product Engineering 11/11/63, based on Stress Concentra-  
tion Around Holes, G. N. Savin.

\*\* See Figure 55 for locations A through J.

Figure 55  
Strain Gage Locations on Test Panels Used for Experimental Test



132

**SECTION VIII**

**DESIGN RECOMMENDATIONS FOR 5.1" X 5.1" SHIELD PANELS**

The following recommended design changes for current heat shield panel designs are based on the structural analysis developed on this program and on the heat shield panel fabrication experience on Contract NASA-1257.

**1. Honeycomb Reinforcement for M-31 Insulation**

Presently specified core configuration for the M-31 insulation reinforcement is Type 8-15 (1/16" cell size - 0.0015" foil core). A slightly heavier core, Type 8-20 (1/16" cell size - 0.001" foil core) is preferred for increased stability in the actual panel brazing as well as the core machining and panel layup operations. The greater stability of the Type 8-20 core during the brazing process will allow the use of a higher vacuum desirable to insure the fit of the panel details than the presently used 30 mercury or 1.5 psi. Likewise both the core machining and panel layup operations will benefit from the increased stability provided by the Type 8-20 core in:

- a. Improving the resistance to deformation caused by shop handling
- b. Reducing the time required for panel layup.

The difference in weight for the Type 8-20 versus 8-15 core (1/16" in thickness) is very slight, amounting to 0.011 lbs. per square foot or 0.21 lbs. for the 30H1257 panel.

**2. Braze Alloy Thickness for Open Faced Honeycomb Core**

The 30H1257 panels produced on Contract NASA-976 utilized 0.002" thick braze alloy (silver-copper-lithium) for the Type 8-15 open face core to facing attachment because of availability and prior experience on other open face honeycomb brazing applications. A thinner base of braze alloy, namely 0.0015", would be advantageous from a weight viewpoint (0.078 lbs/ft<sup>2</sup> versus 0.104 lbs/ft<sup>2</sup> for 0.002" braze alloy) and would provide comparable size braze fillets.

**3. Welded Zee Edge Member Frame**

The 30H1257 panel utilizes a one piece edge member frame fabricated as a subassembly by fusion welding four (4) zee sections at the corners followed by radiographic inspection of the welds and grinding the weld bead flush with the surface. As a consequence of the welded edge member frame, the completed panel is "sealed" with respect to the structural honeycomb core.

**133**

**134**

4. Brazed Zee Edge Member Assembly

The one piece welded edge member frame has many advantages. However, it involves expensive and fabrication operations that could be eliminated by using the fully brazed edge member assembly shown in Figure 56. This arrangement, made up of four zee sections brazed together, is also fully sealed by use of a small piece of facing integrally brazed as a doubler at each corner to provide additional strength and close off the corner gap from the core. This is the assembly that is recommended.

5. Core Sealed Edge Member Assembly

For minimum cost the corner joint sealing can be accomplished with a cost savings by using the corner configuration shown in Figure 57 with a high temperature elastomeric sealer such as Coast Pro Seal 700 applied to the corner opening. This type corner joint uses four (4) separate zee sections brazed to the panel facings and eliminates the welding operation, weld fixture, radiographic inspection and weld bead machining--it has likewise been extensively used in brazed panels for airframe application.

6. Zare Reduction for Zee Section Edge Member

An 0.030" thick zee section edge member will satisfy the design conditions and afford weight savings of approximately 5 lbs. for the 30MH2571 panel configuration. The analysis for the 0.030" edge member and a comparison with the present 0.050" edge member appears in Section II, Stress Analysis.

7. Treatment of the panel edges for the cup type attachment heat shield panels, particularly for exposed panel edges such as the outboard fairing panels, will be required to protect the structural honeycomb core from thermal and mechanical damage. Presumably, this will be accomplished by completely machining out the honeycomb core approximately 1/16" from the edge of the panel facing and filling the resulting slot with M-31 insulation. It appears unlikely that the unreinforced M-31 edge fill will be retained under the severe noise and vibration environment sustained during ignition and flight. A better edge treatment would be to leave a minimum of 0.25" honeycomb on each panel face in the slot area to provide a more positive attachment for the M-31 insulation. The best edge treatment is a complete insulated metal seal.

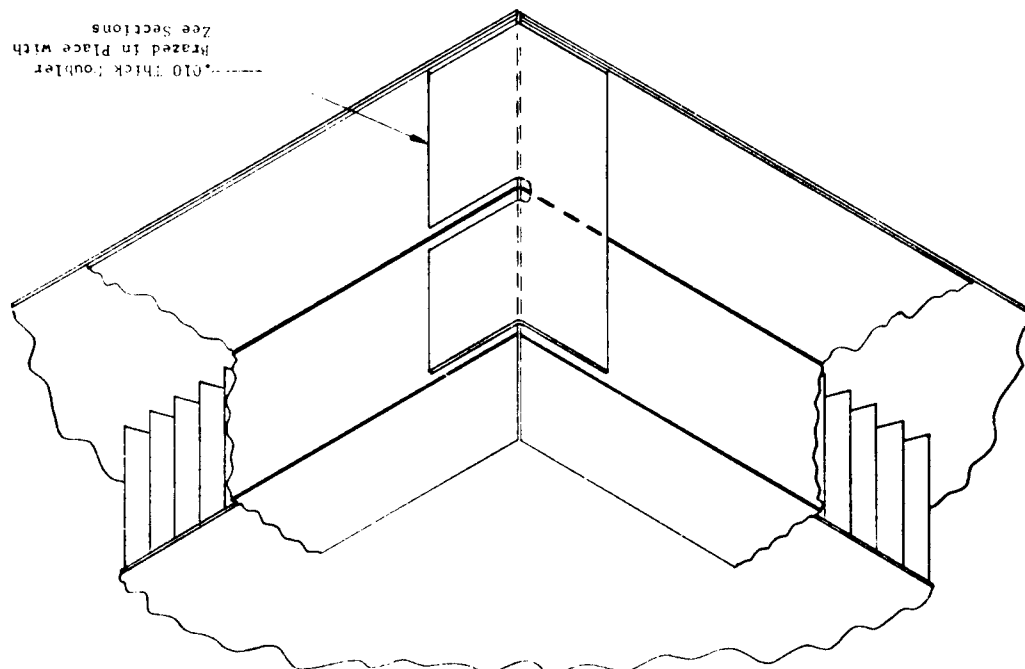
8. The necessity for deformed or crushed open faced honeycomb core to insure the adherence of the M-31 insulation under acoustic and thermal loads was established by the NASA S-IC Heat Shield Panel Test Program. Since the initial core height on both the 30MH2571 and 60B20210 panel designs was 0.125" and then further reduced by deformation or crushing to about 0.075", a thicker open faced core is clearly indicated. A thickness of 0.250" deformed to 0.180" is recommended.

135

136

137

Figure 56 Recommended Zee Section Section Through Joint Assembly



138

Figure 57 Recommended Zee Section Section Through Joint Assembly

